UNIVERSITY OF CALIFORNIA,
IRVINE

Exploring 2.2.2-Cryptand for the Expansion of the +2 and +3 Oxidation State Chemistry of the Rare-Earth and Actinide Metals and X-ray Photoelectron Spectroscopy of Gadolinium Complexes

DISSERTATION

submitted in partial satisfaction of the requirements
for the degree of

DOCTOR OF PHILOSOPHY

in Chemistry

by

Sierra R. Ciccone

Dissertation Committee:
Professor William J. Evans, Chair
Professor Jenny Y. Yang
Professor Andy S. Borovik

2023

DEDICATION

This dissertation is dedicated to my parents, Denise and Patrick, and to my brother and sisters,

Philip, LouAnn, and Kayela.

Thank you for your love and support.

TABLE OF CONTENTS

LIST OF FIGURES

LIST OF TABLES

Acknowledgments

First and foremost, I would like to thank my research mentor and committee chair, Bill Evans. His immense support has helped me reach achievements I never thought possible. His inspiration will be everlasting, and his passion for chemistry and research has inspired me to find my own passions in life. I cannot put into words how grateful I am for such an amazing mentor through my time at UCI. You have always believed in me even when I did not believe in myself and I can never thank you enough.

I would also like to express my gratitude to my committee members Jenny Yang and Andy Borovik for their advice and support throughout my PhD studies. I would like to thank all of you for being on my advancement to candidacy committee and taking the time to talk to me whenever I have needed it. You have taught me so much about chemistry and have given me valuable advice throughout my time in graduate school.

I would like to thank Dr. Joe Ziller for mounting and solving all my crystal structures. I really appreciated all the time that you spent working on my structures. This dissertation and my work throughout graduate school would not have been possible without your work. I would also like to thank the X-ray fellows who worked hard to mount my crystals and solve my structures: Dan Huh, Tyler Kerr, Chen Sun, and Joseph Nguyen. I appreciate the time you spend mounting my crystals and explaining the data to me. Thank you for all the work that the X-ray facility has done throughout my time at UCI.

Thank you to the Evans group members Austin Ryan, Dan Huh, Samuel Moehring, Jessica White, Justin Wedal, Amanda Chung, William Moore, Lauren Anderson-Sanchez, Joseph Nguyen, Kito Gilbert-Bass, Cary Stennett, Joshua Queen, Gabriella Godinho, and Brynn Turpinn for your support and encouragement and some fun times. And thank you to my colleagues and friends in the Yang, Borovik, and Heyduk groups for being supportive during my PhD.

Thank you to all the people I collaborated with throughout my time at UCI. Thank you to Dr. Filipp Furche for the theoretical calculations and DFT on my compounds. I would also like to thank Dr. John Hemminger and Dr. Jared Bruce for all the help with interpreting and understand X-ray photoelectron spectroscopy.

Thank you to Justin Wedal for being there for me in a very scary time during my PhD. I cannot thank you enough for your support and taking care of my guinea pigs. Tom and Giz will love you forever.

I would like to thank Cary Stennett for being such an amazing individual. I have never met someone quite like you and your positive energy pushed me to appreciate the good things in life. Thank you for all the laughs and thought-provoking conversations.

To my friends Amanda Chung, Melanie Skans, and Kito Gilbert-Bass, thank you for your never-ending support, I could not have done this without you all. Thank you for always being there when I have needed you.

I'd also like to give a special thanks to my undergraduate research mentor Jessica Hoover. Thank you for your support and mentorship. You are the original inspiration for pursuing my PhD and you still inspire me to this day. Thank you for all the opportunities you allowed me to have and letting me join your research group. I would not be here without the advice you shared with me.

To my parents, Denise and Patrick, thank you so much for always being there for me. Your endless love and support have really pushed me to reach my goals. I love you two so much and you mean the world to me. Thank you for always taking care of me.

CURRICULUM VITAE

Sierra Ciccone

EDUCATION

University of California, Irvine, California (September 2018 – May 2023)
Ph. D. Graduate Student Researcher. Advisor: Prof. William J. Evans
West Virginia University, Morgantown, West Virginia (August 2014 – May 2018)
B.S. in Chemistry, with minor in Biology. Advisor: Prof. Jessica M. Hoover

EXPERIENCE

Undergraduate Teaching Assistant, West Virginia University (August 2016 – May 2018)
Undergraduate Student Researcher, West Virginia University (January 2017 – May 2018)
Summer Undergraduate Research Experience, West Virginia University (Summer 2017; 2018)
Graduate Teaching Assistant, University of California – Irvine (September 2018 – present)
Assisted in teaching and taught laboratory sections. Teaching assignments included general chemistry, organic chemistry, and inorganic chemistry.
Graduate Research Assistant, University of California – Irvine (September 2018 – present)
Eddleman Quantum Institute Graduate Research Fellow, University of California – Irvine (Summer 2020 – 2022)
Convener, Eddleman Quantum Institute Graduate Student Council, University of California – Irvine (Summer 2020 – 2022)

PUBLICATIONS

1. Green, K.A, Honeycutt, A. P., **Ciccone, S. R.,** Grice, K. A., Baur, A., Peterson, J. L., Hoover, J. M. A Redox Transmetalation Step in Nickel-Catalyzed C–C Coupling Reactions. *ACS Catal.* **2023**, *13*, 6375-6381.
2. Huh, D. N., **Ciccone, S. R.,** Bekoe, S., Roy, S., Ziller, J. W., Furche, F., Evans, W. J. Synthesis of Ln^{II}-in-Cryptand Complexes by Chemical Reduction of Ln^{III}-in-Cryptand Precursors: Isolation of a Nd^{II}-in-Cryptand Complex. *Angew. Chem. Int. Ed.* **2020,** *59*, 16141–16146.
3. Huh, D. N., Bruce, J. P., Balasubramani, S. G., **Ciccone, S. R**., Furche, F., Hemminger, J. C., Evans, W. J. High-Resolution X-ray Photoelectron Spectroscopy of Organometallic $(C_5H_4SiMe_3)_3Ln^{III}$ and $[(C_5H_4SiMe_3)_3Ln^{II}]^{1-}$ Complexes (Ln = Sm, Eu, Gd, Tb). *J. Am. Chem. Soc.* **2021**, *143*, 16610-16620.
4. Huh, D. N., Barlow, J. M., **Ciccone, S. R**., Ziller, J. W., Yang, J. Y., Evans, W. J. Stabilization of U(III) to Oxidation and Hydrolysis by Encapsulation using 2.2.2-Cryptand. *Inorg. Chem*. **2020**, *59*, 17077-17083.

5. Huh, D. N., **Ciccone, S. R.,** Moore, W. N. G., Ziller, J. W., Evans, W. J. Synthesis of Ba(II) Analogs of Ln(II)-in-(2.2.2-Cryptand) and Layered Hexagonal Net Ln(II) Complexes, $[(THF)Cs(\mu\text{-}\eta^5\text{:}\eta^5\text{-}C_5H_4SiMe_3)_3Ln^{II}]_n$. *Polyhedron* **2021**, *210*, 115393.
6. Goodwin, C. A. P., **Ciccone, S. R.,** Bekoe, S., Majumdar, S., Scott, B. L., Ziller, J. W., Gaunt, A. J., Furche, F., Evans, W. J. 2.2.2-Cryptand Complexes of Neptunium(III) and Plutonium(III). *Chem. Comm*. **2022**, *58*, 997-700.

POSTER PRESENTATIONS

1. **Ciccone, S. R.; Hoover, J. M.** *Nickel-Catalyzed Oxidative Decarboxylative Cross Coupling: What is the Role of Silver?* Presented at West Virginia University, Summer Undergraduate Research Experience. Morgantown, WV. 2017
2. **Ciccone, S. R.; Hoover, J. M.** *Catalytic decarboxylative (hetero)arylation reactions: Development and mechanistic insights.* Presented at the 69th Southeastern Regional Meeting for the American Chemical Society. Charlotte, NC. 2017.
3. **Ciccone, S. R.; Hoover, J. M.** *Investigation Transmetallation in Nickel-Catalyzed Oxidative Decarboxylative Coupling Reactions.* Presented at West Virginia University, Summer Undergraduate Research Experience. Morgantown, WV. 2018.

SKILLS

- Synthesis of inorganic, organic, and organometallic compounds
- Manipulation of extremely air sensitive inorganic and organometallic compounds using glovebox, vacuum line, and Schlenk line techniques
- Characterization techniques of multinuclear and paramagnetic NMR spectroscopy, IR spectroscopy, UV-visible spectroscopy, elemental analysis, X-ray crystallography, mass spectrometry, and GCMS.
- Electrochemistry to study reduction potentials of reactive and air sensitive complexes
- Synthesis of complexes for XANES measurements
- X-ray photoelectron spectroscopy to probe the electronic structure of new lanthanide complexes

HONORS AND AWARDS

- West Virginia University Honors Program (2014 – 2018)
- Eberly College of Arts & Sciences Outstanding Graduating Senior in Chemistry, *West Virginia University* (2018)
- ACS Undergraduate Award in Organic Chemistry, *West Virginia University* (2018)
- Phi Beta Kappa Honor Society

Abstract of Dissertation

Exploring 2.2.2-Cryptand for the Expansion of the +2 and +3 Oxidation State Chemistry of the Rare-Earth and Actinide Metals and X-ray Photoelectron Spectroscopy of Gadolinium Complexes

Sierra R. Ciccone

Doctor of Philosophy in Chemistry

University of California, Irvine, 2023

Professor William J. Evans, Chair

This dissertation describes efforts to expand the area of low oxidation state chemistry for the rare-earth metals and the actinides. The use of the spherically encapsulating 2.2.2-cryptand (crypt) for the isolation of new complexes of +3 and +2 ions of these metals was explored. In addition, X-ray photoelectron spectroscopy (XPS) was used to evaluate the electron configurations of Gd(II) complexes by comparison with Gd(III) analogs. Specifically, Chapter 2 describes the isolation of complexes of Sm(III) and Nd(III) with crypt, $[Sm(crypt)(OTf)_2][OTf]$ and $[Nd(crypt)(OTf)_2][OTf]$, and their reduction chemistry. The $[Ln(crypt)(OTf)_2][OTf]$ complexes reacted with KC_8 in THF to form the $Ln^{II}(crypt)(OTf)_2$ counterparts. Chapter 3 describes the synthesis and attempted reduction of $[Ln(crypt)(OTf)_2][OTf]$ complexes for Ln = La, Ce, and Pr. Unlike their Sm and Nd counterparts, neither chemical nor electrochemical reduction was observed for La and Ce. Chapter 4 describes the extension of the crypt ligand to actinides in collaboration with Dr. Andrew Gaunt and Dr. Conrad Goodwin at Los Alamos National Laboratory (LANL) for An = U, Np, and Pu. Small scale reactions with uranium to make $[U(crypt)(OTf)_2][OTf]$ were conducted and used as a method to extend this chemistry to Np and Pu, which are of limited availability. Chapter 5 describes methods using liquid ammonia and sodium metal to attempt

reductions of smaller Ln metals encapsulated in the cryptand ligand. This method was explored because Ln-in-crypt complexes of the smaller lanthanides later in the series are not soluble in THF. Chapter 6 describes the exploration of borohydride, $(BH_4)^{1-}$, and thexylborohydride, $(H_3BCMe_2CMe_2H)^{1-}$, ligands to make THF-soluble Ln^{II}-in-crypt complexes. These ligands were used for both Sm and Dy. While evidence suggests that a THF-soluble $Sm^{II}(crypt)(H_3BCMe_2CMe_2H)_2$ can be generated, Dy-in-crypt complexes with borohydrides were still not THF-soluble. Chapter 7 describes the isolation of a Sm^{II} ion encapsulated in a 2.2.1-cryptand (221crypt) ligand environment, [Sm(221crypt)(OTf)][OTf]. A cryptand with a smaller pocket was explored to see if this could affect the solubility of these cryptand complexes. Instead of making complexes more soluble in THF, the opposite was observed. Chapter 8 describes the isolation of a $[Tm^{II}(crypt)(OTf)][OTf]_2$ complex. In comparison to the reductions described in Chapter 2, this complex was not isolated by chemical reduction of a Tm^{III}-in-crypt complex, but rather the reduction of $Tm^{III}(OTf)_3$ with KC_8 followed by the addition of crypt. Chapter 9 describes X-ray photoelectron spectroscopy (XPS) measurements made on Gd complexes in different coordination environments, specifically, $Gd[(NSiMe_3)_2]_3$, Cp^{tet}_3Gd, $[K(crypt)][Gd[(NSiMe_3)_2]_3]$, and $[K(crypt)][Cp^{tet}_3Gd]$ and a comparison with cyclopentadienyl analogs.

Chapter 1

Introduction

One of the fundamental aspects of a metal that controls its reactivity is its oxidation state. While transition metal ions have been thoroughly studied and have been found to access many oxidation states that allow for a vast variety of applications, rare-earth metals (referring to the group of elements Sc, Y, La, Ce, Pr, Nd, Pm, Sm, Eu, Gd, Tb, Dy, Ho, Er, Tm, Yb and Lu) have not been as thoroughly explored. Rare-earth metals, when compared to transition metals are much more limited in accessing a variety of oxidation states.

Rare-Earth Metals. The most common oxidation state for rare-earth metals is the +3 oxidation state. Lanthanide ions in the +2 oxidation state for Sm, Eu, and Yb were known since 1906.[1-4] However, not until 1997-2000 were the first complexes of Nd, Dy and Tm in the +2 oxidation state reported in the literature.[5-7] Extending the +2 oxidation state to the rest of the lanthanide metals was not thought to be possible since their calculated reduction potentials were so negative that they would decompose solvents, Table 1.1.[8]

Table 1.1. Calculated reduction potentials for Ln(III) to Ln(II) ions (in V vs NHE).

Ln	Potential	Ln	Potential
Eu	–0.35	**Pr**	–2.7
Yb	–1.15	**Y**	–2.8
Sm	–1.55	**Ho**	–2.9
Tm	–2.3	**Er**	–3.1
Dy	–2.5	**La**	–3.1
Nd	–2.6	**Ce**	–3.2
Pm	–2.6	**Tb**	–3.7
Lu	–2.72	**Gd**	–3.9

It was not until 2008 that Lappert and coworkers isolated the first examples of La(II) and Ce(II) complexes, [K(chelate)][Cp"$_3$La^{II}] and [K(18-crown-6)][Cp"$_3$Ce^{II}]·[Cp"$_3$Ce^{III}] (Cp" = $C_5H_3(SiMe_3)_2$; chelate = 18-crown-6, 2.2.2-cryptand) by reducing Cp"$_3$Ln complexes with potassium in the presence of a chelating agent, equation 0.1.[9] Since the reduction potential for potassium is –2.9 V vs NHE,[10] the reduction should not occur based on the redox potentials in Table 1.1. However, Lappert reported that these were not $4f^n + e \rightarrow 4f^{n+1}$ reductions, but rather $4f^n + e \rightarrow 4f^n5d^1$ reactions which had less negative redox potentials.

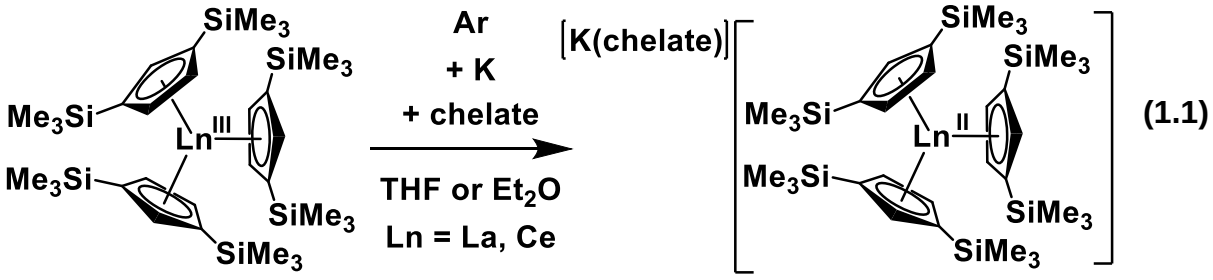

chelate = 18-crown-6 or 2.2.2-cryptand

In 2011, evidence for the +2 oxidation state for Y was found from the EPR data on the product of reducing $Y(NR_2)_3$ (R = $SiMe_3$) with KC_8.[11] By changing the conditions slightly, a molecular Y(II) complex $(Cp'_3Y^{II})^{1-}$ (Cp′ = $C_5H_4SiMe_3$), was isolated later that year., eq 1.2.[12]

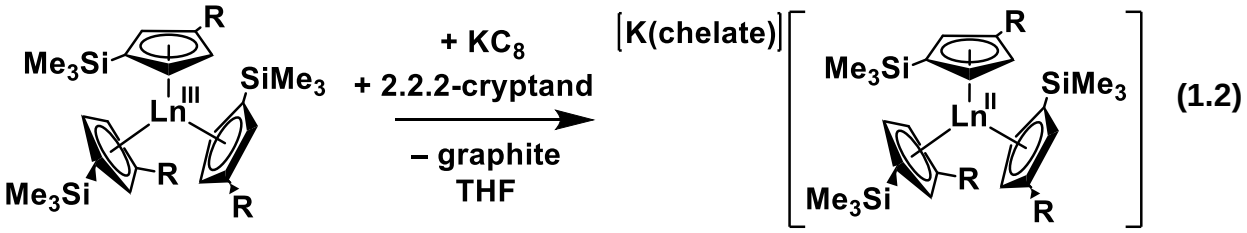

Ln = Y, La, Ce, Pr, Nd, Sm, Gd, Tb, Dy, Ho, Er, Tm, Lu
chelate = 18-crown-6 or 2.2.2-cryptand

Soon after the +2 oxidation state was expanded to the whole lanthanide series, excluding Pm due to its radioactivity, eq 1.2.[13-14] It was found that these new Ln^{II} ions were different in electronic configuration from those that were previously isolated as iodides (Ln =Sm, Eu, Yb, Nd, Dy and Tm) termed traditional ions. These new Ln^{II} ions adopted a $4f^n5d^1$ electron configuration rather than the already known $4f^{n+1}$ electron configuration thus resulting in calling these new Ln ions "non-traditional ions".

Actinides. Unlike the lanthanide series, the actinides have a wider availability of oxidation states.[15] But like the lanthanides, molecular examples of actinides in the +2 oxidation state were also limited. Using strategies similar to the ones used for isolation of Ln(II) complexes, U(II) was isolated in 2013 by reducing Cp'_3U with KC_8 in the presence of 2.2.2-cryptand to form [K(crypt)[Cp'_3U].[16] Similarly to the $4f^n5d^1$ Ln(II) ions, the electron configuration of this U(II) ion was assigned as $5f^36d^1$. Additional examples of U(II) were later isolated with Cp′.[17] This chemistry was also extended to Th(II),[18], Np(II),[19] and Pu(II),[20] equation 1.3.

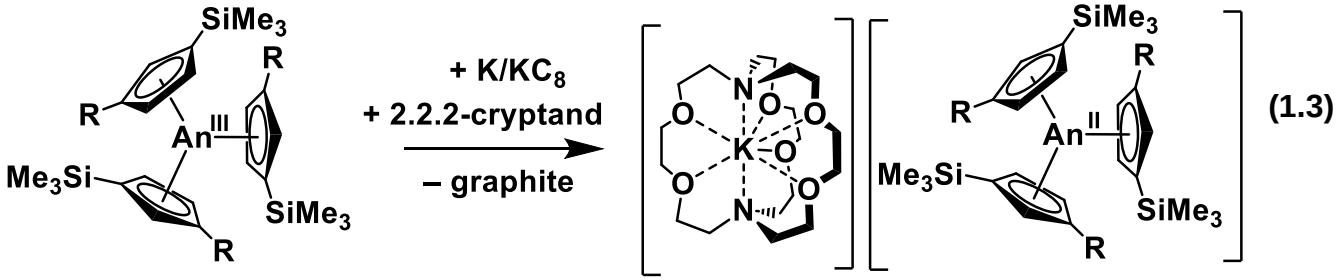

(1.3)

R = H; An = U

R = $SiMe_3$; An = Th, U, Np, Pu

The new Ln(II) ions with $4f^n5d^1$ electron configurations were isolated in trigonal coordination environments which led to a crystal field splitting of the 5d orbitals that put a single d orbital, $5d_z^2$, low in energy such that it could be populated along with the 4f orbitals. It was of

interest to put the new Ln(II) ions in other coordination environments that would test this concept. The 2.2.2-cryptand ligand (crypt), Figure 1.1, was an interesting option since its more spherical coordination environment would not lead to crystal field splitting that would make a single d orbital, the d_z^2, low in energy as seen with the cyclopentadienyl ligands due to their trigonal geometry. Hence $4f^{n+1}$ electron configurations might be preferred for Ln(II) ions inside crypt.

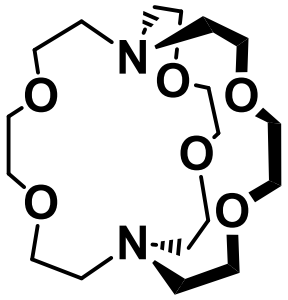

Figure 1.1. 2.2.2-cryptand (crypt) ligand

This dissertation explores the synthesis of crypt complexes of Ln(III) and An(III) ions and their reduction to Ln(II) species. Also included in this dissertation is an X-ray photoelectron spectroscopy study of Gd(III) and Gd(II) complexes designed to explore the reduction of $4f^7$ Gd(III) to $4f^75d^1$ Gd(II).

Chapter 2 describes the isolation of complexes of Sm(III) and Nd(III) with crypt, specifically $[Sm(crypt)(OTf)_2][OTf]$ and $[Nd(crypt)(OTf)_2][OTf]$, and their reduction chemistry. The $[Ln(crypt)(OTf)_2][OTf]$ complexes reacted with KC_8 in THF to form the $Ln^{II}(crypt)(OTf)_2$ counterparts. Traditional electron configurations of $4f^{n+1}$ were assigned to both Sm and Nd using metrical parameters from crystal structures in addition to DFT calculations.

Chapter 3 describes the synthesis and attempted reduction of $[Ln(crypt)(OTf)_2][OTf]$ complexes for Ln = La, Ce, and Pr. Unlike their Sm and Nd counterparts, neither chemical nor

electrochemical reduction was observed for La and Ce. The Pr system was more complicated in that color changes were observed, but new complexes were not isolated for definitive characterization.

Chapter 4 describes the extension of the crypt ligand to actinides in collaboration with Dr. Andrew Gaunt and Dr. Conrad Goodwin at Los Alamos National Laboratory (LANL) for An = U, Np, and Pu. Small scale reactions with uranium to make [U(crypt)$(OTf)_2$][OTf] were conducted and used as a method to extend this chemistry to Np and Pu, which are of limited availability.

Chapter 5 describes methods using liquid ammonia and sodium metal to attempt reductions of smaller Ln metals encapsulated in the cryptand ligand. This method was explored because Ln-in-crypt complexes of the smaller lanthanides later in the series are not soluble in THF. While Birch reductions were successful for the chemical reduction of Sm-in-crypt complexes, reduction could not be extended to the smaller metals nor Nd.

Chapter 6 describes the use of borohydride, $(BH_4)^{1-}$, and thexylborohydride, $(H_3BCMe_2CMe_2H)^{1-}$, to make THF-soluble Ln^{II}-in-crypt complexes. These ligands were used for both Sm and Dy. While evidence suggests that a THF-soluble Sm^{II}(crypt)$(H_3BCMe_2CMe_2H)_2$ could be generated, Dy-in-crypt complexes were still not THF-soluble.

Chapter 7 describes the isolation of a Sm^{II} ion encapsulated in a 2.2.1-cryptand (221crypt) ligand environment, [Sm(221crypt)(OTf)][OTf]. A cryptand with a smaller pocket was explored to see if this could affect the solubility of these cryptand complexes. Instead of making complexes more soluble in THF, the opposite was observed.

Chapter 8 describes the isolation of a [Tm^{II}(crypt)(OTf)][$OTf]_2$ complex. In comparison to the reductions described in Chapter 2, this complex was not isolated by chemical reduction of a

Tm^{III}-in-crypt complex, but rather the reduction of a $Tm^{III}(OTf)_3$ with KC_8 followed by the addition of crypt.

Chapter 9 describes X-ray photoelectron spectroscopy (XPS) measurements made on Gd complexes in different coordination environments, specifically, $Gd[(NSiMe_3)_2]_3$, Cp^{tet}_3Gd, $[K(crypt)][Gd[(NSiMe_3)_2]_3]$, and $[K(crypt)][Cp^{tet}_3Gd]$. Measurements were collected to compare with data reported in 2021[21] for cyclopentadienyl complexes that suggested the valence band of these complexes could be investigated to show the addition of an electron into the 5d orbital. However, no peaks were observed to suggest this for these complexes. Instead, only shifts in binding energies were observed between the +3 and +2 oxidation states.

References

1. Atwood, D. A., The rare earth elements: fundamentals and applications. John Wiley & Sons: 2013.

2. Matignon, C., Cazes, E., Le chlorure samareux. *Ann. Chim. Phys*. **1906**, *8*, 417-426.

3. Jantsch, G., Grubitsch, H., Hoffmann, F., Alber, H., Zur Kenntnis der Halogenide der seltenen Erden. Über die Jodide der Ceriterdenelemente und die Neubestimmung der Schmelzpunkte der Chloride. *Z. Anorg. Allg. Chem*. **1929**, *185* (1), 49-64.

4. Klemm, W., Bommer, H., Contribution to the knowledge of the rare earths. *Z. Anorg. Allg. Chem.* **1937**, *231*, 138-171.

5. Bochkarev, M. N., Fedushkin, I. L., Dechert, S., Fagin, A. A., Schumann, H., $[NdI_2(THF)_5]$, the First Crystallographically Authenticated Neodymium(II) Complex. *Angew. Chem. Int. Ed.* **2001**, *40* (17), 3176-3178.

6. Evans, W. J., Allen, N. T., Ziller, J. W., The Availability of Dysprosium Diiodide as a Powerful Reducing Agent in Organic Synthesis: Reactivity Studies and Structural Analysis of $DyI_2(DME)_3$ and Its Naphthalene Reduction Product. *J. Am. Chem. Soc*. **2000**, *122* (47), 11749-11750.

7. Bochkarev, M. N., Fedushkin, I. L., Fagin, A. A., Petrovskaya, T. V., Ziller, J. W., Broomhall-Dillard, R. N., Evans, W. J., Synthesis and structure of the first molecular thulium(II) complex: $[TmI_2(MeOCH_2CH_2OMe)_3]$. *Angew. Chem. Int. Ed.* **1997**, *36* (1-2), 133-135.

8. Morss, L. R., Thermochemical properties of yttrium, lanthanum, and the lanthanide elements and ions. *Chem. Rev.* **1976**, *76* (6), 827-841.

9. Hitchcock, P. B., Lappert, M. F., Maron, L., Protchenko, A. V., Lanthanum Does Form Stable Molecular Compounds in the +2 Oxidation State. *Angew. Chem. Int. Ed*. **2008**, *47* (8), 1488-1491.

10. Vanysek, P. Electrochemical Series. In *CRC Handbook of Chemistry and Physics*, 92nd ed: CRC Press, 2011; 5-80.

11. Fang, M., Lee, D. S., Ziller, J. W., Doedens, R. J., Bates, J. E., Furche, F., Evans, W. J., Synthesis of the $(N_2)^{3-}$ Radical from Y^{2+} and Its Protonolysis Reactivity To Form $(N_2H_2)^{2-}$ via the $Y[N(SiMe_3)_2]_3/KC_8$ Reduction System. *J. Am. Chem. Soc*. **2011**, *133* (11), 3784-3787.

12. MacDonald, M. R., Ziller, J. W., Evans, W. J., Synthesis of a Crystalline Molecular Complex of Y^{2+}, $[(18\text{-crown-6})K][(C_5H_4SiMe_3)_3Y]$. *J. Am. Chem. Soc.* **2011**, *133* (40), 15914-15917.

13. MacDonald, M. R., Bates, J. E., Ziller, J. W., Furche, F., Evans, W. J., Completing the Series of +2 Ions for the Lanthanide Elements: Synthesis of Molecular Complexes of $Pr^{2+,}$ Gd^{2+}, Tb^{2+}, and Lu^{2+}. *J. Am. Chem. Soc.* **2013**, *135* (26), 9857-9868.

14. MacDonald, M. R., Bates, J. E., Fieser, M. E., Ziller, J. W., Furche, F., Evans, W. J., Expanding Rare-Earth Oxidation State Chemistry to Molecular Complexes of Holmium(II) and Erbium(II). *J. Am. Chem. Soc*. **2012**, *134* (20), 8420-8423.

15. Morss, L. R. Edelstein, N. M., Fuger, J., Katz, J. J., The chemistry of the actinide and transactinide elements. Springer: 2006; Vol. 1

16. MacDonald, M. R., Fieser, M. E., Bates, J. E., Ziller, J. W., Furche, F., Evans, W. J., Identification of the +2 Oxidation State for Uranium in a Crystalline Molecular Complex, [K(2.2.2-Cryptand)][$(C_5H_4SiMe_3)_3U$]. *J. Am. Chem. Soc.* **2013**, *135* (36), 13310-13313.

17. Windorff, C. J., MacDonald, M. R., Meihaus, K. R., Ziller, J. W., Long, J. R., Evans, W. J., Expanding the Chemistry of Molecular U^{2+} Complexes: Synthesis, Characterization, and Reactivity of the $\{[C_5H_3(SiMe_3)_2]3U\}^-$ Anion. *Chem. Eur. J.* **2016**, *22* (2), 772-782.

18. Langeslay, R. R., Fieser, M. E., Ziller, J. W., Furche, F., Evans, W. J., Synthesis, structure, and reactivity of crystalline molecular complexes of the $\{[C_5H_3(SiMe_3)_2]_3Th\}^{1-}$ anion containing thorium in the formal +2 oxidation state. *Chem. Sci.* **2015**, *6* (1), 517-521.

19. Su, J., Windorff, C. J., Batista, E. R., Evans, W. J., Gaunt, A. J., Janicke, M. T., Kozimor, S. A., Scott, B. L., Woen, D. H., Yang, P., Identification of the Formal +2 Oxidation State of Neptunium: Synthesis and Structural Characterization of $\{Np^{II}[C_5H_3(SiMe_3)_2]_3\}^{1-}$. *J. Am. Chem. Soc.* **2018**, *140* (24), 7425-7428.

20. Windorff, C. J., Chen, G. P., Cross, J. N., Evans, W. J., Furche, F., Gaunt, A. J., Janicke, M. T., Kozimor, S. A., Scott, B. L., Identification of the Formal +2 Oxidation State of Plutonium: Synthesis and Characterization of $\{Pu^{II}[C_5H_3(SiMe_3)_2]_3\}^-$. *J. Am. Chem. Soc.* **2017**, *139* (11), 3970-3973.

21. Huh, D. N., Bruce, J. P., Balasubramani, S. G., Ciccone, S. R., Fuche, F., Hemminger, J. C., Evans, W. J. High-Resolution X-ray Photoelectron Spectroscopy of Organometallic $(C_5H_4SiMe_3)_3Ln^{III}$ and $[(C_5H_4SiMe_3)_3Ln^{II}]^{1-}$ Complexes (Ln = Sm, Eu, Gd, Tb). *J. Am. Chem. Soc.* **2021,** *143* (40), 16610-16620

CHAPTER 2

Synthesis of Ln^{II}-in-Cryptand Complexes by Chemical Reduction of Ln^{III}-in-Cryptand Precursors

Introduction*

The identification of +2 oxidation states for the Ln metals as described in Chapter 1 led to a search for other coordination environments that could also support the +2 oxidation state since the initial examples were limited to types of cyclopentadienyl ligands. 2.2.2-Cryptand (crypt) was of interest because of electrochemical reports by Gansow[1] and Allen[2] that suggested that crypt supports lower oxidation states. Complexation of alkali and alkaline-earth metal ions using the crypt ligand was first reported in 1973[3,4], and this crypt encapsulation chemistry was eventually extended to lanthanide ions in 1979.[5] However, in the ensuing four decades, only seventeen crystallographically-characterized Ln-in-crypt complexes were reported in the literature.[5-15] The majority of these complexes involved lanthanides in the common +3 oxidation state. Only in 2010 were Ln(II)-in-crypt complexes identified, but only for the $4f^n$ Ln(II) ions, Ln = Sm, Eu, and Yb.[9-14] These crystallographically-characterized Ln(II)-in-crypt complexes were all formed from Ln(II) precursors, equation 1.1, rather than by reduction of Ln(III)-in-crypt precursors.

*Portions of this chapter have been published in Huh, D. N.; **Ciccone, S. R.**; Bekoe, S.; Roy, S.; Ziller, J. W.; Furche, F.; Evans, W. J., Synthesis of Ln(II)-in-Cryptand Complexes by Chemical Reduction of Ln(III)-in-Cryptand Precursors: Isolation of a Nd(II)-in-Cryptand Complex. *Angew. Chem. Int. Ed.* **2020,** *59* (37), 16141-16146.

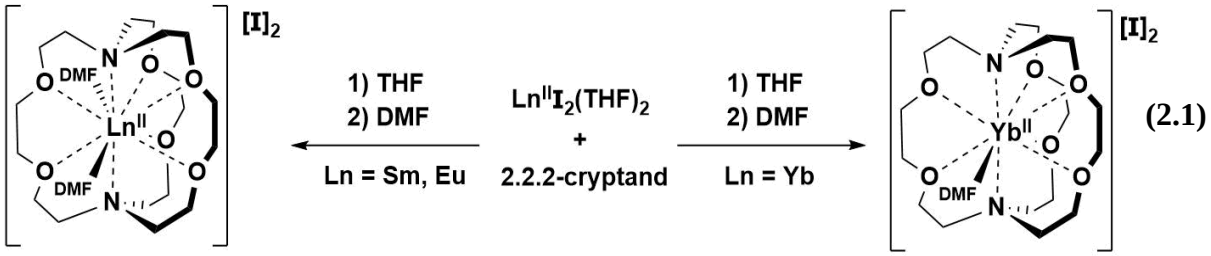

Electrochemical reports suggested that crypt not only may support lower oxidation states, but may actually *favor* lower oxidation states, as presented by Gansow[1] and Allen.[2] It was shown that the redox potential of encapsulated Eu ions were more positive, suggesting the +2 oxidation state of these ions was easier to access. By favoring lower oxidation states, crypt may allow for isolation of different Ln^{II} ions and potentially even Ln(I) ions.

It was of interest to explore the reduction chemistry of Ln-in-crypt complexes further, but already-known complexes, as shown in eq 2.1, were insoluble in the ethereal solvents commonly used in the synthesis to reduce lanthanide compounds. The compounds dissolve in dimethylformamide (DMF) to form DMF adducts,[13] but this complicates the reduction chemistry since alkali metal reducing agents can react with DMF.[16] Thus, THF soluble Ln-in-crypt complexes were sought.

To obtain more information about the chemistry of Ln-in-crypt complexes in general, reactions of lanthanide triflates with crypt were investigated. This Chapter describes the fact that lanthanide triflates, $Ln^{III}(OTf)_3$, of Ln = Nd and Sm form isolable Ln(III)-in-crypt complexes that are soluble in THF, a solvent commonly used for KC_8 and alkali metal reductions. Reduction of these Sm(III) and Nd(III) complexes using KC_8 demonstrates that chemical transformations of Ln(III)-in-crypt to Ln(II)-in-crypt are possible with crystallographically-characterized precursors and products. Moreover, this provided the first example of the Nd(II) ion encapsulated in a

cryptand ligand. Sm and Nd were chosen since reduction of $4f^5$ Sm(III) forms the traditional $4f^6$ Sm(II) ion, whereas $4f^3$ Nd(III) can be reduced to Nd(II) with either the traditional $4f^4$ electron configuration or with a non-traditional $4f^35d^1$ configuration, *i.e.* Nd(II) is a configurational crossover ion. In addition to reporting the isolation of a Nd(II)-in-crypt complex, the electrochemical characterization of this highly reducing Nd(II) species is described. Only one other report of Nd(III)/Nd(II) electrochemistry was previously ~~is~~ published in the literature.[17]

Results and Discussion

$[Ln^{III}(crypt)(OTf)_2][OTf]$, 1-Ln. Addition of THF suspensions of lanthanide triflates, $Ln^{III}(OTf)_3$ (Ln = Nd, Sm), to THF solutions of 2.2.2-cryptand (crypt) generate clear and colorless solutions. Crystallization of these solutions at –35 °C yields THF-soluble products with two triflate ligands coordinated to the Ln(III)-in-crypt, and one outer-sphere triflate,$[Ln(crypt)(OTf)_2][OTf]$, **1-Ln**, eq 2.2, identified by single crystal X-ray diffraction, Figure 2.1.

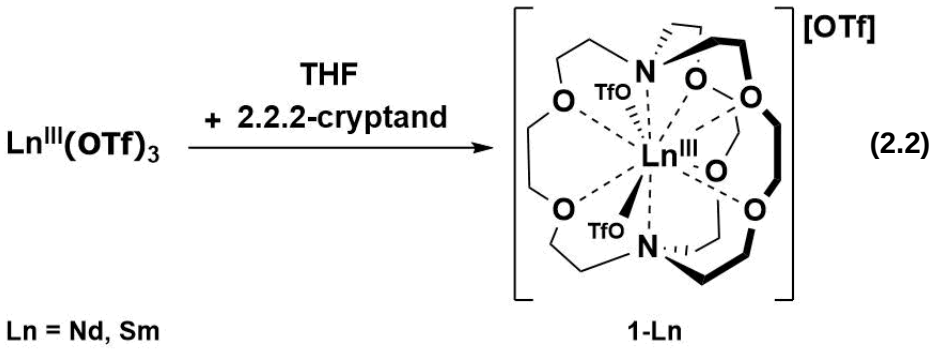

(2.2)

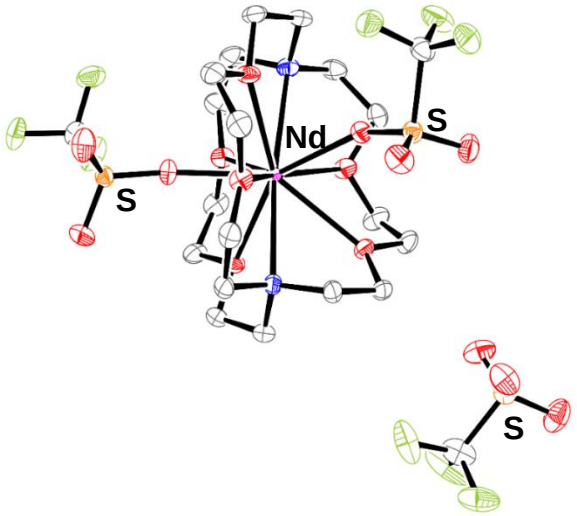

Figure 2.1. ORTEP representation of [Nd(crypt)$(OTf)_2$][OTf], **1-Nd**, with thermal ellipsoids drawn at the 50% probability level. Hydrogen atoms were omitted for clarity. **1-Sm** is isomorphous with **1-Nd**.

Cyclic Voltammetry. Although obtaining reproducible electrochemical data on lanthanide complexes has historically been challenging, electrochemical analysis of the Ln(III)-in-crypt complexes was performed in order to determine the Ln(III)/Ln(II) (Ln = Nd, Sm) reduction potentials. The cyclic voltammograms of these complexes were obtained in a THF solution containing 50 mM $[Bu_4N][OTf]$ as the supporting electrolyte, Figure 2.2. The cyclic voltammogram of [Nd(crypt)$(OTf)_2$][OTf] , **1-Nd**, showed a reduction feature at E_{pc} = –3.45 V and a related oxidation feature at E_{pa} = –2.89 V with a wave separation of 540 mV. These features are centered at E = –3.16 V *versus* $Fc^{+/0}$. In comparison, the cyclic voltammogram of **1-Sm**, showed a reduction feature at E_{pc} = –2.13 V and a related oxidation feature at E_{pa} = –1.57 V with a wave separation of 560 mV. These features are centered at E = –1.85 V *versus* $Fc^{+/0}$. The latter

result is similar to the quasi-reversible reduction potential of –1.66 V *versus* $Fc^{+/0}$ reported for "[Sm(crypt)](OTf)$_3$]" using [Pr_4N][$BAr^F{}_4$] as the supporting electrolyte.[18]

It was uncertain if electrochemical data could be obtained on **1-Nd** because a much more negative value would be expected for Nd versus Sm. Estimates of reduction potentials based on thermochemical and spectroscopic data by Morss were a –2.6 V vs SHE potential for Nd(III)/Nd(II) versus –1.55 V vs SHE for Sm.[19] Hence it was exciting that a cyclic voltammogram of [Nd(crypt)(OTf)$_2$][OTf] could be obtained. The more negative value for Nd versus Sm is consistent with the Morss calculations.[19]

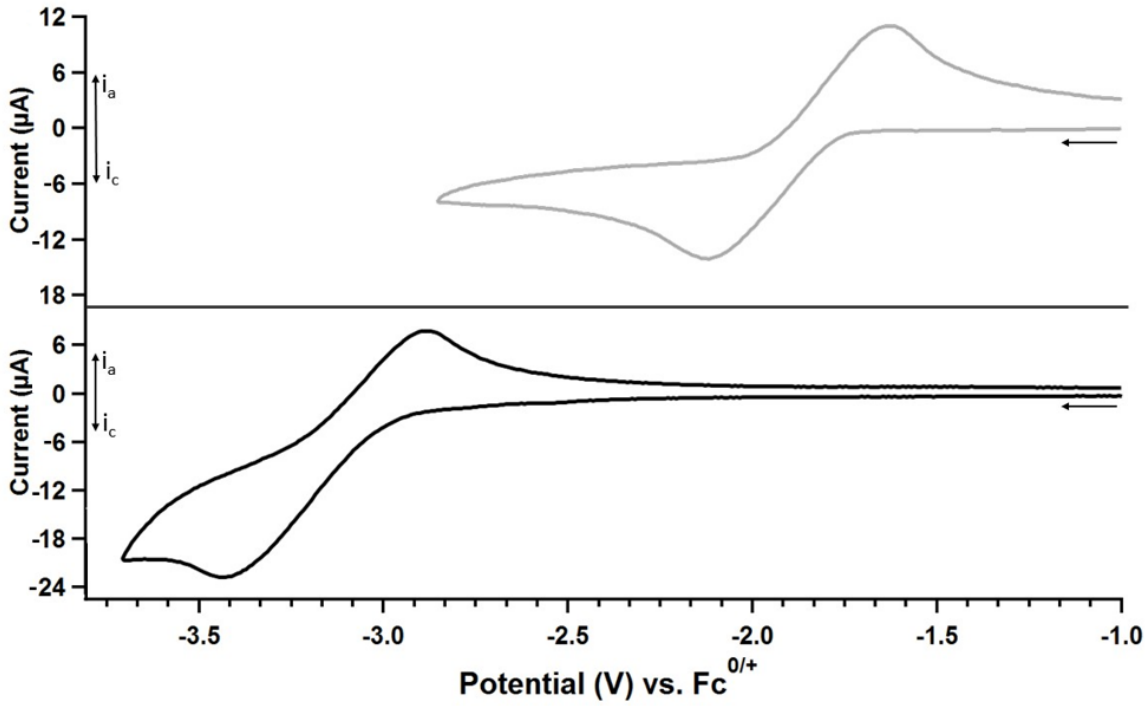

Figure 2.2. **1-Nd** (black, bottom) and **1-Sm** (gray, top) Ln(III)/Ln(II) redox couples in 50 mM [Bu_4N][OTf] THF solution at 25 °C with a scan rate of 200 mV/s using a glassy carbon working electrode, a platinum wire counter electrode, and a silver wire pseudo-reference electrode.

Isolation of [Ln^{II}(crypt)(OTf)$_2$], 2-Ln. The Ln(III)-in-crypt complexes, [Ln(crypt)(OTf)$_2$][OTf] (Ln = Sm, Nd), **1-Ln**, were chemically reduced to form the neutral Ln(II)-in-crypt complexes [Ln(crypt)(OTf)$_2$], **2-Ln**, eq 1.3. A THF solution of **1-Ln** was added to KC_8 to form a red solution in the case of Sm and a dark blue solution in the case of Nd. The reduction products, **2-Ln**, were crystallographically-characterized and the Ln metal center was found to retain both inner-sphere triflate ligands, Figure 1.3.

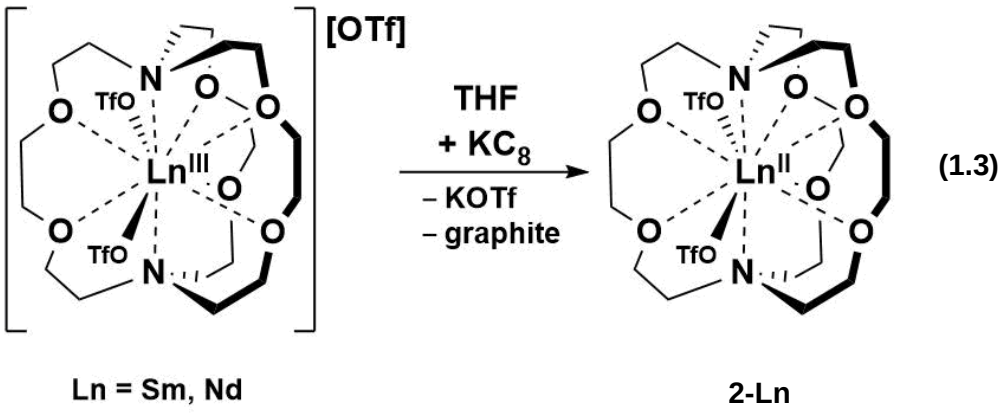

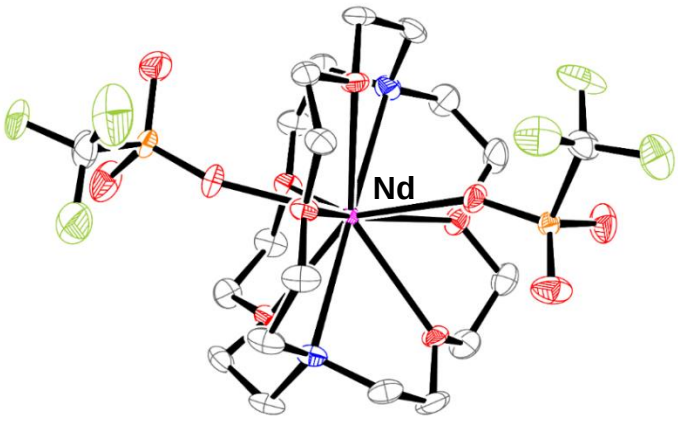

Figure 2.3. ORTEP representation of [Nd(crypt)(OTf)$_2$], **2-Nd**, with thermal ellipsoids drawn at the 50% probability level. Hydrogen atoms and disorder of a coordinated triflate were omitted for clarity. **2-Sm** is isomorphous with **2-Nd**.

Structural Details of $[Ln^{III}(crypt)(OTf)_2][OTf]$. The M(III)–O(crypt) and M(III)–N(crypt) bond distances of the **1-Ln** (Ln= Nd, Sm) complexes are similar to other reported rare-earth cryptate complexes.[5-15] In these complexes, the metal is encapsulated by crypt with two inner-sphere triflates and one outer-sphere triflate. The geometry of these rare-earth complexes is a 10-coordinate tetra-capped trigonal prism with the nitrogen donors capping both trigonal faces and the triflate oxygens capping two of the rectangular faces. This geometry has been reported for other Ln-in-crypt complexes, $[Ln^{II}(crypt)(DMF)_2][X]_2$ (Ln= Sm, Eu; X= I, BPh_4),[8] $[La^{III}(crypt)(OH_2)(Cl)][Cl]_2$,[8] $[La^{III}(crypt)(DMF)(OTf)][OTf]_2$,[15] and $[La(crypt)^{III}Cl_2][Cl]$.[15]

Table 2.1. Selected bond distances (Å) of $[Ln^{III}(crypt)(OTf)_2][OTf]$, **1-Ln**.

	Ln–O(crypt)	**Ln–N(crypt)**	**Ln–OTf**
1-Nd	2.551(2)-2.652(4)	2.769(4)-2.803(4)	2.413(3)-2.452(3)
1-Sm	2.522(2)-2.644(3)	2.755(4)-2.785(4)	2.381(3)-2.419(3)

Structural Details of $[Ln^{II}(crypt)(OTf)_2]$, 2-Ln. The structures of **2-Nd and 2-Sm** are isomorphous and have the 10-coordinate tetra-capped trigonal prism geometry as found for the Ln(III)-in-crypt complexes. The average Nd–O(crypt) bond distance of $[Nd^{II}(crypt)(OTf)_2]$ is 0.137 Å longer the average Nd–O(crypt) bond distance in $[Nd^{III}(crypt)(OTf)_2][OTf]$. The average Sm–O(crypt) bond distance in $[Sm^{II}(crypt)(OTf)_2]$ is 0.141 Å longer than the average Sm–O(crypt) bond distance in $[Sm^{II}(crypt)(OTf)_2][OTf]$, Table 2.2. Similarly, the average Nd–N(crypt) and Sm–N(crypt) bond distances are 0.129 and 0.142 Å longer than their Ln(III)-in-crypt counterparts. The Nd–OTf and Sm–OTf bond distances are 0.184 Å longer than their Ln(III)-in-crypt counterparts. These large differences in bond distances are consistent with $4f^{n+1}$ instead of $4f^n5d^1$

electron configurations.[20] Complexes of the $4f^n5d^1$ Ln(II) ions typically have distances 0.02-0.06 Å larger than their Ln(III) analogs.

Table 2.2. Difference in bond distances (Å) between **1-Nd** and **2-Nd** and between **1-Sm** and **2-Sm.**

	Ln–O(crypt)		Ln–N(crypt)		Ln–OTf	
	Average	**Difference**	**Average**	**Difference**	**Average**	**Difference**
1-Nd/2-Nd	2.62(3)/2.75(2)	0.137	2.79(2)/2.916(7)	0.129	2.43(2)/2.617(2)	0.184
1-Sm/2-Sm	2.60(4)/2.74(2)	0.141	2.77(2)/2.913(7)	0.142	2.40(2)/2.59(2)	0.184

UV-Visible Spectra. The UV-vis spectra of **2-Nd** and **2-Sm** are shown in Figure 1.4 with their simulations calculated from $[Nd(crypt)]^{2+}$ and $[Sm(crypt)]^{2+}$ by Samuel Bekoe and Saswata Roy in the group of Professor Filipp Furche. Consistent with the $4f^4$ assignment from the DFT calculations provided from the Furche group, the experimental extinction coefficients of **2-Nd** are low (< 1000 M^{-1} cm^{-1}). For comparison, the extinction coefficients of reported Nd(II) complexes with assigned $4f^35d^1$ electron configurations range from 4700 to as high as 5800 M^{-1} cm^{-1}.[20,21] In contrast, the extinction coefficients reported for $NdI_2(DME)_3$, a complex with an assigned $4f^4$ electron configuration, are much lower, with a maximum value of 420 M^{-1} cm^{-1}.[22] The **2-Sm** complex also has extinction coefficents less than 1000 M^{-1} cm^{-1} which is consistent with a $4f^6$ electron configuration.

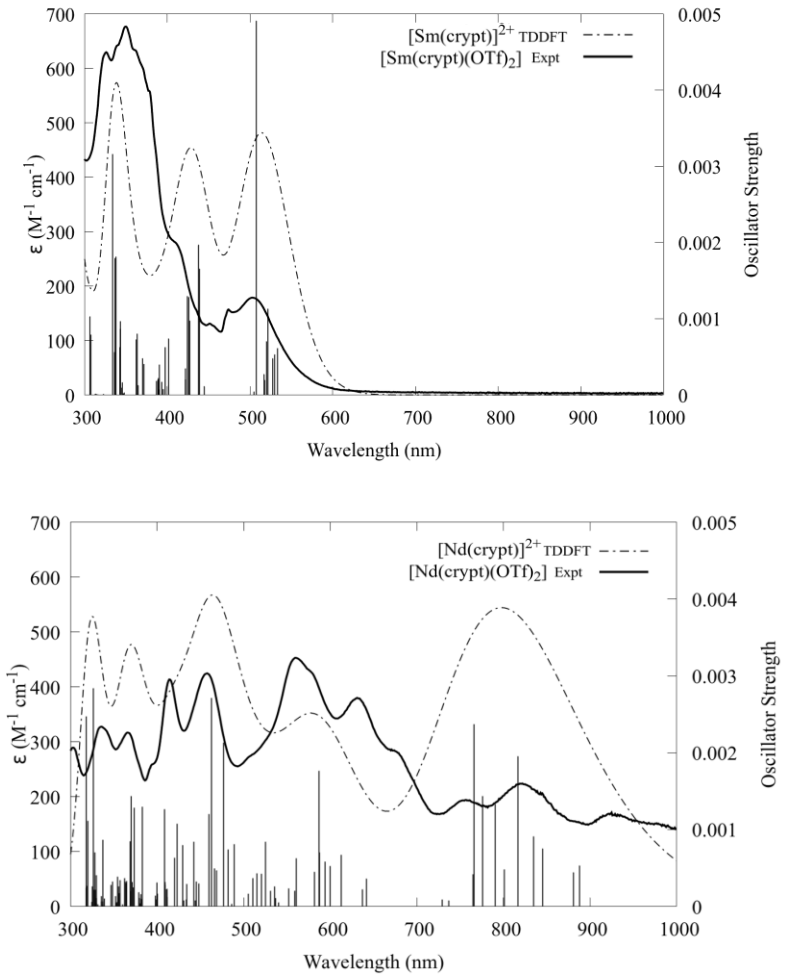

Figure 2.4. Observed UV-vis spectrum of [Sm(crypt)$(OTf)_2$], **2-Sm** (solid, top), in THF (7 mM) and calculated spectrum of $[Sm(crypt)]^{2+}$ spectrum (dash, top). Observed UV-vis spectrum of [Nd(crypt)$(OTf)_2$, **2-Nd** (solid, bottom) in THF (5 mM) and calculated spectrum of $[Nd(crypt)\}^{2+}$ (dash, bottom).

Conclusion

The isolation of *THF-soluble* Ln(III)-in-crypt complexes, $[Ln^{III}(crypt)(OTf)_2][OTf]$, **1-Ln**, (Ln = Nd, Sm; crypt = 2.2.2-cryptand; OTf = SO_3CF_3) by adding crypt to lanthanide triflate precursors allows the KC_8 reduction chemistry of these species to be investigated. These Ln(III)-in-crypt precursors can be chemically reduced using KC_8 to form the neutral complexes

[Ln^{II}(crypt)$(OTf)_2$], **2-Ln**, thereby demonstrating chemical reduction of crystallographically-characterizable Ln(III)-in-crypt precursors to crystallographically-characterizable Ln(II)-in-crypt complexes is possible. Moreover, this provided the first example of a Nd(II) ion sequestered in a cryptand ligand. The only other Ln(II)-in-cryptand complexes involved just Eu, Yb, and Sm. For both Nd and Sm, the crypt ligand preferentially retains the lanthanide metal and is not displaced by potassium upon reduction. The electrochemical data on the Ln(III)/Ln(II) redox couples of **1-Sm** and **1-Nd** suggest that the Ln(III) ions in these Ln(III)-in-crypt complexes are not substantially easier to reduce than in other ligand environments, but the crypt environment did provide a rare example of a Nd(III)/Nd(II) couple. Interestingly the crypt ligand environment enforces a traditional electron configuration, $4f^4$, rather than a non-traditional electron configuration, $4f^35d^1$, for Nd. While the $4f^35d^1$ Nd(II) complexes have trigonal symmetry that allows a $5d_z^2$ orbital to be comparable in energy to the 4f orbitals, the 10-coordinate crypt ligand environment does not split the 5d shell strongly enough to make 5d orbitals accessible.

Experimental

All manipulations and syntheses described below were conducted with the rigorous exclusion of air and water using standard glovebox and high-vacuum line techniques under an argon atmosphere. Solvents were sparged with UHP argon and dried by passage through columns containing Q-5 and molecular sieves prior to use. Deuterated tetrahydrofuran (THF-d_8) was dried over NaK alloy, degassed by three freeze-pump-thaw cycles, and vacuum transferred before use. ^{1}H NMR spectra were recorded on GN500, or CRYO500 MHz spectrometers at 298 K unless otherwise stated and referenced internally to residual protio-solvent resonances. $Ln(OTf)_3$ (Ln= Nd, Sm, Tm) (Fischer Scientific) were dried under high vacuum (10^{-5} Torr) for 48 h at 220 °C before use. 2.2.2-Cryptand (4,7,13,16,21,24-hexaoxa-1,10-diazabicyclo[8.8.8]hexacosane,

Aldrich) was placed under vacuum (1 x 10^{-3} Torr) for 12 h before use. Infrared spectra were recorded as compressed solids on an Agilent Cary 630 ATR-FTIR. Elemental analyses were conducted on a PerkinElmer 2400 Series II CHNS elemental analyzer. Electrochemical measurements were recorded using a glassy carbon working electrode, a Pt counter electrode, and a Ag wire pseudo-reference electrode with a Princeton Applied Research PARSTAT 2273 Advanced Electrochemical System. UV-Visible spectra were collected in THF using a Varian Cary 50 scan UV/Vis spectrophotometer.

[Sm(crypt)(OTf)$_2$][OTf], 1-Sm. A solution of crypt (32 mg, 0.08 mmol) in 5mL of THF was added to a stirred suspension of Sm(OTf)$_3$ (50 mg, 0.08 mmol) in 10 mL of THF. The solution was left to stir overnight and went from a cloudy suspension to a clear solution. After 24 h, the solution was concentrated to 1 mL and placed in the freezer at –25 °C. After 1d, colorless crystals of **1-Sm** suitable for X-ray crystallography were obtained (62 mg, 80%). ^{1}H NMR (THF-d_8): δ 3.01, 3.37, 3.93. IR (cm^{-1}): 2905w, 1462w, 1358w, 1313m, 1263m, 1234m, 1206s, 1157m, 1105m, 1072s, 1019s, 961m, 838w, 754w. Anal. Calcd for $C_{21}H_{36}F_9N_2O_{15}Sm$ (MW 974.04): C, 25.90; H, 3.73; N, 2.88. Found: C, 26.09; H, 4.01; N, 2.63.

[Nd(crypt)(OTf)$_2$][OTf], 1-Nd. A solution of crypt (32 mg, 0.08 mmol) in 5 mL of THF was added to a stirred suspension of Nd(OTf)$_3$ (50 mg, 0.08 mmol) in 10 mL of THF. After 24 h, the solution was concentrated to 1 mL and placed in the freezer at −25 °C. After 1d, colorless crystals of **1-Nd** suitable for X-ray crystallography were obtained (60 mg, 71%). IR (cm^{-1}): 2906w, 1458w, 1357w, 1314m, 1263m, 1234m, 1207s, 1154m, 1105m, 1073s, 1020s, 960m, 837w, 756w. Anal. Cacld for $C_{21}H_{36}F_9N_2O_{15}Nd$ (MW 967.93): C, 26.06; H, 3.75; N, 2.89. Found: C, 25.68; H, 3.62; N, 2.68. `

[Sm(crypt)(OTf)$_2$], 2-Sm. In an argon filled glovebox, a colorless THF (5 mL) solution of **1-Sm** (60 mg, 0.06) chilled to –25 °C was added to a vial of KC_8 (12 mg, 0.09 mmol) chilled to –35 °C. The reaction mixture became red and was stirred for 1 min. The red mixture was filtered to remove graphite and afforded a red solution. The solution was then placed in the freezer at –35 °C. After 3 days, red crystals of **2-Sm** suitable for X-ray crystallography were obtained (21 mg, 43%). ^{1}H NMR (THF-d_8): δ 1.65, 3.14, 3.42. IR (cm^{-1}): 2878w, 1482w, 1447w, 1358w, 1284s, 1245m, 1149m, 1089m, 1031s, 953m, 832w, 756w. UV-vis (THF) λ_{max} nm (ε, M^{-1}cm^{-1}): 289 (450), 326 (630), 350 (680), 412 (270), 452 (130), 474 (160), and 504 (180). Anal. Calcd for $C_{20}H_{36}F_6N_2O_{12}S_2Sm$: C, 29.12; H, 4.40; N, 3.40. Found: C, 29.22; H, 4.51; N, 3.25.

[Nd(crypt)(OTf)$_2$], 2-Nd. As described for **2-Sm**, a colorless THF (5 mL) solution of **1-Nd** (60 mg, 0.06 mmol) was added to a vial of KC_8 (12 mg, 0.09 mmol) forming a black mixture. The black mixture was filtered to remove graphite and afforded a dark blue solution which was layered into Et_2O and placed into a –35 °C freezer. After 1 d, black crystals of **2-Nd** suitable for X-ray crystallography were obtained 1(0 mg, 20%). IR (cm^{-1}): 2889w, 1476w, 1355w, 1264w. 1224w, 1151m, 1106m, 1030s, 950w, 830w, 751w. UV-vis (THF) λ_{max} nm (ε, M^{-1}cm^{-1}): 285 (210), 304 (230), 335 (260), 366 (250), 393 (200), 414 (330), 458 (340), 560 (360), 581 (340), 632 (300), 677 (230), 754 (150), 820 (180), and 925 (140). Anal. Calcd for $C_{20}H_{36}F_6N_2O_{12}S_2Nd$: C, 29.33; H, 4.43; N, 3.42. Found: C, 29.51; H, 4.25; N, 3.34.

References

1. Yee, E. L.; Gansow, O. A.; Weaver, M. J., Electrochemical studies of europium and ytterbium cryptate formation in aqueous solution. Effects of varying the metal oxidation state upon cryptate thermodynamics and kinetics. *J. Am. Chem. Soc.* **1980,** *102* (7), 2278-2285.

2. Gamage, N.-D. H.; Mei, Y.; Garcia, J.; Allen, M. J., Oxidatively Stable, Aqueous Europium(II) Complexes through Steric and Electronic Manipulation of Cryptand Coordination Chemistry. *Angew. Chem. Int. Ed.* **2010,** *49* (47), 8923-8925.

3. Dietrich, B.; Lehn, J. M.; Sauvage, J. P.; Blanzat, J., Cryptates—X: Syntheses et proprietes physiques de systemes diaza-polyoxa-macrobicycliques. *Tetrahedron.* **1973**, *29* (11), 1629-1645.

4. Dietrich, B.; Lehn, J. M.; Sauvage, J. P., Cryptates—XI: Complexes macrobicycliques, formation, structure, proprietes. *Tetrahedron.* **1973**, *29* (11), 1647-1658.

5. Burns, J. H., Crystal and molecular structure of a cryptate complex of samarium: $C_{18}H_{36}O_6N_2Sm_2(NO_3)_6 \cdot H_2O$. *Inorg. Chem.* **1979,** *18* (11), 3044-3047.

6. Benetollo, F.; Bombieri, G.; Cassol, A.; De Paoli, G.; Legendziewicz, J., Coordination chemistry of lanthanides with cryptands. An X-ray and spectroscopic study of the complex $Nd_2(NO_3)_6$ $[C_{18}H_{36}O_6N_2] \cdot H_2O$. *Inorg. Chem. Acta*. **1985,** *110* (1), 7-13.

7. Yang, G.; Liu, S.; Jin, Z., Coordination chemistry and structure characterization of $C_{18}H_{36}O_6N_2Eu_2(NO_3)_6 \cdot H_2O$. *Inorg. Chem. Acta.* **1987,** *131* (1), 125-128.

8. Mao, J.; Jin, Z., Synthesis and structure characterization of lanthanum [2,2,2]cryptates, $[LaCl[2,2,2](H_2O)]Cl_2 \cdot H_2O$ and $[La(CF_3SO_3)[2,2,2](DMF)](CF_3SO_3)_2$. *Polyhedron.* **1994,** *13* (2), 319-323.

9. Gamage, N.-D. H.; Mei, Y.; Garcia, J.; Allen, M. J., Oxidatively Stable, Aqueous Europium(II) Complexes through Steric and Electronic Manipulation of Cryptand Coordination Chemistry. *Angew. Chem. Int. Ed.* **2010,** *49* (47), 8923-8925.

10. Lenora, C. U.; Carniato, F.; Shen, Y.; Latif, Z.; Haacke, E. M.; Martin, P. D.; Botta, M.; Allen, M. J., Structural Features of Europium(II)-Containing Cryptates That Influence Relaxivity. *Chem. Eur. J.* **2017,** *23* (61), 15404-15414.

11. Ekanger, L. A.; Polin, L. A.; Shen, Y.; Haacke, E. M.; Martin, P. D.; Allen, M. J., A EuII-Containing Cryptate as a Redox Sensor in Magnetic Resonance Imaging of Living Tissue. *Angew. Chem. Int. Ed.* **2015,** *54* (48), 14398-14401.

12. Huh, D. N.; Ziller, J. W.; Evans, W. J., Facile Encapsulation of Ln(II) Ions into Cryptate Complexes from $LnI_2(THF)_2$ Precursors (Ln = Sm, Eu, Yb). *Inorg. Chem.* **2019,** *58* (15), 9613-9617.

13. Huh, D. N.; Kotyk, C. M.; Gembicky, M.; Rheingold, A. L.; Ziller, J. W.; Evans, W. J., Synthesis of rare-earth-metal-in-cryptand dications, $[Ln(2.2.2\text{-cryptand})]^{2+}$, from Sm^{2+}, Eu^{2+}, and Yb^{2+} silyl metallocenes $(C_5H_4SiMe_3)_2Ln(THF)_2$. *Chem. Commun.* **2017,** *53* (62), 8664-8666.

14. T. C. Jenks, A. N. W. Kuda-Wedagedara, M. D. Bailey, C. L. Ward, M. J. Allen. Specroscopic and electrochemical trends in divalent lanthanides through modulation of coordination environment. *Inorg. Chem.* **2020**, *59*, 2613-2620.

15. Huh, D. N.; Windorff, C. J.; Ziller, J. W.; Evans, W. J., Synthesis of uranium-in-cryptand complexes. *Chem. Commun.* **2018,** *54* (73), 10272-10275.

16. Paul, R. C. A., B. N.; Kapoor, R., Preparation & Characterization of Alkali Metal Dimethylformamidyls. *Indian J. Chem.* **1975,** *13*, 1338-1340

17. Halter, D. P., Palumbo, C. T., Ziller, J. W., Gembicky, M., Rheingold, A. L., Evans, W. J., Meyer, K. Electrocatalytic H_2O Reduction with f-Elements: Mechanistic Insight and Overpotential Tuning in a Series of Lanthanide Complexes *J. Am. Chem. Soc.* **2018,** *140*, 2587-2594.

18. Marsh, M. L.; White, F. D.; Meeker, D. S.; McKinley, C. D.; Dan, D.; Van Alstine, C.; Poe, T. N.; Gray, D. L.; Hobart, D. E.; Albrecht-Schmitt, T. E., Electrochemical Studies of Selected Lanthanide and Californium Cryptates. *Inorg. Chem.* **2019,** *58* (15), 9602-9612.

19. Morss, L. R., Thermochemical properties of yttrium, lanthanum, and the lanthanide elements and ions. *Chem. Rev.* **1976,** *76* (6), 827-841.

20. Fieser, M. E.; MacDonald, M. R.; Krull, B. T.; Bates, J. E.; Ziller, J. W.; Furche, F.; Evans, W. J., Structural, Spectroscopic, and Theoretical Comparison of Traditional vs Recently Discovered Ln^{2+} Ions in the $[K(2.2.2\text{-cryptand})][(C_5H_4SiMe_3)_3Ln]$ Complexes: The Variable Nature of Dy^{2+} and Nd^{2+}. *J. Am. Chem. Soc.* **2015,** *137* (1), 369-382.

21. Jenkins, T. F.; Woen, D. H.; Mohanam, L. N.; Ziller, J. W.; Furche, F.; Evans, W. J., Tetramethylcyclopentadienyl Ligands Allow Isolation of Ln(II) Ions across the Lanthanide Series in $[K(2.2.2\text{-cryptand})][(C_5Me_4H)3Ln]$ Complexes. *Organometal.* **2018**, *37* (21), 3863-3873.

22. Bochkarev, M. N.; Fagin, A. A., A New Route to Neodymium(II) and Dysprosium(II) Iodides. *Chem. Eur. J.* **1999**, *5*, 2990-2992.

Chapter 3

Early Lanthanide Metals and Dy-in-crypt Complexes

Introduction

As described in Chapter 2, only a few complexes with Ln(II) ions in 2.2.2-cryptand (crypt) were known even 30 years after the first Ln(III)-in-crypt complex was reported.[1-13] Initially, these Ln(II)-in-crypt complexes were synthesized using Ln(II) precursors of the most stable Ln(II) ions, Sm, Eu, and Yb, and were not obtained through chemical reduction. In contrast, the Ln(II)-in-crypt complexes for Ln = Sm and Nd in Chapter 2 required the development of THF-soluble Ln(III)-in-crypt complexes involving the use of triflates as ligands, utilizing $Ln(OTf)_3$ complexes as precursors, equations 3.1 and 3.2.

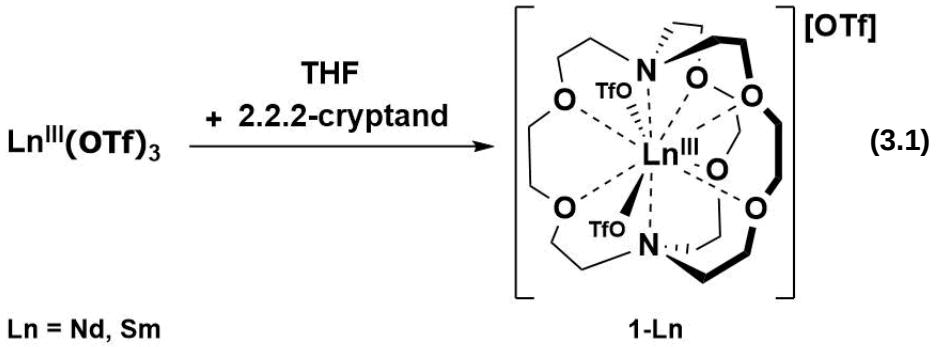

(3.1)

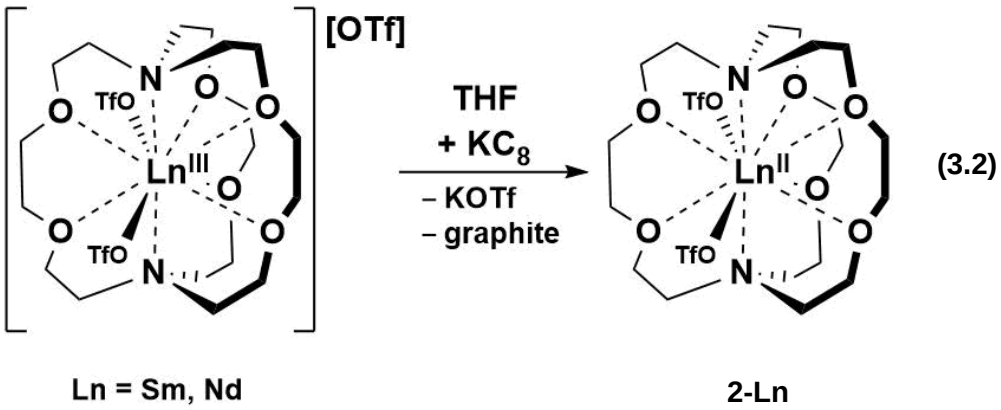

(3.2)

One reason these Ln-in-crypt complexes are of interest is because of the coordination environment. As part of the discovery that Ln(II) ions can be obtained for all the Ln metals, except Pm due to radioactivity,[14-19] it was found that the new ions beyond the traditional Eu, Yb, Sm, Tm. Dy and Nd metals with $4f^{n+1}$ electron configurations could adopt an unexpected non-traditional electron configuration, $4f^n5d^1$. In the trigonal tris(cyclopentadienyl) coordination environments of the new Ln(II) ions, apparently the $5d_z^2$ orbital was comparable in energy to the 4f orbitals. The crypt ligand provides a more spherical ligand environment compared to the trigonal environments.

In Chapter 2, it is reported that the Nd(II)-in-crypt complex, a configuration cross-over ion which can either adopt a $4f^4$ or $4f^35d^1$ electron configuration, adopts the traditional electron configuration $4f^4$. This may be due to the more spherical environment which would not allow the d_z^2 to be comparable in energy to the 4f orbitals. Thus, it was desired to see if the coordination environment could push the barrier for configurational crossover ions to metals other than Dy as had been observed for C_5Me_4H versus $C_5H_4SiMe_3$.[14, 20]

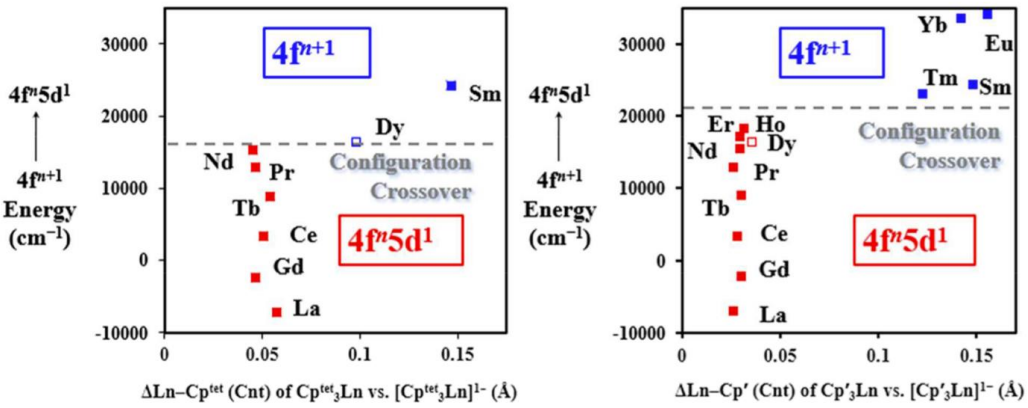

Figure 3.1. Configuration crossover ions depend on the ligand set. (Left) For the Cp^{tet} ligand, a crossover plot shows that Dy adopts a traditional electron configuration of $4f^{n+1}$. (Right)

For the Cp′ ligand, a crossover plot shows that Dy adopts a non-traditional electron configuration of $4f^n5d^1$.

In this Chapter, the syntheses of additional Ln(III)-in-crypt complexes using $Ln(OTf)_3$ as precursors are described along with the attempts to reduce them to the Ln(II)-in-crypt counterpart. By examining a range of metals including the largest lanthanide La, to a smaller lanthanide Dy, there was an attempt to understand the capacity of crypt to support low oxidation states for lanthanide metals as well as its influence on electronic configuration.

In the search for more soluble Ln-in-crypt complexes, La(III), Ce(III), Pr(III), and Dy(III) complexes were isolated in addition to the Sm(III)-in-crypt and Nd(III)-in-crypt complexes described in Chapter 2. In comparison to the Sm(III) and Nd(III) complexes discussed in Chapter 2, reduction of these complexes did not result in any isolable Ln(II) complexes. Attempts to reduce Dy(III) only resulted in isolation of K(crypt)(OTf) salts.

Results and Discussion

$[Ln^{III}(crypt)(OTf)_2][OTf]$, 1-Ln. Addition of THF suspensions of lanthanide triflates, $Ln^{III}(OTf)_3$ (Ln = La, Ce, Nd, Sm), to THF solutions of crypt generate colorless solutions. Crystallizations of these solutions from THF at –35 °C yield products with two triflate ligands coordinated to the Ln(III)-in-crypt and one outer-sphere triflate, $[Ln(crypt)(OTf)_2][OTf]$, **1-Ln**, eq 3.1. Structures were solved by X-ray diffraction for La, Ce, Nd, and Sm complexes, Figure 3.1. Importantly, these new complexes were THF soluble. As described in Chapter 2, THF solubility is important for alkali metal reductions of Ln(III) to Ln(II) complexes that cannot be carried out in more polar organic solvents such as acetonitrile or DMF.[21]

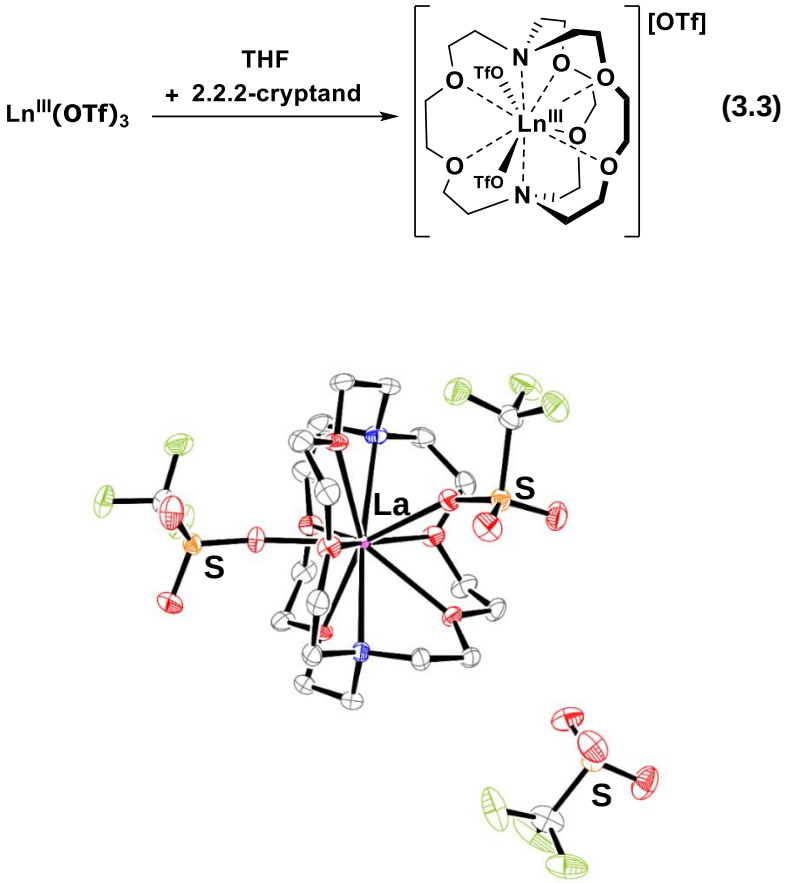

Figure 3.2. ORTEP representation of [Nd(crypt)$(OTf)_2$][OTf], **1-La**, thermal ellipsoids drawn at the 50% probability level. Hydrogen atoms were omitted for clarity. **1-La** and **1-Ce** are isomorphous.

[**Ln(crypt)(OH_2)(OTf)][OTf]$_2$, 2-Ln.** In some reactions of Pr and Nd triflates, a product other than **1-Ln** was isolated. With these two metals, the water adduct, [Ln(crypt)(OH_2)(OTf)][OTf]$_2$, **2-Ln**, was found by X-ray crystallography. Subsequent examination of the IR spectra of the starting triflates revealed O-H stretches which suggested that the water came from the starting material. A Pr(III)-in-crypt without an aqua ligand has yet to be crystallographically-characterized.

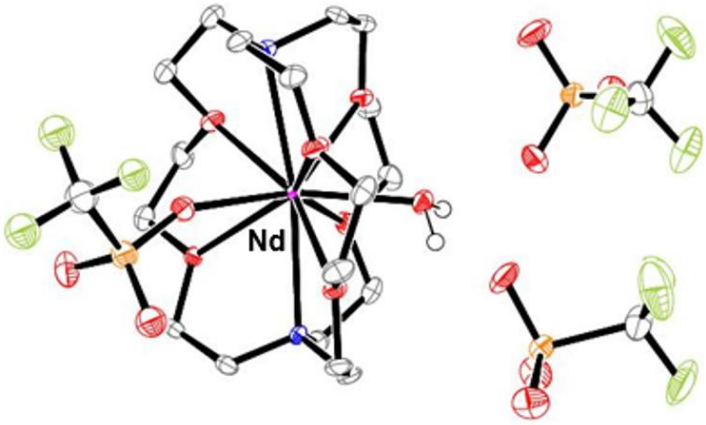

Figure 3.3. ORTEP representation of $[Nd(crypt)(OH_2)(OTf)][OTf]_2$, **3-Nd**, with thermal ellipsoids drawn at the 50% probability level. Hydrogen atoms were omitted for clarity. The structure of **3-Pr** is isomorphous.

Structural Details of $[Ln^{III}(crypt)(OTf)_2][Otf]$, 1-Ln Complexes. The M(III)–O(crypt) and M(III)–N(crypt) bond distances of the **1-Ln** (Ln= La, Ce, Nd, Sm) complexes in this Chapter are similar to previously reported rare-earth cryptate complexes.[2, 3, 5-13] In these complexes, the metal is encapsulated by crypt with two inner-sphere triflates and one outer-sphere triflate. The geometry of these rare-earth complexes is a 10-coordinate tetra-capped trigonal prism with the nitrogen donors capping both trigonal faces and the triflate oxygens capping two of the rectangular faces. This geometry has been previously reported for other Ln-in-crypt complexes, $[Ln^{II}(crypt)(DMF)_2][X]_2$ (Ln= Sm, Eu; X= I, BPh_4),[9] $[La^{III}(crypt)(OH_2)(Cl)][Cl]_2$,[12] $[La^{III}(crypt)(DMF)(OTf)][OTf]_2$,[12] and $[La(crypt)^{III}Cl_2][Cl]$.[8]

Table 3.1. Selected Bond Distances (Å) of $[Ln^{III}(crypt)(OTf)_2][OTf]$, **1-Ln**, and $[Ln^{III}(crypt)(OH_2)(OTf)][OTf]_2$, **2-Ln**.

	Ln–O(crypt)	Ln–N(crypt)	Ln–OTf	Ln–OH_2
1-La	2.600(2)-2.679(3)	2.084(3)-2.823(3)	2.473(3)-2.506(2)	
1-Ce	2.573(2)-2.671(3)	2.787(4)-2.815(3)	2.447(3)-2.485(3)	
3-Pr	2.582(2)-2.698(2)	2.792(2)-2.797(2)	2.463(2)	2.456(2)
1-Nd	2.551(2)-2.652(4)	2.769(4)-2.803(4)	2.413(3)-2.452(3)	
3-Nd	2.561(3)-2.690(3)	2.773(4)-2.784(4)	2.439(4)	2.439(3)
1-Sm	2.522(2)-2.644(3)	2.755(4)-2.785(4)	2.381(3)-2.419(3)	

Attempts to Reduce $[La(crypt)(OTf)_2][OTf]$ and $[Ce(crypt)(OTf)_2][OTf]$ Complexes. Upon reaction of $[La(crypt)(OTf)_2][OTf]$ and $[Ce(crypt)(OTf)_2][OTf]$ with KC_8 in THF at – 35 °C, no change in color was observed, in contrast to observations of color change from colorless to red and colorless to dark blue for Sm and Nd, respectively. Additionally, electrochemical studies showed no reduction nor oxidation events within the THF solvent window which spans from approximately – 3 V to 1 V vs. SCE.[22] This reductive window should be enough to capture at least a Ce redox wave as known Ce(IV/III) redox potentials have not been reported beyond the – 2 V to 1 V range in non-aqueous solvents.[23] Curiously, attempted reductions using what is presumed to be the $[Pr(crypt)(OTf)_2][OTf]$ resulted in a color change to pale blue that faded to pale green within minutes. Lower temperature reactions, at – 78 °C, of Pr-in-crypt with KC_8 were attempted as well. At this temperature, the blue color persisted but faded to the pale green once the cold well began to warm up. Another attempt was carried out in an M-tube, a modified H-tube with an extra side arm. The reduction was carried out at – 78 °C on a Schlenk line with the extra side arm filled with

Et_2O, Figure 3.3. However, this method was not successful and resulted in the same color change as before, from pale blue to pale green.

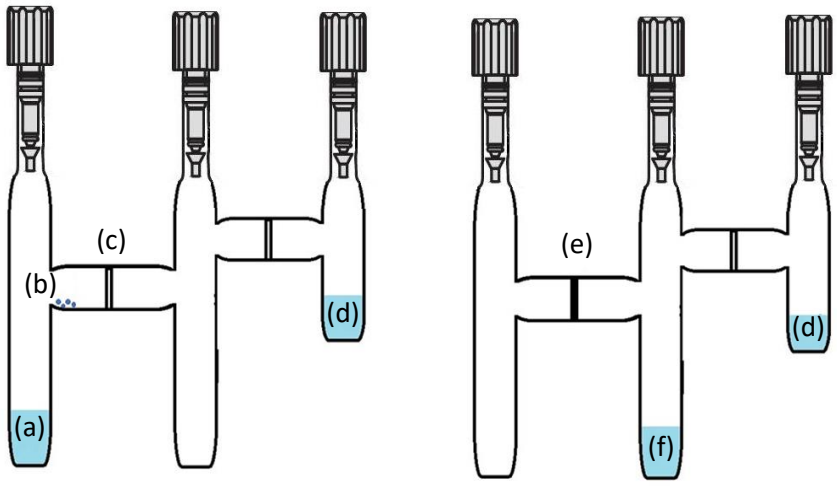

Figure 3.4. (1) M-tube apparatus before reduction. (a) A solution of $Pr(crypt)(OTf)_3$ in THF cooled to – 78 °C. (b). KC_8 is placed on the side to be tapped into the $Pr(crypt)(OTf)_3$ solution for reduction. (c) A frit for removal of reacted KC_8 for after reduction. (d) Et_2O to diffuse on the reduced THF solution. (2) M-tube apparatus after reduction. (e) Filtered graphite. (f) Reduced $Pr(crypt)(OTf)_3$ solution. (d) Et_2O to diffuse into reduced THF solution.

Electrochemical studies of the Pr-in-crypt complex were also attempted which resulted in the observation of a weak reduction wave close to the end of the solvent window at -3.9 V vs $Fc^{0/+}$, but nothing definitive to confidently assign as a Pr(III)/Pr(II) reduction event. However, this is promising as a Pr(III) to Pr(II) reduction as Pr is calculated to have a lower reduction potential[24] compared to Sm and Nd, which were reported as -2.13 V and -3,45 V, respectively.

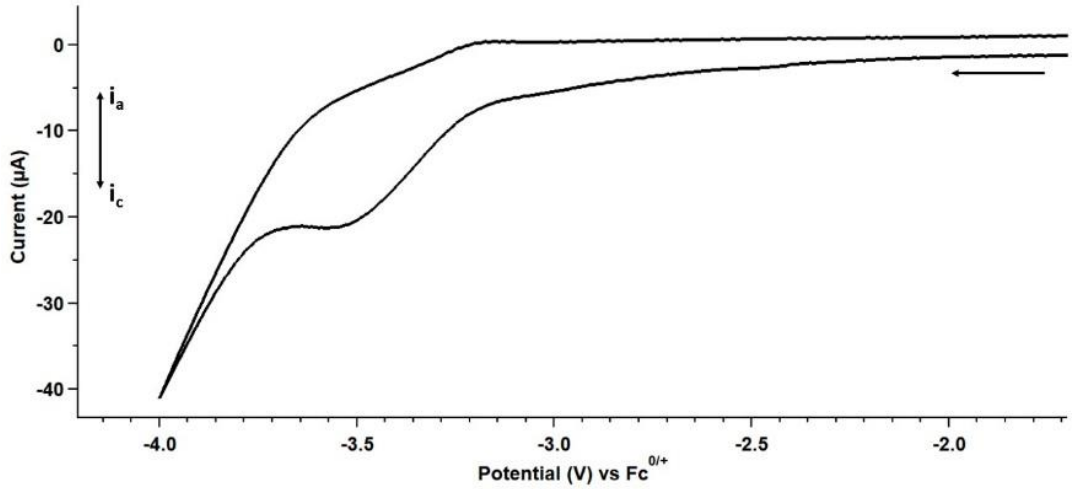

Figure 3.5. Voltammogram of the [Pr(crypt)$(OTf)_2$][OTf] complex in 50 mM [Bu_4N][OTf] in THF solution at 25 °C with a scan rate of 200 mV/s using a glassy carbon working electrode, a platinum wire counter electrode, and a silver wire pseudo-reference electrode.

Attempts to reduce a Dy(III)-in-crypt Triflate Complex. The results reported above are for the larger lanthanide metals with 8-coordinate Ln(III) radii of 1.16 – 1.079 Å.[25] These gave THF-soluble complexes. However, this was not the case for the smaller metal Dy, which has an 8-coordinate radius of 1.027 Å.[25] Reaction of $Dy(OTf)_3$ with crypt in THF resulted in a colorless solid that was not soluble. The complex, however, was soluble in MeCN. From crystallization in MeCN, it could be determined that this Dy(III) complex was structurally different from the early lanthanide metals, most likely due to the difference in ionic radius. Rather than a structure that has two triflate ligands bound to the metal center, only one triflate was bound to Dy with two outer-sphere triflate anions, [Dy(crypt)(OTf)][$OTf]_2$. It is believed that the reduced interaction with triflate ligands is what leads to the poor solubility of the late lanthanide metals in the cryptand coordination environment.

Reductions were attempted in MeCN using KC_8. Upon addition of KC_8 to a solution of $[Dy(crypt)(OTf)_2][OTf]$ in MeCN, no color change in solution was observed. However, the KC_8 changed in color from golden/copper to black suggesting it had reacted, but no Dy(II) was isolated. Attempts to reduce the THF-insoluble Dy complex in THF were also conducted, yet almost all reactions resulted in no color change and no isolation of X-ray quality crystals. In one attempt at a Birch reduction of the Dy complex, the reaction between $[Dy(crypt)(OTf)_2][OTf]$ and Na^0 in liquid ammonia resulted in a color change from colorless to dark blue. Dark blue solids were isolated after removing the liquid ammonia under vacuum over approximately 2 hours. The dark blue solids, which survived upon transfer to the glovebox, were dissolved in THF, and layered with Et_2O to yield blue crystals suitable for X-ray diffraction, but upon collection, it was determined that the crystal was only [Na(crypt)][OTf]. Other attempted Birch reductions yielded solids that were not soluble in DMF, MeCN, dichloromethane, and THF. This result leads to the assumption that alkali metals may displace the Dy ion in the cryptand pocket due to their preferability to bind to that coordination environment.[10, 11]

Conclusion

Although using triflates as a ligand for Ln-in-crypt complexes allowed for the synthesis and isolation of THF-soluble complexes, reductions of larger lanthanide metals, Ln = La, Ce and Pr, have not been successful. It has not yet been possible to find a way to get rare-earth metals in the +2 oxidation state encapsulated within the cryptand ligand, other than Eu, Sm Yb, and Nd. The 2.2.2-cryptand environment differs from the commonly used cyclopentadienyl ligand environment as it is more spherical. As described in Chapter 2, it is believed that cryptand does not allow the d_z^2 orbital to be comparable in energy to the *f*-orbitals due to its symmetry as the cyclopentadienyl ligands have been shown to do. This is a possible explanation as to why La and Ce could not be

isolated in the +2 oxidation, as their reduction potentials from the $4f^n$ to a $4f^{n+1}$ electron configuration has been calculated as too negative for isolation in common solvents.[24]

Experimental

All manipulations and syntheses described below were conducted with the rigorous exclusion of air and water using standard glovebox and high-vacuum line techniques under an argon atmosphere. Solvents were sparged with UHP argon and dried by passage through columns containing Q-5 and molecular sieves prior to use. Deuterated tetrahydrofuran (THF-d_8) was dried over NaK alloy, degassed by three freeze-pump-thaw cycles, and vacuum transferred before use. ^{1}H NMR spectra were recorded on GN500, or CRYO500 MHz spectrometers at 298 K unless otherwise stated and referenced internally to residual protio-solvent resonances. The $Ln(OTf)_3$ (Ln= Nd, Sm, Tm) precursors (Fischer Scientific) were dried under high vacuum (10^{-5} Torr) for 48 h at 220 °C before use. 2.2.2-Cryptand (4,7,13,16,21,24-hexaoxa-1,10-diazabicyclo[8.8.8]hexacosane, Aldrich) was placed under vacuum (1 x 10^{-3} Torr) for 12 h before use.

[La(crypt)$(OTf)_2$][OTf], 1-La. A solution of crypt (32 mg, 0.085 mmol) in 5 mL of THF was added to a stirred suspension of $La(OTf)_3$ (50 mg, 0.08 mmol) in 10 mL of THF. After 24 h, the solution was concentrated to 1 mL and placed in the freezer at −25 °C. After 1d, colorless crystals of **1-La** suitable for X-ray crystallography were obtained. ^{1}H NMR (THF-d_8): δ 3.02 (t, 12H), δ 4.08 (t, 12H), δ 4.13 (s, 12H).

[Ce(crypt)$(OTf)_2$][OTf], 1-Ce. As described for **1-La**, a solution of crypt (32 mg, 0.085 mmol) in 5 mL of THF was added to a stirred suspension of $Ce(OTf)_3$ (50 mg, 0.08 mmol) in 10 mL of THF. After 24 h, the solution was concentrated to 1 mL and placed in the freezer at −25 °C. After 1d, colorless crystals of **1-Ce** suitable for X-ray crystallography were obtained.

[Nd(crypt)(OH_2)(OTf)][$OTf]_2$, 2-Nd . A 5 mL THF solution of crypt (32 mg, 0.085 mmol) was added to a stirred suspension of $Nd(OTf)_3$ (50 mg, 0.08 mmol), that had an absorption in its IR spectrum at 3418 cm^{-1} suggesting the presence of water. After 24 h, the solution was concentrated to 1 mL and placed in the freezer at −25 °C. After 1d, colorless crystals of **2-Nd** suitable for X-ray crystallography were obtained.

[Pr(crypt)(OH_2)(OTf)][$OTf]_2$, 2-Pr. A 5 mL THF solution of crypt (32 mg, 0.085 mmol) was added to a stirred suspension of $Pr(OTf)_3$ (50 mg, 0.08 mmol) that had an absorption in its IR spectrum at 3421 cm^{-1} suggesting the presence of water. After 24 h, the solution was concentrated to 1 mL and placed in the freezer at −25 °C. After 1d, colorless crystals of **2-Pr** suitable for X-ray crystallography were obtained.

References

1. B. Dietrich, J. M. L., J. P. Sauvage and J. Blanzat Synthesis et Proprietes Physiques de Systemes Diaza-polyoxa-macrobicycliques. *Tetrahedron.* **1973,** *29*, 1629-1645.

2. Benetollo, F. B., G.; Cassol, A.; De Paoli, G.; Legendziewicz, J., Coordination chemistry of lanthanides with cryptands. An X-ray and spectroscopic study of the complex $Nd_2(NO_3)_6[C_{18}H_{36}O_6N_2]\cdot H_2O$. *Inorg. Chem. Acta.* **1985,** *110*, 7-13.

3. Burns, J. H., Crystal and molecular structure of a cryptate complex of samarium: $C_{18}H_{36}O_6N_2Sm_2(NO_3)_6\cdot H2O$. *Inorg. Chem.* **1979,** *18*, 3044-3047.

4. Dietrich, B. L., J. M.; Sauvage, J. P., Cryptates—XI: Complexes macrobicycliques, formation, structure, proprietes. *Tetrahedron.* **1973,** *29*, 1647-1658.

5. Ekanger, L. A.; Polin, L. A.; Shen, Y.; Haacke, E. M.; Martin, P. D.; Allen, M. J., A Eu(II)-Containing Cryptate as a Redox Sensor in Magnetic Resonance Imaging of Living Tissue. *Angew. Chem. Int. Ed.* **2015,** *54* (48), 14398-401.

6. Gamage, N. D.; Mei, Y.; Garcia, J.; Allen, M. J., Oxidatively stable, aqueous europium(II) complexes through steric and electronic manipulation of cryptand coordination chemistry. *Angew. Chem. Int. Ed.* **2010,** *49* (47), 8923-5.

7. Huh, D. N.; Kotyk, C. M.; Gembicky, M.; Rheingold, A. L.; Ziller, J. W.; Evans, W. J., Synthesis of rare-earth-metal-in-cryptand dications, $[Ln(2.2.2\text{-cryptand})]^{2+}$, from Sm^{2+}, Eu^{2+}, and Yb^{2+} silyl metallocenes $(C_5H_4SiMe_3)_2Ln(THF)_2$. *Chem. Commun.* **2017,** *53* (62), 8664-8666.

8. Huh, D. N.; Windorff, C. J.; Ziller, J. W.; Evans, W. J., Synthesis of uranium-in-cryptand complexes. *Chem Commun.* **2018,** *54* (73), 10272-10275.

9. Huh, D. N.; Ziller, J. W.; Evans, W. J., Facile Encapsulation of Ln(II) Ions into Cryptate Complexes from $LnI_2(THF)_2$ Precursors (Ln = Sm, Eu, Yb). *Inorg. Chem.* **2019,** *58* (15), 9613-9617.

10. Jenks, T. C.; Kuda-Wedagedara, A. N. W.; Bailey, M. D.; Ward, C. L.; Allen, M. J., Spectroscopic and Electrochemical Trends in Divalent Lanthanides through Modulation of Coordination Environment. *Inorg. Chem.* **2020,** *59* (4), 2613-2620.

11. Lenora, C. U.; Carniato, F.; Shen, Y.; Latif, Z.; Haacke, E. M.; Martin, P. D.; Botta, M.; Allen, M. J., Structural Features of Europium(II)-Containing Cryptates That Influence Relaxivity. *Chemistry* **2017,** *23* (61), 15404-15414.

12. Mao, J. J., Z., Synthesis and structure characterization of lanthanum [2,2,2]cryptates, [LaCl[2,2,2](H_2O)]Cl_2·H_2O and [La(CF_3SO_3)[2,2,2](DMF)](CF_3SO_3)$_2$. *Polyhedron* **1994,** *12*, 319-323.

13. Yang, G. L., S.; Jin, Z., Coordination chemistry and structure characterization of $C_{18}H_{36}O_6N_2Eu_2(NO_3)_6$·$H_2O$. *Inorg. Chem. Acta.* **1987,** *131*, 125-128.

14. Fieser, M. E.; MacDonald, M. R.; Krull, B. T.; Bates, J. E.; Ziller, J. W.; Furche, F.; Evans, W. J., Structural, spectroscopic, and theoretical comparison of traditional vs recently discovered Ln(2+) ions in the [K(2.2.2-cryptand)][($C_5H_4SiMe_3$)$_3$Ln] complexes: the variable nature of Dy(2+) and Nd(2+). *J Am Chem Soc* **2015,** *137* (1), 369-82.

15. Hitchcock, P. B.; Lappert, M. F.; Maron, L.; Protchenko, A. V., Lanthanum does form stable molecular compounds in the +2 oxidation state. *Angew Chem Int Ed Engl* **2008,** *47* (8), 1488-91.

16. MacDonald, M. R.; Bates, J. E.; Fieser, M. E.; Ziller, J. W.; Furche, F.; Evans, W. J., Expanding rare-earth oxidation state chemistry to molecular complexes of holmium(II) and erbium(II). *J. Am. Chem. Soc.* **2012,** *134* (20), 8420-3.

17. MacDonald, M. R.; Bates, J. E.; Ziller, J. W.; Furche, F.; Evans, W. J., Completing the series of +2 ions for the lanthanide elements: synthesis of molecular complexes of Pr^{2+}, Gd^{2+}, Tb^{2+}, and Lu^{2+}. *J. Am. Chem. Soc.* **2013,** *135* (26), 9857-68.

18. MacDonald, M. R.; Ziller, J. W.; Evans, W. J., Synthesis of a crystalline molecular complex of Y^{2+}, [(18-crown-6)K][($C_5H_4SiMe_3$)$_3$Y]. *J. Am. Chem. Soc.* **2011,** *133* (40), 15914-7.

19. Woen, D. H.; Chen, G. P.; Ziller, J. W.; Boyle, T. J.; Furche, F.; Evans, W. J., Solution Synthesis, Structure, and CO_2 Reduction Reactivity of a Scandium(II) Complex, Sc[N($SiMe_3$)$_2$]$_3$. *Angew. Chem. Int. Ed.* **2017,** *56* (8), 2050-2053.

20. Jenkins, T. F.; Woen, D. H.; Mohanam, L. N.; Ziller, J. W.; Furche, F.; Evans, W. J., Tetramethylcyclopentadienyl Ligands Allow Isolation of Ln(II) Ions across the Lanthanide Series in [K(2.2.2-cryptand)][(C_5Me_4H)$_3$Ln] Complexes. *Organometal.* **2018,** *37* (21), 3863-3873.

21. R. C. Paul, P. K., Prepartion and Characterization of Alkali Metal Dimethylformamidyls. *Indian J. Chem.* **1975,** *13*, 1338-1340.

22. Elgrishi, N.; Rountree, K. J.; McCarthy, B. D.; Rountree, E. S.; Eisenhart, T. T.; Dempsey, J. L., A Practical Beginner's Guide to Cyclic Voltammetry. *J. Chem. Ed.* **2017,** *95* (2), 197-206.

23. Piro, N. A.; Robinson, J. R.; Walsh, P. J.; Schelter, E. J., The electrochemical behavior of cerium(III/IV) complexes: Thermodynamics, kinetics and applications in synthesis. *Coord. Chem. Rev.* **2014,** *260*, 21-36.

24. Morss, L. R., Thermochemical Properties of Yttrium, Lanthanum, and the Lanthanide Elements and Ions. *Chem. Rev. 76*, 827-841.

25. Shannon, R. D., Revised Effective Ionic Radii and Systematic Studies of Interatomic Distances in Halides and Chalcogenides. *Acta*. *Cryst.* **1976,** *A32*, 751-767.

Chapter 4

Uranium-in-2.2.2-Cryptand

Introduction*

As described in Chapter 2, it took a long time to develop the chemistry of rare earth metals in cryptand ligands. For the actinide metals, incorporation into cryptands was even slower. In 2018, the first crystal structures of uranium-in-cryptand complexes were reported for $[U(crypt)I_2][I]$, $[U(crypt)(OH)_2][I]_2$, and $[U(crypt)I(OH_2)][I][BPh_4]$.[1] Unfortunately, these uranium-in-cryptand complexes were only soluble in polar organic solvents such as DMF and MeCN. This limited the utility of this cryptand ligand environment for developing further actinide reaction chemistry. Thus, it was soughtto extend the triflate ligand system described in Chapter 2 to uranium.

In the process of studying new U-in-crypt complexes, it was of interest to see if this coordination environment could be extended to the transuranium metals such as Np and Pu. The limited availability of transuranium isotopes to basic research laboratories coupled with their radiological hazards limits their ability to be studied. Uranium is much more available to study,[2-8] allowing for the modeling of scaled down syntheses that can be expanded to metals such as Np and Pu. In this Chapter a THF-soluble U(III)-in-crypt triflate complex is described that can be generated and crystallized quickly on a small scale such that the synthesis is viable for analogous Np(III) and Pu(III) complexes. In collaboration with Drs. Andrew J. Gaunt and Conrad A. P. Goodwin at Los Alamos National Laboratory, this has provided Np and Pu in the crypt coordination environment. *Portions of this chapter have been published in Goodwin, C. A. P., **Ciccone, S. R.,** Bekoe, S., Majumdar, S., Scott, B. L., Ziller, J. W., Gaunt, A. J., Furche, F., Evans, W. J. 2.2.2-Cryptand Complexes of Neptunium(III) and Plutonium(III). *Chem. Comm*. **2022**, *58*, 997-700.

Results and Discussion

$[U^{III}(crypt)(OTf)_2][OTf]$, 1-U. First attempts to synthesize a THF-soluble U(III)-in-crypt complex involved the reaction of a solution of KOTf with the THF-insoluble brown-green complex $[U(crypt)I_2][I]$. This generated a green solution that upon workup was found to be $[U(crypt)(OTf)_2][OTf]$, **1-U**. While this method provided a route to yield single crystals of **1-U**, it was difficult to isolate analytically pure material and the crystals grew slowly. Therefore, for Np and Pu an alternative synthesis using Me_3SiOTf as the triflate ligand source was explored.

In an inert atmosphere argon glovebox, Me_3SiOTf reacts with $[U(crypt)I_2][I]$, equation 4.1, as a suspension in benzene to form a green oil that, upon workup and recrystallization from THF/Et_2O, quickly gives pure single crystals of green **1-U**, Figure 4.1, in 66% yield on a 100 mg scale. Various small-scale (11 mg) recrystallizations of crude **1-U** were examined, but the THF/Et_2O combinations provided the best single crystals.

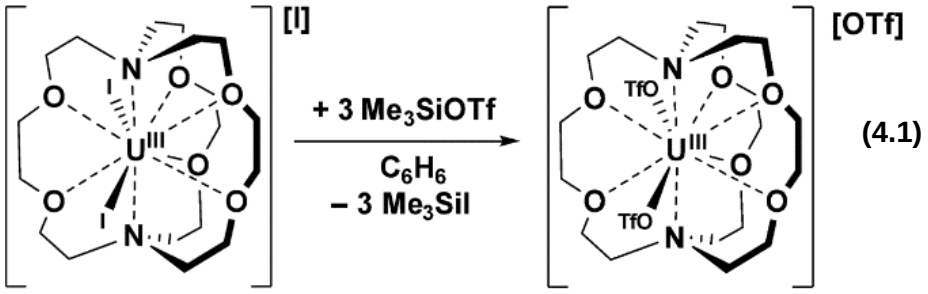

(4.1)

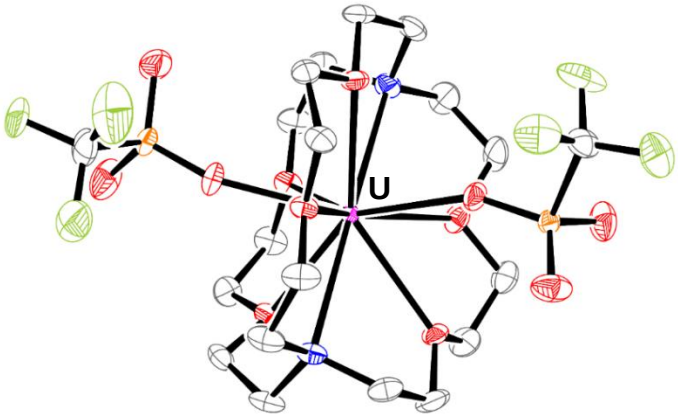

Figure 4.1. Representation of **1-U** with atomic displacement parameters drawn at the 30% probability level. Hydrogen atoms are omitted for clarity. **1-Np** and **1-Pu** are isomorphous.

$[Np(crypt)(OTf)_2][OTf]$ and $[Pu(crypt)(OTf)_2][OTf]$. Np and Pu complexes were made analogously at Los Alamos National Lab by Drs. Andrew J. Gaunt and Conrad A. P. Goodwin

conducted in a radiation laboratory equipped with high efficiency particulate air filtered hoods and in negative pressure gloveboxes fixed with either UHP argon or UHP helium. Just as in the synthesis of **1-U**, the synthesis of these Np and Pu analogues started from the triiodide precursor, $[AnI_3(THF)_4]$ for An = Np and Pu. These were reacted with crypt to give what is presumed to be the $[An(crypt)I_2][I]$. In the case of Np, the yellow compound was suspended in benzene and reacted with Me_3SiOTf to form a THF-soluble compound, $[Np(crypt)(OTf)_2][OTf]$, **1-Np**, identified by X-ray crystallography. In the case of Pu, the cream-colored compound was reacted with Me_3SiOTf in benzene to form $[Pu(crypt)(OTf)_2][OTf]$, **1-Pu**, identified by X-ray crystallography. These complexes are isomorphous with $[U(crypt)(OTf)_2][OTf]$.

Structural Details. Structural data on **1-U** obtained at UCI and the data on **1-Np** and **1-Pu** obtained at LANL are presented in Table 4.1. The complexes crystallize in the $P\bar{1}$ space group and are isomorphous. Each structure contains an $[An(crypt)(OTf)_2]^{1+}$ cation that approximates to a 10-coordinate tetra-capped trigonal prism with the nitrogen donors capping both trigonal faces and the triflate oxygens capping two of the rectangular faces. A third triflate anion is present and well separated from the $[An(crypt)(OTf)_2]^{1+}$ cations. In **1-Pu**, the Pu–O(OTf) range is 2.439(9)–2.512(9) Å across six unique bond distances (see Table 4.1). These Pu–O distances to the triflate anions are shorter than the range of Pu–O(crypt) distances (2.565(12)–2.677(13) Å) to the neutral oxygen donor sites of the crypt. The range of Pu–N(crypt) distances in 1-Pu (2.731(14)–2.834(17) Å) is the largest of the **1-An** series, containing both the shortest and longest An–N bonds.

Table 4.1. Selected bond distances in $[An(crypt)(OTf)_2][OTf]$, **1-An**.

	An–O(OTf) (Å)	An–O(crypt) (Å)	An–N(crypt) (Å)
1-U	2.454(4) –2.518(4)	2.566(4) – 2.677(4)	2.754(5) – 2.809(5)
1-Np	2.427(9) – 2.512(9)	2.570(11) – 2.659(13)	2.734(14) – 2.775(17)

1-Pu	2.439(9) – 2.512(9)	2.565(12) – 2.677(13)	2.731(14) – 2.834(17)

There is no clear evidence of the expected trend of bond shortening due to increased charge density from U^{III} to Np^{III} to Pu^{III}.[9] This could simply be due to the magnitude of error values in the data associated with the individual metal–ligand distances to relatively light O and N atoms, along with the wide spread of values precluding useful comparison of average values (large standard deviation). Higher resolution data may have revealed a trend. Unfortunately, the scarcity of single crystal X-ray structural data across homologous trivalent series extending from U–Pu, with neutral O-donor ligands provides limited contextualization of the **1-An** data.

NMR. The ^{19}F NMR resonances of **1-U** (–79.93 ppm), **1-Np** (–82.22 ppm), and **1-Pu** (–79.77 ppm) in THF-d_8 all show a single resonance which indicates that the triflate anions are equivalent in solution, presumably due to rapid exchange on the NMR timescale. They are only slightly shifted from that of KOTf at 79.54 ppm. Similarly, the ^1H NMR spectra of **1-Np** and **1-Pu** each show just a single set of three resonances assigned to the crypt ligand: **1-Np**, 10.85, 6.12, and 1.14 ppm; **1-Pu**, 4.29, 4.05, and 3.23 ppm, indicating that in solution it is in a symmetric environment. This indicates that in solution there is C_3 symmetry in contrast to the solid-state structures that contain two coordinated OTf anions. These ^1H NMR resonances are shifted slightly from the values for free crypt at 3.60, 3.52, and 2.57 ppm. These small shifts are consistent with other NMR spectra of Np(III) and Pu(III).[10-14] The room temperature ^1H NMR spectrum of **1-U** in THF-d_8 has a single discernible broad signal at 8.25 ppm within a window of 300 ppm to 150 ppm. This differs from the ^1H NMR spectrum of [U(crypt)I_2][I] in MeCN-d_3 which contains resonances at 8.39, 6.86 and 5.97 ppm. The broad resonance of **1-U** splits into several broad resonances at 260 K, but a clearly resolved three-line spectrum was not obtained down to 245 K.

UV-Visible Spectra. The experimental solution UV-vis-NIR spectra of the **1-An** compounds are shown in Figure 4.2 (black lines) alongside TDDFT simulated spectra (see below). Each complex has numerous weak transitions at low energy in the f–f transition region (ca. 7,000–15,000 cm^{-1} ; 700–1400 nm) and large absorptions at energies over 20,000 cm-^{1} (500 nm) that extend into the UV region which are plausibly charge transfer bands or 5f - 6d transitions.

Electronic structure calculations on the $[An(crypt)(OTf)_2]^{1+}$ complexes were carried out by Samuel Bekoe and Sourav Majumdar in the group of Professor Filipp Furche to evaluate the ground state nature of these complexes and their UV-visible spectra. The calculations indicated quartet $5f^3$, quintet $5f^4$, and sextet $5f^5$ ground state configurations for $[U(crypt)(OTf)_2]^{1+}$, $[Np(crypt)(OTf)_2]^{1+}$, and $[Pu(crypt)(OTf)_2]^{1+}$, respectively. The calculated average An–O and An–N bond distances are within 0.02 Å of the experimental values in $[An(crypt)(OTf)_2][OTf]$. TDDFT calculations of the simulated UV-vis-NIR spectra are shown in Fig. 4.2 (green lines). For all three complexes $[U(crypt)(OTf)_2]^{1+}$, $[Np(crypt)(OTf)_2]^{1+}$, and $[Pu(crypt)(OTf)_2]^{1+}$, the calculations indicate that there are very weak 5f - 5f transitions in the 7,000–20,000 cm^{-1} region and intense 5f - 6d transitions at energies over 20,000 cm^{-1}. Although scalar relativistic DFT calculations do not provide accurate estimates of intensity and splitting patterns of these 5f - 5f transitions, the overall match of the UV-visible spectra in the 5f - 6d region and the absence of 6d - 7p transitions (characteristic of divalent actinide compounds with $6d^1$ ground states)[15] supports the assignment of $5f^n$ ground states with no 6d occupation. The onset of 5f - 6d transitions occurs

at higher energies in the order U < Np < Pu, in keeping with the increasing stabilization of the 5f manifold relative to the 6d orbitals as the actinide series is traversed from U to Np to Pu.

Figure 4.2. Black lines show solution UV-vis-NIR spectra of (a) $[U(crypt)(OTf)_2][OTf]$ (**1-U**) (5 mM), (b) **1-Np** (1.89 mM), and (c) **1-Pu** (2.05 mM) in THF at ambient temperature. Green lines show simulated UV-vis-NIR spectra of (a) $[U(crypt)(OTf)_2]^{1+}$, (b) $[Np(crypt)(OTf)_2]^{1+}$, and (c) $[Pu(crypt)(OTf)_2]^{1+}$ with computed TDDFT oscillator strengths shown as vertical lines. The experimental spectrum is shown in black for comparison. A Gaussian line broadening of 0.10 eV was applied. The computed intensities were scaled to ease comparison with the experiment spectrum.

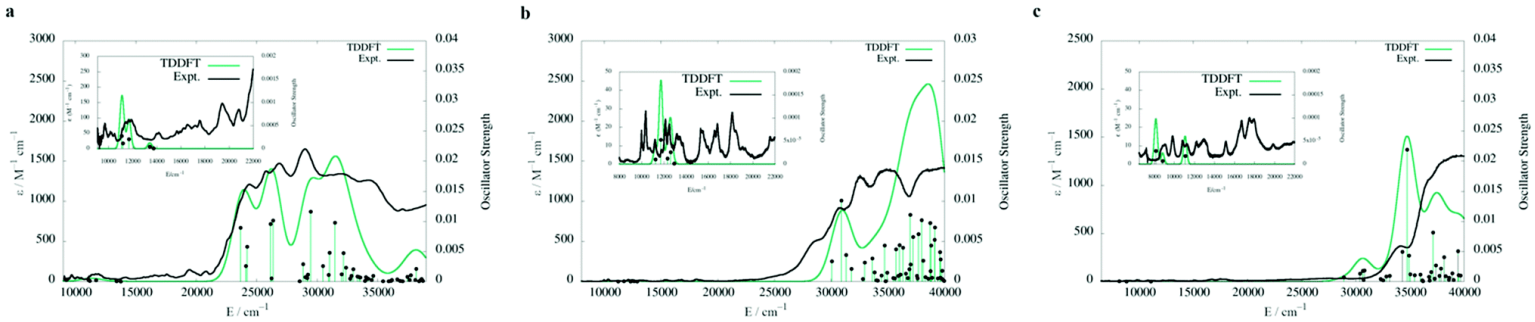

Conclusion

In summary, the coordination chemistry of 2.2.2-cryptand was expanded to Np(III) and Pu(III) through methods initially found to be successful for U(III). The U(III)-in-crypt complex, $[U(crypt)I_2][I]$, reacts with Me_3SiOTf to generate $[U(crypt)(OTf)_2][OTf]$. Using analogous procedures, crystallographically characterizable $[An(crypt)(OTf)_2][OTf]$ complexes of Np and Pu could be prepared and isolated by LANL. The transuranium complexes are isomorphous with the U analog and all are THF-soluble. The solubility provides the opportunity to use this encapsulating coordination environment for further development of transuranium chemistry. DFT calculations reveal $5f^n$ ground-state electronic configurations in accord with that expected for trivalent ions.

These combined theoretical/experimental results reveal a clear and simple physical manifestation of increased 5f–6d energetic separation across the series from U to Np to Pu.

Experimental

[U(crypt)(OTf)$_2$][OTf], 1-U. *Method 1.* To a stirring suspension of [U(crypt)(I)$_2$][I] (50 mg, 0.05 mmol), KOTF (28 mg, 0.15 mmol) was added. The reaction was left to stir overnight. Insoluble material was removed by centrifugation, and the resulting green solution was layered over Et_2O. After 3d, green crystals of **1-U** suitable for X-ray diffraction were obtained.

Method 2. A suspension of [U(crypt)(I)$_2$][I] (100 mg, 100 μmol) in C_6H_6 (10 mL) was added to a stirring solution of Me_3SiOTf (300 μmol) in C_6H_6 (5 mL). During the course of addition, the solids dissolved quickly and then deposited a small quantity of green solids that appeared oily or greasy. The mixture was then left to stir overnight. The next day, the mixture was centrifuged to yield a green oily deposit and a colorless clear supernatant. The supernatant was decanted and the oil was taken up in THF, and the green solution was filtered and dried in vacuo to give a fluffy green solid (70 mg, 66% yield). The green solid was dissolved in THF, layered with Et_2O, and placed at −35 °C. Pale green plates of [U(2.2.2-crypt)(OTf)$_2$][OTf] (**1-U**) formed overnight, from which the structure was determined. ^{1}H NMR (THF-d_8, 400.13 MHz, 298 K): δ = 8.24. ^{19}F{^{1}H} NMR (THF-d_8, MHz, 298 K): δ = −80.32 (OTf, O_3SCF_3 × 3) UV-vis-NIR (THF): λmax (cm^{-1}; ε) = 252 (39,680, 962), 271 (36,900, 890), 291 (34,360, 1,261), 310 (32,260, 1,337), 346 (28,900, 1,643), 374 (26,740, 1,472), 388 (25,770, 1,375), 412 (24,270, 1,198), 425 (23,530, 950), 444 (22,520, 490), 480 (20,830, 127), 515 (19,420, 146), 553 (18,080, 57), 570 (17,540, 90), 582 (17,180, 75), 603 (16,580, 78), 618 (16,180, 54), 627 (15,950, 53), 639 (15,650, 55), 704 (14,200, 51), 841 (11,890, 94), 856 (11,680, 93), 874 (11,440, 86), 895 (11,170, 64), 950 (10,530, 48), 979

(10,210, 50), 986 (10,140, 53), 1032 (971, 80). Anal. Calcd for $US_2F_6O_{12}N_2C_{20}H_{36}SO_3CF_3$: C, 23.16; H, 3.42; N, 2.64. Found: C, 23.81; H, 3.26; N, 2.24.

References

1. Huh, D. N.; Windorff, C. J.; Ziller, J. W.; Evans, W. J., Synthesis of uranium-in-cryptand complexes. *Chem Commun.* **2018,** *54* (73), 10272-10275.

2. Morss, L. R. Edelstein, N. M., Fuger, J., Katz, J. J., The chemistry of the actinide and transactinide elements. Springer: 2006; Vol. 1

3. Gilson, S. E.; Burns, P. C., The crystal and coordination chemistry of neptunium in all its oxidation states: An expanded structural hierarchy of neptunium compounds. *Coord. Chem. Rev.* **2021,** *445*, 1-59.

4. Minasian, S. G.; Krinsky, J. L.; Arnold, J., Evaluating f-element bonding from structure and thermodynamics. *Chem. Eur. J.* **2011,** *17* (44), 12234-45.

5. Albrecht-Schmitt, T. E., Organometallic and Coordination Chemistry of the Actinides. Springer: 2008

6. Jones, M. B.; Gaunt, A. J., Recent developments in synthesis and structural chemistry of nonaqueous actinide complexes. *Chem. Rev.* **2013,** *113* (2), 1137-98.

7. Liddle, S. T., The Renaissance of Non-Aqueous Uranium Chemistry. *Angew. Chem. Int. Ed.* **2015,** *54* (30), 8604-41.

8. Ephritikhine, M., The vitality of uranium molecular chemistry at the dawn of the XXIst century. *Dalton. Trans.* **2006,** (21), 2501-16.

9. Shannon, R. D., Revised Effective Ionic Radii and Systematic Studies of Interatomie Distances in Halides and Chaleogenides *Acta. Cryst.* **1978,** *A32*, 751-767.

10. Goodwin, C. A. P.; Janicke, M. T.; Scott, B. L.; Gaunt, A. J., $[AnI_3THF_4]$ (An = Np, Pu) Preparation Bypassing An^0 Metal Precursors: Access to Np^{3+}/Pu^{3+} Nonaqueous and Organometallic Complexes. *J. Am. Chem. Soc.* **2021,** *143* (49), 20680-20696.

11. Su, J.; Windorff, C. J.; Batista, E. R.; Evans, W. J.; Gaunt, A. J.; Janicke, M. T.; Kozimor, S. A.; Scott, B. L.; Woen, D. H.; Yang, P., Identification of the Formal +2 Oxidation State of Neptunium: Synthesis and Structural Characterization of $Np^{II}[C_5H_3(SiMe_3)_2]_3$. *J. Am. Chem. Soc.* **2018,** *140* (24), 7425-7428.

12. Windorff, C. J.; Chen, G. P.; Cross, J. N.; Evans, W. J.; Furche, F.; Gaunt, A. J.; Janicke, M. T.; Kozimor, S. A.; Scott, B. L., Identification of the Formal +2 Oxidation State of Plutonium: Synthesis and Characterization of $Pu^{II}[C_5H_3(SiMe_3)_2]_3$. *J. Am. Chem. Soc.* **2017,** *139* (11), 3970-3973.

13. Windorff, C. J.; Sperling, J. M.; Albrecht-Schonzart, T. E.; Bai, Z.; Evans, W. J.; Gaiser, A. N.; Gaunt, A. J.; Goodwin, C. A. P.; Hobart, D. E.; Huffman, Z. K.; Huh, D. N.; Klamm, B. E.; Poe, T. N.; Warzecha, E., A Single Small-Scale Plutonium Redox Reaction System Yields Three Crystallographically-Characterizable Organoplutonium Complexes. *Inorg. Chem.* **2020,** *59* (18), 13301-13314.

14. Myers, A. J.; Tarlton, M. L.; Kelley, S. P.; Lukens, W. W.; Walensky, J. R., Synthesis and Utility of Neptunium(III) Hydrocarbyl Complex. *Angew. Chem. Int. Ed.* **2019,** *58* (42), 14891-14895.

15. Wedal, J. C.; Bekoe, S.; Ziller, J. W.; Furche, F.; Evans, W. J., C–H Bond Activation via U(II) in the Reduction of Heteroleptic Bis(trimethylsilyl)amide U(III) Complexes. *Organometallics.* **2020,** *39* (18), 3425-3432.

Chapter 5

Birch Reductions of Rare-Earth Metal Cryptand Complexes

Introduction

Rare-earth metal-in-cryptand complexes have low solubility which limits the reduction methods possible for these ions with extremely low reduction potentials, so other reduction methods were sought. Reduction methods for rare-earth metal complexes are not extensive. Many of the isolated rare-earth metal complexes in the +2 oxidation state have been reduced in similar ways. In 2008, Lappert showed that it was possible for La and Ce ions to exist in the +2 oxidation state by reducing the Ln^{III} precursor in THF or Et_2O in the presence of a chelate (18-crown-6 or 2.2.2-cryptand) and K metal at room temperature.[1] Following this discovery, Matt MacDonald from the Evans group isolated a Y^{II} complex by reduction of a Y^{III} in Et_2O in the presence of chelate and KC_8 at – 45 °C.[2] This method of using an ethereal solvent in the presence of chelate with K or KC_8 as a reductant paved the way for the isolation of many more rare-earth metals in the +2 oxidation state.[3-14]

In addition to these methods, it has also been shown that Ln metal complexes could be reduced through gamma irradiation,[15] as well as reduction in non-donor solvents such as toluene, cyclohexane and benzene with KC_8 as a reductant.[16-18] While KC_8 reductions in THF were suitable for reduction of $[Nd(crypt)(OTf)_2][OTf]$ and $[Sm(crypt)(OTf)_2][OTf]$ complexes, they were not suitable for the smaller lanthanide metals or $[U(crypt)(I)_2][I]$ due to poor solubility in ethereal solvents. Additionally, gamma irradiation in non-polar solvents would not be a suitable route for reduction due to, again, poor solubility. Thus, Birch reductions, using liquid ammonia as a solvent, were investigated as a new method for reduction of these crypt complexes. Ammonia being polar as well as tolerating alkali metal reductions led to Birch reductions as a possible way to reduce the rare-earth metal complexes with limited solubility.

Lanthanide metals Eu and Yb have been reported to dissolve in ammonia to presumably form the metal hexaammoniate, $[Ln(NH_3)_n]^{2+}$, upon removal of the solvent.[19] Additionally,

uranium halides have been reacted with ammonia to also show generation of uranium ammoniates.[20] As far as alkali metal reduction of rare-earth metal complexes in ammonia, only UBr_3 and UBr_4 have been reacted with potassium metal in ammonia to result in insoluble dark grey powders.[20] With limited knowledge on how rare-earth metal complexes will react with alkali metals in ammonia, and with the need for a polar solvent that would tolerate alkali metals, Birch reductions were carried out with the Ln-in-crypt and U-in-crypt complexes.

Results and Discussion

Reduction of Sm and Nd Compounds. Birch reductions with rare-earth metal complexes are unexplored, so complexes that were known to reduce with the common method that employed KC_8 as a reductant in ethereal solvents were investigated first. $[Sm(crypt)(OTf)_2][OTf]$ was dissolved in ammonia to give a colorless solution and was then reacted with a sub-stoichiometric amount of sodium metal. When small amounts of sodium metal were dissolved in the ammonia, a blue color appeared and then quickly dissipated back to colorless. After a couple of additions of sodium, the solution turned to a persistent red color. The red solids isolated upon workup were determined to be the reduced complex, $Sm(crypt)(OTf)_2$, by X-ray crystallography.

In addition to this Sm complex, the Birch reduction of $[Sm(221\text{-}crypt)(OTf)][OTf]_2$, discussed in Chapter 7, was conducted. Again a color change occurred, this time to green. The reduced Sm product, [Sm(221crypt)(OTf)][OTf] was isolated and identified by X-ray crystallography. For both these reductions, it is important to use sub-stoichiometric amounts of sodium metal as a reductant. If excess amounts of sodium are used, insoluble white products are isolated.

In contrast to the Sm reductions, reductions for Nd did not generate the dark blue Nd(crypt)$(OTf)_2$ as expected. Even though it is known that the [Nd(crypt)$(OTf)_2$][OTf] complex can be reduced in THF with KC_8, the Birch reductions of this complex resulted in no color change. When small amounts of sodium metal were added to the complex, the blue color associated with solvated electron appeared and quickly dissipated, as in the case of Sm, but the expected color change to dark blue of the Nd(crypt)$(OTf)_2$ complex was not observed.

Reduction of [Dy(crypt)(OTf)][OTf]$_2$. Multiple attempts were made to try to reduce [Dy(crypt)(OTf)][OTf]$_2$ by Birch reduction. In the initial attempt to isolate a Dy^{II} ion within the cryptand coordination environment, ammonia was condensed onto the [Dy(crypt)(OTf)][OTf]$_2$ complex. Upon addition of small amounts of sodium metal to the mixture , a blue solution was formed. After removal of the ammonia, the blue residue was extracted into THF and layered with Et_2O to produce blue colored crystals at –35 °C. Unfortunately these crystals were only [Na(crypt)][OTf] and not a Dy^{II} complex. Subsequent attempts resulted in reactions that were analogous to the Nd reductions, i.e., no color change was observed.

Reduction of [U(crypt)(I)$_2$]I. Birch reductions of [U(crypt)$(I)_2$][I] were explored because this uranium complex was only soluble in polar solvents such as DMF and MeCN, which are unsuitable for alkali metal reductions. When [U(crypt)$(I)_2$][I] is reacted with a sub-stoichiometric amount of sodium metal, the green solution undergoes a slight color change. Upon workup, both green and red solids are isolated, neither of which could be definitively characterized. Interestingly, when this complex is reacted with an excess amount of sodium metal, white insoluble solids are isolated as in the case of the Sm reductions.

Conclusion

While liquid ammonia had the potential to be a solvent suitable for reductions of rare-earth metal cryptand complexes, evidence of productive reduction under these conditions was only obtained for Sm. While the precursor Ln(III) complexes do show solubility in ammonia, the reductions with Nd do not proceed as they do in THF with KC_8. One important difference is that there cannot be an excess of alkali metal in the liquid ammonia reactions. In contrast to the THF/KC_8 reductions, an excess of metal results in a white insoluble product.

Experimental

All manipulations and syntheses described below were conducted with the rigorous exclusion of air and water using standard glovebox and high-vacuum line techniques under an argon atmosphere. [Ln(crypt)$(OTf)_2$][OTf] and [U(crypt)$(I)_2$][I] complexes were synthesized as previously reported. UHP anhydrous ammonia was supplied by Airgas and condensed at either –35 °C or –78 °C on the Schlenk line in to a Schlenk flask equipped with its own bubbler.

Reduction of [Sm(crypt)$(OTf)_2$][OTf] in Ammonia with Sodium. [Sm(crypt)$(OTf)_2$][OTf] (50 mg, 0.051 mmol) was placed in a Schlenk flask with a sub-stoichiometric amount of sodium smeared on the top half of the flask. The flask was connected to a Schlenk line equipped with anhydrous ammonia. Ammonia was condensed onto the [Sm(crypt)$(OTf)_2$][OTf] to dissolve the complex at–35 °C in some reactions or –78 °C in other reactions. Once liquid ammonia was condensed, the flask was manipulated to dissolve small amounts of Na at a time. With each addition of sodium metal, a blue color appeared and dissipated. As more sodium was added, the solution turned to red, the color of Sm^{II}(crypt)$(OTf)_2$. The red color persisted after ammonia was removed by first passing argon gas over the solution to blow off the ammonia and then placing the residues under vacuum. The red residues were collected in THF and layered with Et_2O. Red crystals grown at –35 °C showed the product to be

$Sm^{II}(crypt)(OTf)_2$. If excess amounts of Na metal were added, a dark blue color persisted in solution and after removal of the ammonia an insoluble white powder was isolated.

Reduction of [Sm(221crypt)(OTf)][OTf]$_2$ in Ammonia with Sodium. [Sm(221crypt)$(OTf)_2$][OTf] (50 mg, 0.054 mmol) was placed in a Schlenk flask with a sub-stoichiometric amount of sodium smeared on the top half of the flask. The flask was connected to a Schlenk line equipped with anhydrous ammonia. Ammonia was condensed on to the [Sm(221crypt)(OTf)][OTf_2] to dissolve the complex at either –35 °C or –78 °C. Once liquid ammonia was condensed, the flask was tipped to dissolve small amounts of Na at a time. With each addition of sodium metal, a blue color appeared. As more sodium was added, the solution turned to green, the color of $[Sm^{II}(crypt)(OTf)][OTf]$.

Reduction of [Nd(crypt)(OTf)$_2$][OTf] in Ammonia with Sodium. Attempts to reduce [Nd(crypt)$(OTf)_2$][OTf] were carried out with both potassium and sodium. Both metals resulted in the same outcome. [Nd(crypt)$(OTf)_2$][OTf] (50 mg, 0.052 mmol) was loaded in a Schlenk flask with either Na or K metal smeared to the upper half of the flask. The flask was attached to a Schlenk line equipped with anhydrous ammonia. Ammonia was condensed into the flask to dissolve the Nd complex at either –35 °C or –78 °C and the solution was swirled to add small amounts of metal at a time. When the alkali metal was added, a blue color appeared and then quickly dissipated. This was repeated several times, but unlike the Sm reaction in which a Sm^{II} color was observed, there was no color change observed for Nd even though the reaction could be carried out with KC_8 in THF.

Reduction of [Dy(crypt)(OTf)][OTf]$_2$ in Ammonia with Sodium. [Dy(crypt)(OTf)][OTf_2] (50 mg, 0.051 mmol) was loaded in a Schlenk flask with Na metal smeared to the upper half of the flask. The flask was attached to a Schlenk line equipped with

anhydrous ammonia. Ammonia was condensed into the flask to dissolve the Nd complex at either –35 °C or –78 °C and the solution was swirled to add small amounts of metal at a time. When the alkali metal was added, a blue color appeared and then quickly dissipated. This was repeated several times. In one instance, there was a color change to dark blue, but subsequent attempts resulted in no color change.

Reduction of [U(crypt)(I)$_2$][I] in Ammonia with Sodium. [U(crypt)(I)$_2$][I] (50 mg, 0.058 mmol) were loaded in to a Schlenk flask with Na metal smeared to the upper half of the flask. Ammonia was condensed into the flask to dissolve the uranium compound at either –35 °C or –78 °C. The green solution was swirled to add small amounts of sodium. The solution changed to a darker green and upon removal of the solvent, green and red solids were isolated.

References

1. Hitchcock, P. B.; Lappert, M. F.; Maron, L.; Protchenko, A. V., Lanthanum does form stable molecular compounds in the +2 oxidation state. *Angew. Chem. Int. Ed.* **2008,** *47* (8), 1488-91.

2. MacDonald, M. R.; Ziller, J. W.; Evans, W. J., Synthesis of a crystalline molecular complex of Y2+, [(18-crown-6)K][($C_5H_4SiMe_3$)$_3$Y]. *J. Am. Chem. Soc.* **2011,** *133* (40), 15914-7.

3. Anderson-Sanchez, L. M.; Yu, J. M.; Ziller, J. W.; Furche, F.; Evans, W. J., Room-Temperature Stable Ln(II) Complexes Supported by 2,6-Diadamantyl Aryloxide Ligands. *Inorg. Chem.* **2023,** *62* (2), 706-714.

4. Huh, D. N.; Ciccone, S. R.; Bekoe, S.; Roy, S.; Ziller, J. W.; Furche, F.; Evans, W. J., Synthesis of Ln(II)-in-Cryptand Complexes by Chemical Reduction of Ln(III)-in-Cryptand Precursors: Isolation of a Nd(II)-in-Cryptand Complex. *Angew. Chem. Int. Ed.* **2020,** *59* (37), 16141-16146.

5. Jenkins, T. F.; Woen, D. H.; Mohanam, L. N.; Ziller, J. W.; Furche, F.; Evans, W. J., Tetramethylcyclopentadienyl Ligands Allow Isolation of Ln(II) Ions across the Lanthanide Series in [K(2.2.2-cryptand)][$(C_5Me_4H)_3$Ln] Complexes. *Organometal.* **2018,** *37* (21), 3863-3873.

6. Kelly, R. P.; Maron, L.; Scopelliti, R.; Mazzanti, M., Reduction of a Cerium(III) Siloxide Complex To Afford a Quadruple-Decker Arene-Bridged Cerium(II) Sandwich. *Angew .Chem.* **2017,** *56* (49), 15663-15666.

7. Langeslay, R. R.; Fieser, M. E.; Ziller, J. W.; Furche, F.; Evans, W. J., Synthesis, structure, and reactivity of crystalline molecular complexes of the($[C_5H_3(SiMe_3)_2]_3Th)^{1-}$ anion containing thorium in the formal +2 oxidation state. *Chem Sci* **2015,** *6* (1), 517-521.

8. MacDonald, M. R.; Bates, J. E.; Fieser, M. E.; Ziller, J. W.; Furche, F.; Evans, W. J., Expanding rare-earth oxidation state chemistry to molecular complexes of holmium(II) and erbium(II). *J. Am. Chem. Soc.* **2012,** *134* (20), 8420-3.

9. MacDonald, M. R.; Bates, J. E.; Ziller, J. W.; Furche, F.; Evans, W. J., Completing the series of +2 ions for the lanthanide elements: synthesis of molecular complexes of Pr^{2+}, Gd^{2+}, Tb^{2+}, and Lu^{2+}. *J. Am. Chem. Soc.* **2013,** *135* (26), 9857-68.

10. MacDonald, M. R.; Fieser, M. E.; Bates, J. E.; Ziller, J. W.; Furche, F.; Evans, W. J., Identification of the +2 oxidation state for uranium in a crystalline molecular complex, [K(2.2.2-cryptand)][$(C_5H_4SiMe_3)_3$U]. *J. Am. Chem. Soc.* **2013,** *135* (36), 13310-3.

11. Moehring, S. A.; Miehlich, M.; Hoerger, C. J.; Meyer, K.; Ziller, J. W.; Evans, W. J., A Room-Temperature Stable Y(II) Aryloxide: Using Steric Saturation to Kinetically Stabilize Y(II) Complexes. *Inorg. Chem.* **2020,** *59* (5), 3207-3214.

12. Su, J.; Windorff, C. J.; Batista, E. R.; Evans, W. J.; Gaunt, A. J.; Janicke, M. T.; Kozimor, S. A.; Scott, B. L.; Woen, D. H.; Yang, P., Identification of the Formal +2 Oxidation State of Neptunium: Synthesis and Structural Characterization of $Np^{II}[C_5H_3(SiMe_3)_2]_3$. *J. Am. Chem. Soc.* **2018,** *140* (24), 7425-7428.

13. Windorff, C. J.; Chen, G. P.; Cross, J. N.; Evans, W. J.; Furche, F.; Gaunt, A. J.; Janicke, M. T.; Kozimor, S. A.; Scott, B. L., Identification of the Formal +2 Oxidation State of

Plutonium: Synthesis and Characterization of $Pu^{II}[C_5H_3(SiMe_3)_2]_3$. *J. Am. Chem. Soc.* **2017,** *139* (11), 3970-3973.

14. Windorff, C. J.; MacDonald, M. R.; Meihaus, K. R.; Ziller, J. W.; Long, J. R.; Evans, W. J., Expanding the Chemistry of Molecular U^{2+} Complexes: Synthesis, Characterization, and Reactivity of the $[C_5H_3(SiMe_3)_2]_3U^-$ Anion. *Eur. J. Chem.* **2016,** *22* (2), 772-82.

15. Moore, W. N. G.; White, J. R. K.; Wedal, J. C.; Furche, F.; Evans, W. J., Reduction of Rare-Earth Metal Complexes Induced by gamma Irradiation. *Inorg. Chem.* **2022,** *61* (44), 17713-17718.

16. Florian Jaroschik, F. N., Xavier Frederie Le Goff, Louis Ricard, Isolation of Stable Organodysprosium(II) Complexes by Chemical Reduction of Dysprosium(III) Precursors. *Organometal.* **2007,** *26*, 1123-1125.

17. Gould, C. A.; McClain, K. R.; Yu, J. M.; Groshens, T. J.; Furche, F.; Harvey, B. G.; Long, J. R., Synthesis and Magnetism of Neutral, Linear Metallocene Complexes of Terbium(II) and Dysprosium(II). *J. Am. Chem. Soc.* **2019,** *141* (33), 12967-12973.

18. Jaroschik, F.; Nief, F.; Ricard, L., Synthesis of a new stable, neutral organothulium(II) complex by reduction of a thulium(III) precursor. *Chem. Commun.* **2006,** (4), 426-8.

19. Korst, J. C. W. a. W. L., Solution of Europium and Ytterbium Metals in Liquid Ammonia. *J. Phys. Chem.* **1956,** *60*, 1590-1591.

20. Rudel, S. S., Baer, Sebastian A., Woidy, Patrick, Müller, Thomas G., Deubner, H.-Lars, Scheibe, Benjamin and Kraus, Florian, Recent advances in the chemistry of uranium halides in anhydrous ammonia. *Zeitschrift für Kristallographie - Crystalline Materials* **2018,** *233*, 817-844.

Chapter 6

Synthesis of 2.2.2-Cryptand Encapsulated Lanthanide Thexylborohydride Complexes, $Ln(crypt)(H_3BCMe_2CMe_2H)_3$

Introduction

As described in Chapters 2 and 3, only a few complexes with Ln(II) ions in 2.2.2-cryptand (crypt) were known even 30 years after the first Ln(III)-in-crypt complex was reported. Moreover, initially all of these Ln(II)-in-crypt complexes involved the most stable Ln(II) ions of Sm, Eu, and Yb. The formation of the M(II)-in-crypt complexes in Chapter 2 required the development of THF soluble Ln(III)-in-crypt complexes which were obtained by using $Ln(OTf)_3$ precursors, equations 6.1 and 6.2.

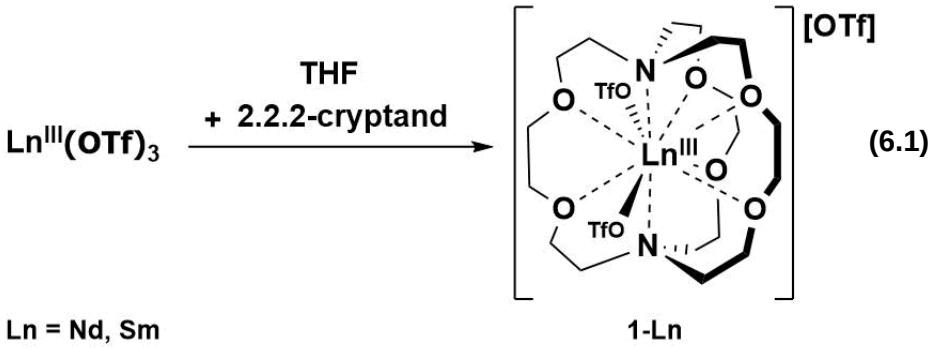

(6.1)

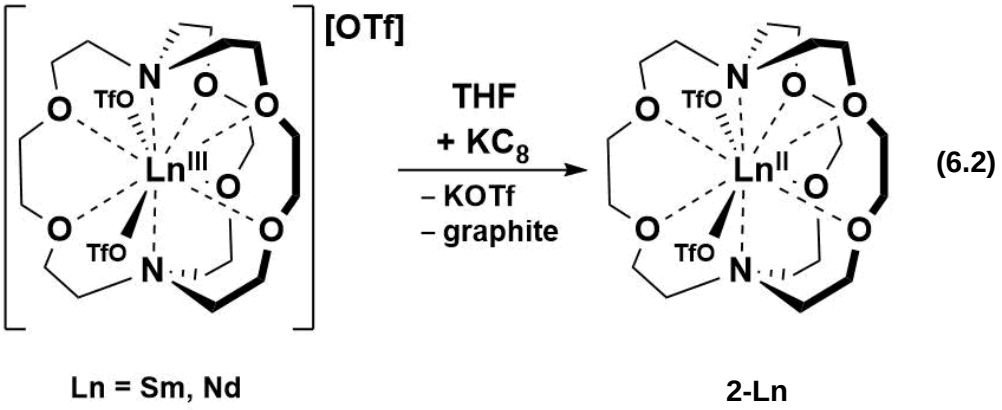

(6.2)

Additionally, it was shown that solubility of these Ln(III)-in-crypt complexes, which was essential to the alkali metal reduction to achieve the +2 oxidation state, was limited to the larger lanthanide metals, Figure 6.1. Only chemical reduction was definitively observed for Sm and Nd.

Attempts to expand this chemistry to the smaller metals was not successful because the Ln(III) precursors precipitated out of solvents that were suitable for alkali metal reduction. Thus, the search for solubilizing ligands continued.

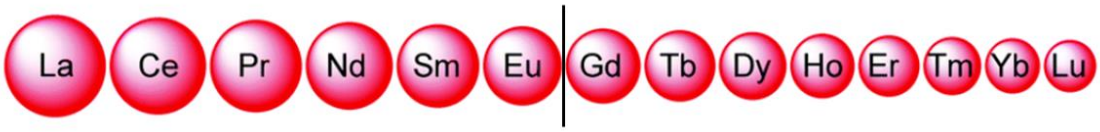

Figure 6.1. The lanthanide series showing decreasing size of ions across the period. A cutoff in solubility of Ln-in-crypt complexes in THF was found to be between Eu and Gd.

Routes to molecular lanthanide borohydride complexes from $LnCl_3$ and $NaBH_4$ have been known since the 1970s.[1] These lanthanide borohydride complexes are claimed to have superior solubility over the $LnCl_3$ precursors in THF, which has proven to be an advantage in the syntheses of a wide range of organolanthanide complexes.[2-4] This made the borohydride an interesting candidate as a ligand to solubilize these Ln-in-cryptand complexes to expand reductive chemistry to the smaller lanthanide metals. In addition to this borohydride ligand, Ephritikine showed in 1995 that $U(BH_4)_4$ could add a borohydride B–H bond to an alkene double bond, giving the corresponding alkylborohydride derivative, $U(H_3BCMe_2CMe_2H)_4$.[5]

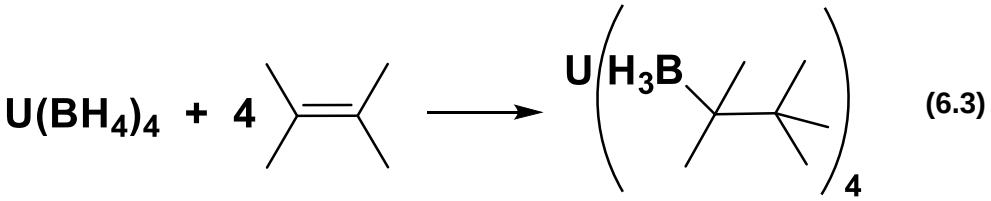

(6.3)

These "thexylborohydride" complexes demonstrated the existence of a new ligand with a hydrocarbon chain that could add solubility. Thexylborohydride ligands seemed promising as ligands to solubilize the Ln-in-cryptand complexes.

In this Chapter, the synthesis of Ln(III)-in-crypt complexes from borohydrides is described along with the synthesis of Ln(III)-in-crypt complexes supporting the thexylborohydride ligand. Attempts to reduce these complexes to the +2 oxidation state with Sm and Dy were investigated because of the established chemistry with Sm and the goal to expand this chemistry to smaller lanthanide metals such as Dy.

Results and Discussion

Synthesis of Ln Thexylborohydride Complexes, Ln = Sm, Dy. To make the thexylborohydride complexes, the $Ln(BH_4)_3$ complexes were reacted with tetramethylethylene. This allowed the thexylborohydride compounds, $Ln(H_3BCMe_2CMe_2H)_3$, to be isolated.

For Sm, tetraethylmethylene was added to a colorless solution of $Sm(BH_4)_3$ in benzene. The solution remained clear. Upon removal of solvent, a colorless solid was isolated. Characterization of this solid by ^1H NMR spectroscopy in C_6D_6 shows signals that support the insertion of tetramethylethylene into the B–H bond.

For Dy, since $Dy(BH_4)_3$ is not soluble in benzene, reactions were carried out in THF. $Dy(BH_4)_3$ was added to THF to make a colorless solution. After addition of tetramethylethylene, the solution remained clear. This solution was used for the reactions described below.

Syntheses of Ln-in-crypt Borohydride Complexes. Because the borohydride complexes proved to be more soluble than the $LnCl_3$ precursors that have been used to synthesize Ln-in-crypt complexes, attempts to make a THF-soluble Ln-in-crypt complex from borohydrides were carried out. Unfortunately, upon the addition of the chelate to the $Ln(BH_4)_3$ complexes in THF, precipitation occurred that showed this was not a route to soluble Ln-in-crypt complexes.

Syntheses of Ln-in-crypt Thexylborohydride Complexes, Ln = Sm, Dy. To make the crypt encapsulated $Ln(H_3BCMe_2CMe_2H)_3$, crypt was added to the thexylborohydride complexes, $Ln(H_3BCMe_2CMe_2H)_3$. In the case of Sm, no precipitation was observed after addition of crypt, in THF. However, for Dy, even with the thexylborohydride ligands, solids precipitated upon addition of crypt. Reductions were carried out with the $Sm(crypt)(H_3BCMe_2CMe_2H)_3$ complex while alternative routes to obtain a crypt encapsulated Dy(II) ion were attempted as described below.

It is important to note that the steps taken in the synthesis of these complexes is crucial. It is necessary to generate the lanthanide thexylborohydride complex, $Ln(H_3BCMe_2CMe_2H)_3$, first and then add cryptand or the insertion of tetramethylethylene into the B–H bond will not occur. If cryptand is added to the $Sm(BH_4)_3$ first, the resulting solid does react with tetramethylethylene to make the benzene soluble product formed from the thexylborohydride.

Reduction of the Sm-in-crypt Thexylborohydride Complex. $Sm(crypt)(H_3BCMe_2CMe_2H)_3$ is soluble in both toluene and THF. Thus, this complex can be reacted with KC_8 to give a reduced product in both toluene and THF. In both cases, addition of KC_8 resulted in a color change from colorless to pink. Where previous complexes could barely be solubilized in THF, it is remarkable that this crypt encapsulated complex could also be reduced in toluene. Crystallization was achieved by placing a THF solution of the reduced complex layered with Et_2O at – 35 °C overnight to give a complex believed to be $Sm^{II}(crypt)(H_3BCMe_2CMe_2H)_2$, equation 6.4 due to a color change from colorless to pink. Unfortunately, the X-ray diffraction data collected on the crystal was of insufficient quality to provide even a connectivity structure.

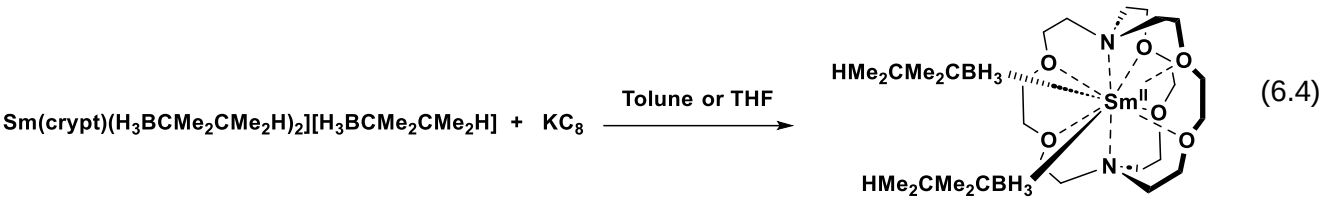

(6.4)

Even though the $Dy(crypt)(H_3BCMe_2CMe_2H)_3$ was not soluble in THF, the complex was still reacted with KC_8. Unfortunately, the colorless dysprosium compound remained colorless while the KC_8 remained a copper gold color suggesting that no reduction took place. Because of this, reduction $Dy(BH_4)_3$ with KC_8 followed by the addition of crypt was carried out to see if this was a way that a Dy(II) could be encapsulated in the crypt ligand. Reaction of $Dy(BH_4)_3$ with KC_8 in THF resulted in a color change to orange-brown. Addition of cryptand to this orange brown solution caused orange-brown solids to precipitate. It was also attempted to layer the reduced $Dy(BH_4)_3$ with a solution of crypt in THF, but this also resulted in orange-brown insoluble material.

Conclusion

The isolation of THF-soluble Ln-in-cryptand complexes for the smaller lanthanide metals has not been achieved. Even though the thexylborohydride ligand system made it possible to have a Ln-in-crypt complex that is soluble in toluene, $Sm(crypt)(H_3BCMe_2CMe_2H)_3$, this chemistry still could not be expanded to metals such as Dy. Even though the attempted goal has not been reached there is promise that a Dy(II) ion could be encapsulated in crypt through the route of reducing the $Dy(BH_4)_3$ complex followed by encapsulation of crypt, similar to the synthesis of $Tm(crypt)(OTf)_2$ reported in Chapter 8.

Experimental

All manipulations and syntheses described below were conducted with the rigorous exclusion of air and water using standard glovebox and high-vacuum line techniques under an argon atmosphere. Solvents were sparged with UHP argon and dried by passage through columns containing Q-5 and molecular sieves prior to use. Deuterated tetrahydrofuran (THF-d_8) and deuterated benzene (C_6D_6) were dried over NaK alloy, degassed by three freeze-pump-thaw cycles, and vacuum transferred before used. ^{1}H NMR spectra were recorded on a GN500 or CRYO500 MHz spectrometer at 298K unless otherwise stated and referenced internally to residual protio-solvent resonances. Tetramethylethylene was dried over sieves and degassed by three freeze-pump-thaw cycles prior to use. $Ln(BH_4)_3$ complexes were synthesized according to the literature.[6]

$Sm(H_3BCMe_2CMe_2H)_3$. Tetramethylethylene (0.13 mL, 0.93 mmol) was added to a solution of $Sm(BH_4)_3$, (60 mg 0.31 mol) in 10 mL of benzene. The reaction was left to stir overnight and the next day the reaction remained a clear solution. The solvent was removed to give $Sm(H_3BCMe_2CMe_2H)_3$. ^{1}H NMR (C_6D_6): δ 1.26 (s, 6H, $Sm(H_3BC\mathbf{Me_2}CMe_2H)_3$), δ 1.29 (d, 6H, $Sm(H_3BCMe_2C\mathbf{Me_2}H)_3$), δ 1.76 (sept., 1H, $Sm(H_3BCMe_2CMe_2\mathbf{H})_3$), δ3.56 (s, 3H, $Sm(\mathbf{H_3}BCMe_2CMe_2H)_3$).

$Dy(H_3BCMe_2CMe_2H)_3$. Tetramethylethylene (0.086 mL, 0.72 mol) was added to a solution of $Dy(BH_4)_3$ (50 mg, 0.24 mol) in 10 mL of THF. The reaction was left to stir overnight. The solvent was removed to give white solids presumed to be $Dy(H_3BCMe_2CMe_2H)_3$. This compound was soluble in THF only unlike its Sm analogue.

Sm^{III}(crypt)$(H_3BCMe_2CMe_2H)_3$. $Sm(H_3BCMe_2CMe_2H)_3$ (50 mg, 0.11 mmol) was dissolved in toluene and cryptand (41 mg, 0.11 mmol) was added. The solution was left to stir overnight. Upon the removal of solvent, colorless solids were obtained.

Sm^{II}(crypt)($H_3BCMe_2CMe_2H$)$_2$. The Sm(crypt)($H_3BCMe_2CMe_2H$)$_3$ precursor (90 mg, 0.11 mol) was dissolved in THF and cooled to – 35 °C. KC_8 (14 mg, 0.11 mmol) was added to this cooled solution which resulted in a color change from colorless to pink. To reduced solution was filtered, layered with Et_2O and placed in the freezer at – 35 °C. The next day, pink crystals were obtained (35 mg, 43% yield). Unfortunately, the crystal data were not of sufficient quality to reveal the structure.

References

1. Marks. T. J. Covalent Transition Metal, Lanthanide, and Actinide Tetrahydroborate Complexe. *Chem. Rev.* **1977**, 263-293.

2. Visseaux, M.; Bonnet, F., Borohydride complexes of rare earths, and their applications in various organic transformations. *Coord. Chem. Rev.* **2011,** *255* (3-4), 374-420.

3. Makhaev, V. D., Structural and dynamic properties of tetrahydroborate complexes. *Russ. Chem Rev.* **2000,** *69*, 727-746.

4. Ephritikhine, M., Synthesis, Structure, and Reactions of Hydride, Borohydride, and Aluminohydride Compounds of the f-Elements. *Chem. Rev.* **1997,** *97*, 2193-2242.

5. Ephritikhine, C. V. a. M., Novel Hydroboration of Highly Substituted Alkenes catalysed by Borohydride Complexes of Uranium, Neodymium and Zirconium. *J. Chem. Soc., Chem. Commun.* **1995**, 979-980.

6. Ortu, F.; Packer, D.; Liu, J.; Burton, M.; Formanuik, A.; Mills, D. P., Synthesis and structural characterization of lanthanum and cerium substituted cyclopentadienyl borohydride complexes. *J. Organometal. Chem.* **2018,** *857*, 45-51.

Chapter 7

Encapsulating Sm(II) in 2.2.1-Cryptand

Introduction

As described in previous Chapters 2 and 3, only the larger traditional Ln(II) ions, Nd(II) Sm(II) and Eu(II)[1] have been isolable in 2.2.2-cryptand (crypt); the smaller traditional Ln(II) ions, Dy(II) and Yb(II), have not yet been isolated in this coordination environment. One reason for this is that crypt complexes of the smaller Ln(III) ions have poor solubility in ethereal solvents suitable for alkali metal reduction. Thus, synthetic routes alternative to reduction of Ln(III)-in-crypt were pursued to encapsulate these late metals.

Another possible problem with incorporating the late lanthanide metals into crypt beyond the poor solubility of the Ln(III)-in-crypt compounds was that it was also possible that there may be competition between potassium with these smaller metals for the cryptand pocket.[1,2] Since potassium optimally fits the 2.2.2-cryptand pocket, a smaller cryptand,[3] 2.2.1-cryptand, was investigated to determine if this would be more suitable for the late lanthanides. Since 1987, only four crystallographically characterized complexes have been reported in the literature for this coordination environment: $[Pr(221crypt)(CH_3CN)_2]\cdot 3[ClO_4]$, $[Eu(221crypt)(H_2O)_2][Cl]_2$, $[La(221crypt)(NO_3)_2][H_2(221crypt)][La(NO_3)_6]$, and $[La(221crypt)(Cl)_2][Cl]$.[2,4-6] Like Ln-in-crypt complexes, 2.2.1-cryptand Ln complexes have been mostly limited to the +3 oxidation state with the larger metals Pr(III) and La(III), and only explored for the +2 oxidation state with Eu(II). This Chapter reports the exploration of the 2.2.1-cryptand ligand with Sm.

Results and Discussion

Addition of a slurry of colorless $Sm(OTf)_3$ in THF to a THF solution of 2.2.1-cryptand results in a THF-insoluble product, different from the reaction of $Sm(OTf)_3$ with 2.2.2-cryptand in which a THF-soluble product is formed.. Although this product was not soluble in THF, its reduction as a slurry with KC_8 was investigated. After about 30 seconds, the mixture generated a green soluble product. The mixture was filtered through a Kimwipe-packed pipette to remove solids and provide a clear green solution. This green solution was layered with Et_2O to give green crystals of $[Sm^{II}(221crypt)(OTf)(THF)][OTf]$. Although the proposed Sm(III) complex $[Sm(221crypt)(OTf)][OTf]_2$ precursor has not been isolated, a Sm(II) complex, $[Sm^{II}(221crypt)(OTf)(THF)][OTf$], equation 7.1, [[there is no eq 7.1 so I think this should be eq

7.1]]was characterizable by X-ray crystallography, Figure 7.1 Although connectivity could be established, the data was overall disordered and poorly resolved. Attempts to reproduce this result were not successful, as the KC_8 reduction of $[Sm(crypt)(OTf)][OTf]_2$ did not always proceed. However, as described in Chapter 5, reductions could be carried out reproducibly using liquid ammonia with Na^0.

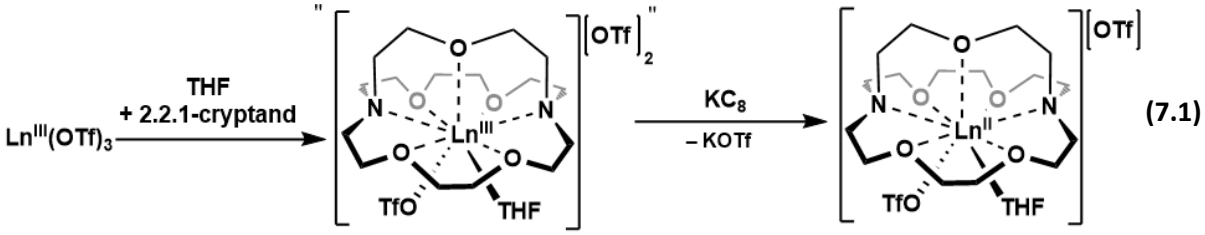

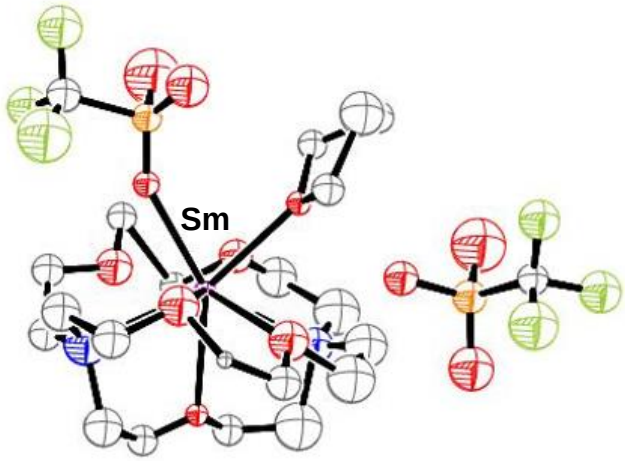

Figure 7.1. ORTEP representation of $[Sm^{II}(221crypt)(OTf)(THF)][OTf]$ with thermal ellipsoids drawn at the 30% probability level. Hydrogen atoms were omitted for clarity.

Conclusion

Chemical reduction of a Sm ion encapsulated by 221crypt to give the isolable [Sm^{II}(221crypt)(OTf)(THF)][OTf] complex demonstrates it is possible to expand on cryptands as ligands for the stabilization of lanthanides in the +2 oxidation state beyond 2.2.2-cryptand.

Experimental

All manipulations and syntheses described below were conducted with the rigorous exclusion of air and water using standard glovebox and high-vacuum line techniques under an argon atmosphere. Solvents were sparged with UHP argon and dried by passage through columns containing Q-5 and molecular sieves prior to use. $Ln(OTf)_3$ (Ln = Sm) (Fischer Scientific) was dried under high vacuum (10^{-5} Torr) for 48 h at 220 °C before use. 2.2.2-cryptand (4,7,13,16,21,24-hexaoxa-1,10-diazabicyclo[8.8.8]hexacosane, Aldrich) was placed under vacuum (1 x 10^{-3} Torr) for 12 h before use. 2.2.1-Cryptand was prepared as a 10 mM solution in THF and dried over sieves and degassed by three freeze-pump-thaw cycles.

[Sm(221crypt)(OTf)(THF)][OTf]. 2.2.1-Cryptand as a 10 mmol solution in THF (250 µL, 0.07 mmol) was added to a suspension of $Sm(OTf)_3$ (40 mg, 0.7 mmol) in THF. After 24 h, KC_8 was added to the suspension, and the supernatant changed from colorless to green. Crystals of [Sm(221crypt)(OTf)(THF)][OTf] suitable for X-ray crystallography were obtained from layering Et_2O onto the filtered THF solution. Alternatively, the complex could be isolated by reducing the solids from the reaction of 2.2.1-cryptand with $Sm(OTf)_3$ via Birch reduction as described in Chapter 5.

References

1. T. C. Jenks, Akhila, N. W. Kuda-Wedagedara, M. D. Bailey, C. L. Ward, M. J. Allen. Spectroscopic and Electrochemical Trends in Divalent Lanthanides through Modulation of Coordination Environment *Inorg. Chem.* **2020**, *59*, 2613-2620.

2. Lenora, C. U., Staples, R. J, Allen, M. J. Measurement of the Dissociation of Eu^{II}-Containing Cryptates Using Murexide. *Inorg. Chem.* **2020,** *59*, 86-93.

3. Lehn, J. M., Cryptates: The Chemsitry of Macropolycyclic Inclusion Complexes. *Acc. Chem.* **1978**, (11), 49-57.

4. Rebizant, J., Spirlet, M. R., Barthelemy, P. P., Desreux, J. F. Solid state and solution structures of the lanthanide complexes with cryptand (2.2.1): Crystallographic and NMR studies of a dimeric praseodymium (2.2.1) cryptand containing two μ-hydroxo bridges. *J. Inclusion. Phenom. Mol. Recog. Chem.* **1987**, *5*, 505-513

5. Jiang-Gao, M., Zhong-Sheng, J., Jia-Zuan, N. *Chin. J. Struct. Chem.* **1992**, *11*, 302.

6. Oh, S. J., Song, K. H., Whang, D., Kim, K., Yoon, T. H., Moon, H., Park, J. W. Catalytic Hydrolysis of Phosphate Diester by Lanthanide(III) Cryptate (2.2.1) Complexes. *Inorg. Chem.* **1996**, *35*, 3780-3785.

Chapter 8

Encapsulating Tm(II) and Sm(II) in 2.2.2-Cryptand

As described in Chapters 2 and 3, only a few complexes with Ln(II) ions in 2.2.2-cryptand (crypt) were known even 30 years after the first Ln(III)-in-crypt complex was reported.[1-13] Moreover, initially all of these Ln(II)-in-crypt complexes involved the most stable Ln(II) ions of Sm, Eu, and Yb. The formation of the M(II)-in-crypt complexes in Chapter 2 required the development of THF soluble Ln(III)-in-crypt complexes which were obtained by using $Ln(OTf)_3$ precursors, equations 8.1 and 8.2.

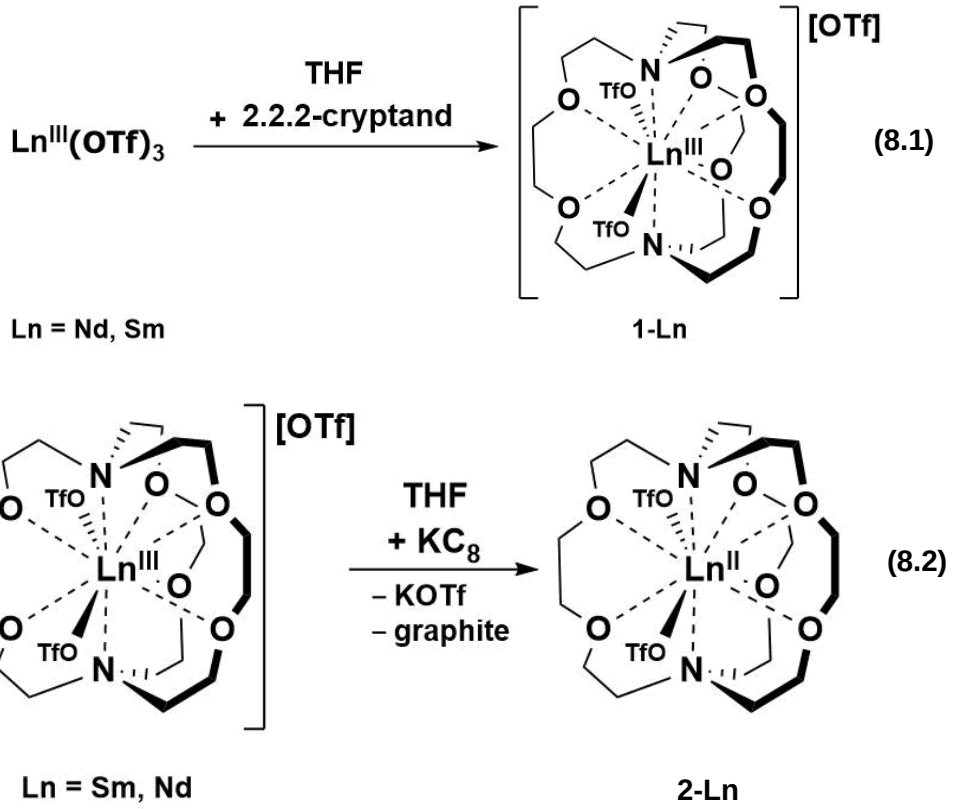

Additionally, it was shown that solubility of these Ln(III)-in-crypt complexes, which was essential to the alkali metal reduction to achieve the +2 oxidation state, was limited to the larger lanthanide metals. Only chemical reduction was definitively observed for Sm and Nd. Attempts to expand this chemistry to the smaller metals was not successful because the Ln(III) precursors precipitated out of solvents that were suitable for alkali metal reduction. Thus, synthetic routes alternative to reduction of Ln(III)-in-crypt were pursued to encapsulate these late metals.

Attempts to make Ln(II)-in-crypt complexes of the smaller lanthanides, Ln = Gd, Tb, Dy, Ho, Er, Tm, and Yb, are complicated because Ln(III)-in-crypt complexes for these ions are not soluble in THF. With Ln = Sm, it is possible to reduce $Sm(OTf)_3$ to generate a solution presumed to be "$Sm^{II}(OTf)_2$".[14] Reduction of $Ln(OTf)_3$, such as $Sm(OTf)_3$, $Dy(OTf)_3$ and $Tm(OTf)_3$ were

investigated followed by the addition of crypt to see if Ln(II)-in-crypt complexes could be isolated in this way.

Results and Discussion

Isolation of Sm^{II}(crypt)$(OTf)_2$. A suspension of $Sm^{III}(OTf)_3$ in THF reacts with KC_8 to generate a dark red solution presumed to be "$Sm^{II}(OTf)_2$". Addition of crypt to this purple solution results in a color change to pink. Isolation of the product is achieved by layering the pink THF solution with Et_2O at – 35 °C which yields Sm^{II}(crypt)$(OTf)_2$, which was identified by X-ray crystallography.

Isolation of [Tm^{II}(crypt)(OTf)][OTf]. A solution of $Tm^{III}(OTf)_3$ in THF reacts with KC_8 to generate a dark purple solution presumed to be "$Tm^{II}(OTf)_2$". Addition of crypt to this purple solution results in a slight color change to a different hue of purple. Isolation of the product is achieved by layering the purple THF solution with Et_2O at – 35 °C which yields [Tm^{II}(crypt)(OTf)][OTf]. The product has one triflate ligand coordinated to the metal and one outer-sphere triflate, identified by single crystal X-ray diffraction, Figure 8.3.

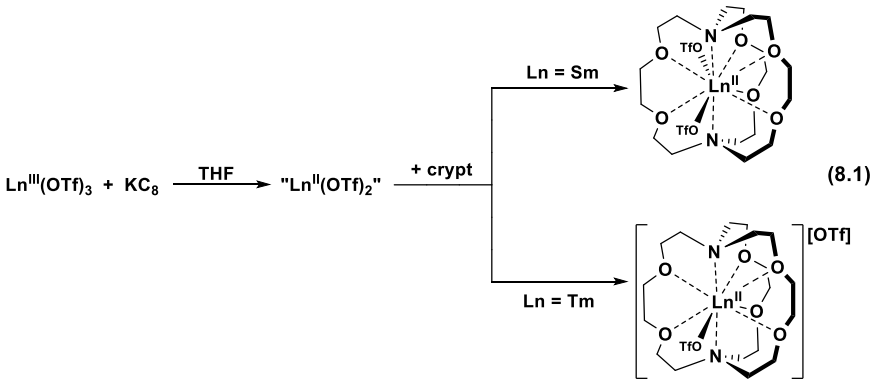

(8.1)

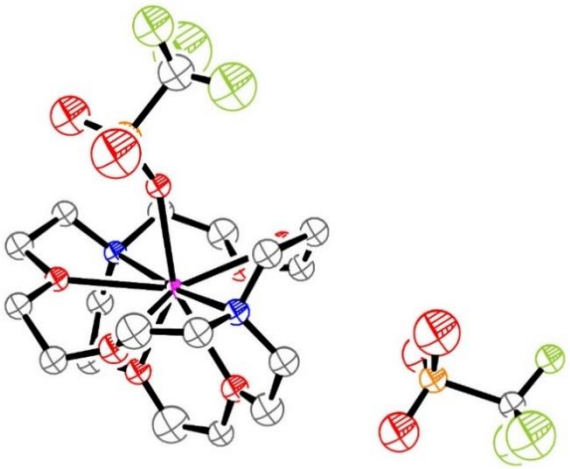

Figure 8.1. ORTEP representation of $[Tm^{II}(crypt)(OTf)][OTf]_2$ with thermal ellipsoids drawn at the 30% probability level. Hydrogen atoms were omitted for clarity.

Attempted Reduction of $Dy(OTf)_3$. Because it was possible to isolate a Sm(II)-in-crypt and a Tm(II)-in-crypt complex by reducing the $Ln(OTf)_3$ precursor, this was also attempted with $Dy(OTf)_3$. When KC_8 was added to a suspension of $Dy(OTf)_3$, no color change was observed and the KC_8 remained a copper color indicating that it was unreacted. The $Dy(OTf)_3$, unlike $Sm(OTf)_3$ and $Tm(OTf)_3$, could not be reduced.

Conclusion

As reported in Chapter 2, a $[Sm^{III}(crypt)(OTf)_2][OTf]$ complex can be chemically reduced by KC_8 reduction to generate a $Sm^{II}(crypt)(OTf)_2$ complex. Here it is described that it is possible to reduce the $Sm(OTf)_3$ precursor followed by encapsulation of crypt to produce the same $Sm^{II}(crypt)(OTf)_2$ complex through this different route. Although chemical reduction of a Tm(III)-in-crypt precursor has not yet been fruitful, it is possible to isolate a Tm(II)-in-crypt complex by reacting a solution of $Tm(OTf)_3$ that has been reduced using KC_8 with crypt to yield

$[Tm^{II}(crypt)(OTf)][OTf]$. While this was possible with $Sm(OTf)_3$ and $Tm(OTf)_3$, reductions of $Dy(OTf)_3$ did not proceed.

Experimental

All manipulations and syntheses described below were conducted with the rigorous exclusion of air and water using standard glovebox and high-vacuum line techniques under an argon atmosphere. Solvents were sparged with UHP argon and dried by passage through columns containing Q-5 and molecular sieves prior to use. $Ln(OTf)_3$ (Ln = Sm, Tm) (Fischer Scientific) were dried under high vacuum (10^{-5} Torr) for 48 h at 220 °C before use. 2.2.2-Cryptand (4,7,13,16,21,24-hexaoxa-1,10-diazabicyclo[8.8.8]hexacosane, Aldrich) was placed under vacuum (1×10^{-3} Torr) for 12 h before use.

[Sm(crypt)(OTf)$_2$]. In an argon filled glovebox, a colorless THF (5 mL) solution of $Sm(OTf)_3$ (60 mg, 0.06 mmol) chilled to – 25 °C was added to a vial of KC_8 (12 mg, 0.088 mmol) chilled to –35 °C. The reaction mixture became pink and was stirred for 1 min. The reaction mixture was filtered on to a solution of crypt (20 mg, 0.06 mmol) which resulted in an immediate color change to red. Red crystals were isolated by layering the red THF solution with Et_2O at – 35 °C that were determined to be $Sm(crypt)(OTf)_2$ by X-ray crystallography.

[Tm(crypt)(OTf)][OTf]. A 5 mL solution of $Tm(OTf)_3$ (50 mg, 0.08 mmol) in THF was chilled to −35 °C. When KC_8 (16 mg, 0.12 mmol) was added to the colorless solution, it turned dark purple. Crypt (27 mg, 0.08 mmol) was added to the dark purple solution. The purple solution was filtered over chilled Et_2O. After 1d, dark purple crystals of [Tm(crypt)(OTf)][OTf] suitable for X-ray crystallography were obtained.

References

1. Dietrich, B., Lehn, J. M., Sauvage, J. P., Blanzat, J. Synthesis et Proprietes Physiques de Systemes Diaza-polyoxa-macrobicycliques. *Tetrahedron.* **1973,** *29*, 1629-1645.

2. Benetollo, F. B., G.; Cassol, A.; De Paoli, G.; Legendziewicz, J., Coordination chemistry of lanthanides with cryptands. An X-ray and spectroscopic study of the complex $Nd_2(NO_3)_6$ $[C_{18}H_{36}O_6N_2]\cdot H_2O$. *Inorg. Chem. Acta.* **1985,** *110*, 7-13.

3. Burns, J. H., Crystal and molecular structure of a cryptate complex of samarium: $C_{18}H_{36}O_6N_2Sm_2(NO_3)_6\cdot H_2O$. *Inorg. Chem.* **1979,** *18*, 3044-3047.

4. Dietrich, B. Lehn, J. M., Sauvage, J. P., Cryptates—XI: Complexes macrobicycliques, formation, structure, proprietes. *Tetrahedron.* **1973,** *29*, 1647-1658.

5. Ekanger, L. A.; Polin, L. A.; Shen, Y.; Haacke, E. M.; Martin, P. D.; Allen, M. J., A Eu(II)-Containing Cryptate as a Redox Sensor in Magnetic Resonance Imaging of Living Tissue. *Angew. Chem. Int. Ed.* **2015,** *54* (48), 14398-401.

6. Gamage, N. D.; Mei, Y.; Garcia, J.; Allen, M. J., Oxidatively stable, aqueous europium(II) complexes through steric and electronic manipulation of cryptand coordination chemistry. *Angew. Chem. Int. Ed.* **2010,** *49* (47), 8923-5.

7. Huh, D. N.; Kotyk, C. M.; Gembicky, M.; Rheingold, A. L.; Ziller, J. W.; Evans, W. J., Synthesis of rare-earth-metal-in-cryptand dications, $[Ln(2.2.2\text{-cryptand})]^{2+}$, from Sm^{2+}, Eu^{2+}, and Yb^{2+} silyl metallocenes $(C_5H_4SiMe_3)_2Ln(THF)_2$. *Chem. Commun.* **2017,** *53* (62), 8664-8666.

8. Huh, D. N.; Windorff, C. J.; Ziller, J. W.; Evans, W. J., Synthesis of uranium-in-cryptand complexes. *Chem. Commun.* **2018,** *54* (73), 10272-10275.

9. Huh, D. N.; Ziller, J. W.; Evans, W. J., Facile Encapsulation of Ln(II) Ions into Cryptate Complexes from $LnI_2(THF)_2$ Precursors (Ln = Sm, Eu, Yb). *Inorg. Chem.* **2019,** *58* (15), 9613-9617.

10. Jenks, T. C.; Kuda-Wedagedara, A. N. W.; Bailey, M. D.; Ward, C. L.; Allen, M. J., Spectroscopic and Electrochemical Trends in Divalent Lanthanides through Modulation of Coordination Environment. *Inorg. Chem.* **2020,** *59* (4), 2613-2620.

11. Lenora, C. U.; Carniato, F.; Shen, Y.; Latif, Z.; Haacke, E. M.; Martin, P. D.; Botta, M.; Allen, M. J., Structural Features of Europium(II)-Containing Cryptates That Influence Relaxivity. *Eur. J. Chem.* **2017,** *23* (61), 15404-15414.

12. Mao, J. J., Z., Synthesis and structure characterization of lanthanum [2,2,2]cryptates, $[LaCl[2,2,2](H_2O)]Cl_2 \cdot H_2O$ and $[La(CF_3SO_3)[2,2,2](DMF)](CF_3SO_3)_2$. *Polyhedron.* **1994,** *12*, 319-323.

13. Yang, G. L., S.; Jin, Z., Coordination chemistry and structure characterization of $C_{18}H_{36}O_6N_2Eu_2(NO_3)_6 \cdot H_2O$. *Inorg. Chem. Acta.* **1987,** *131*, 125-128.

14. Maisano, T.; Tempest, K. E., Sadasivam, D. V.; Flowers, R. A., 2nd, A convenient pathway to Sm(II)-mediated chemistry in acetonitrile. *Org. Biomol. Chem.* **2011,** *9* (6), 1714-6.

Chapter 9

X-ray Photoelectron Spectroscopy of $[Gd^{III}[N(SiMe_3)_2]_3]$, $[K(2.2.2\text{-cryptand})][Gd^{II}[N(SiMe_3)_2]_3]$, $(C_5Me_4H)_3Gd^{III}$, and $[K(2.2.2\text{-cryptand})][(C_5Me_4H)_3Gd^{II}]$ Complexes

Introduction*

One of the major advances in the chemistry of the lanthanide elements was the discovery that Ln(II) ions are accessible in soluble molecular complexes for not only Eu, Yb, Sm, Tm, Dy, and Nd, but also for all the rest of the lanthanides except radioactive Pm.[1-6] For the complexes of all the new Ln(II) ions, structural, spectroscopic, and magnetic data as well as analysis by density

functional theory (DFT) indicated that the product of the reduced $4f^n$ Ln(III) ion was not the expected $4f^{n+1}$ Ln(II), but instead a $4f^n5d^1$ Ln(II) ion. The unusual nature of the $4f^n5d^1$ mixed principal quantum number configuration of the non-traditional Ln(II) ions made the complexes an interesting topic for detailed spectroscopic studies.

In 2017, the electronic structure of [K(2.2.2-cryptand)][Cp′$_3$Ln] complexes of Ln = Pr, Nd, Sm, Gd, Tb, Dy, Ho, Er, Tm, Yb, and Lu were examined by X-ray absorption near-edge spectroscopy (XANES).[7] The L-edge XANES spectra of the $4f^{n+1}$ Ln(II) ions exhibited ~ 7 eV lower energy than their Ln(III) precursors. However, the $4f^n5d^1$ Ln(II) ions were only ~ 0.5 eV different from those of their Ln(III) precursors.

* Portions of this chapter have been published in Huh, D. N., Bruce, J. P., Balasubramani, S. G., **Ciccone, S. R**., Furche, F., Hemminger, J. C., Evans, W. J. High-Resolution X-ray Photoelectron Spectroscopy of Organometallic $(C_5H_4SiMe_3)_3Ln^{III}$ and $[(C_5H_4SiMe_3)_3Ln^{II}]^{1-}$ Complexes (Ln = Sm, Eu, Gd, Tb). *J. Am. Chem. Soc.* **2021**, *143*, 16610-16620.

Electronic calculations revealed that the difference between the spectra of the $4f^{n+1}$ and $4f^n5d^1$ ion could be attributed to the greater Coulombic repulsion experienced by the 2p-electrons from the 4f-electrons compared to the 5d-electrons.[7] A complementary approach to defining electronic structure is X-ray photoelectron spectroscopy (XPS).

XPS provides an evaluation of the core and valence orbitals. For organometallic lanthanide complexes, few have been characterized by XPS, with most studies focusing on the metals, metal oxides, chalcogenides, phosphates, and alloys. In 2021, XPS data were reported on the Cp′ ligand system for both the +3 and +2 oxidation state, extending the scope of available data for XPS data of lanthanide complexes.[8] Data were obtained on Sm, Eu, Gd and Tb to compare the spectra of ions with a $4f^{n+1}$ electron configuration to the spectra of ions with a $4f^n5d^1$ electron configuration.

Figure 9.1. The Ln 4d regions of the Ln(III) and Ln(II) complexes were identified and compared, and the 4d peaks were used to identify a consistent shift of ~ 1 eV between the two oxidation states. The study also reported the tentative assignment of the $5d^1$ electron in the Gd(II) spectrum, consistent with a $4f^n5d^1$ electron configuration, Figure 9.2.[8]

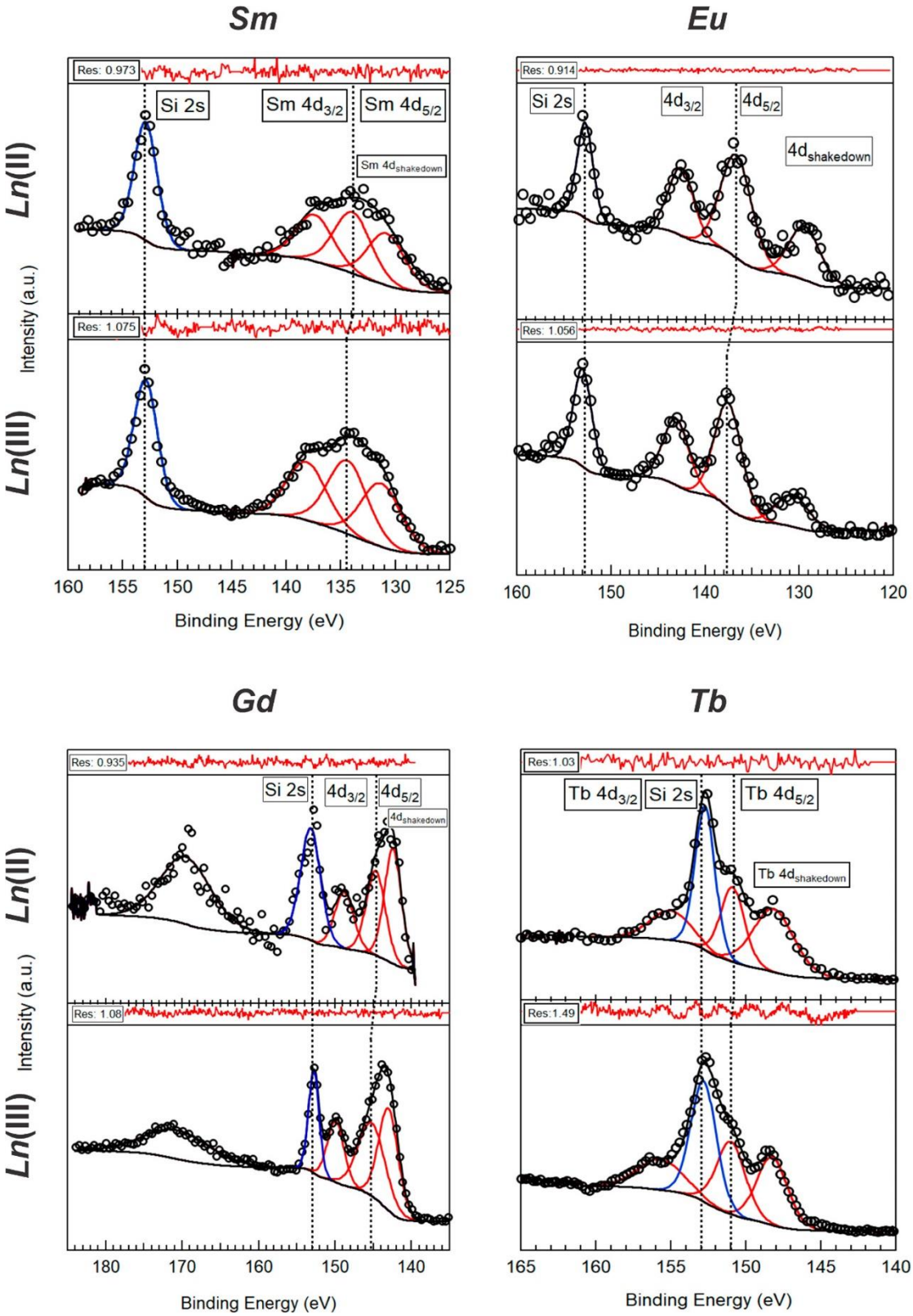
Sm
Res: 0.973
Si 2s
Sm 4d3/2
Sm 4d5/2
Sm 4dshakedown
Res: 1.075
Ln(II)
Ln(III)
Intensity (a.u.)
160 155 150 145 140 135 130 125
Binding Energy (eV)
Eu
Res: 0.914
Si 2s
4d3/2
4d5/2
4dshakedown
Res: 1.056
160 150 140 130 120
Binding Energy (eV)
Gd
Res: 0.935
Si 2s
4d3/2
4d5/2
4dshakedown
Res: 1.08
180 170 160 150 140
Binding Energy (eV)
Tb
Res:1.03
Tb 4d3/2
Si 2s
Tb 4d5/2
Tb 4dshakedown
Res:1.49
165 160 155 150 145 140
Binding Energy (eV)

Figure 9.1. Ln 4d spectra of [K(crypt)][Cp'_3Ln^{II}] (top) and Cp'_3Ln^{III} (bottom) for Ln = Sm, Eu, Gd, and Tb. The red peaks are modeled for the Ln 4d peaks, while blue peaks are Si 2s peaks that occur in the same region. Shifts in all spectra from Ln(III) to Ln(II) show a shift of the 4d regions to lower binding energies.[8]

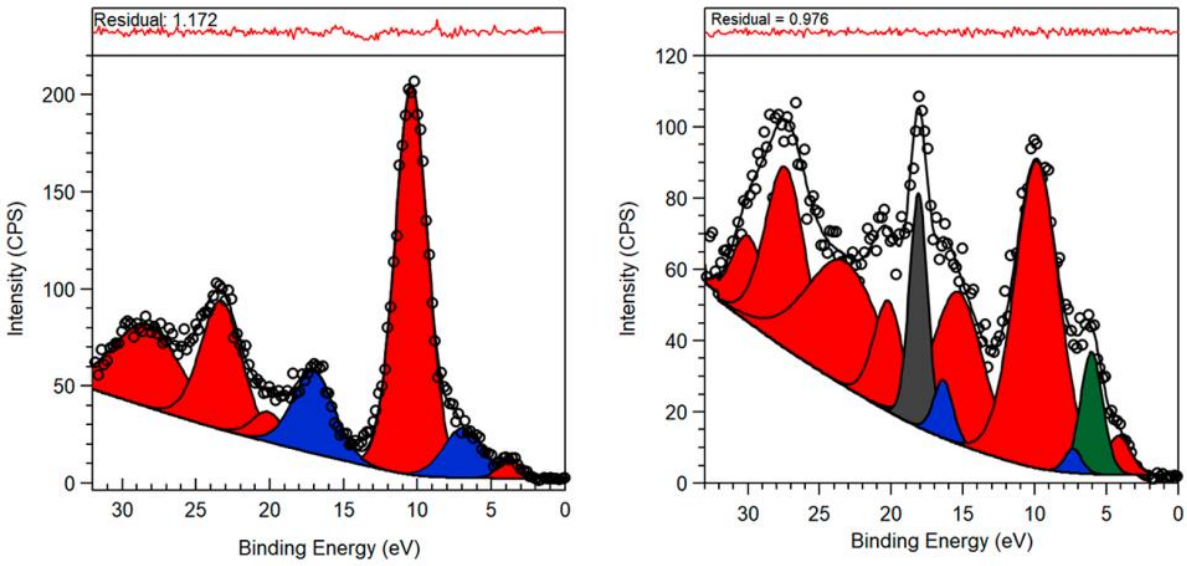

Figure 9.2. Valence XPS region of Cp'_3Gd^{III} (left) and [K(crypt)][Cp'_3Gd^{II}] (right). The red peaks represent valence orbitals associated with Gd, the blue peaks represent orbitals associated with the Cp′ ligand, the gray peak represents the K 2p orbital, and the green peak is assigned to the Gd 5d orbital.[8]

To follow up on these XPS studies, [$Gd[N(SiMe_3)_2]_3$], [K(crypt)][$Gd[N(SiMe_3)_2]_3$], $(C_5Me_4H)_3Gd$ and [K(crypt)][$(C_5Me_4H)_3Gd$] were examined for comparison as described in this Chapter.

Results and Discussion

Carbon 1s Region. The C 1s region for $Gd(NR_2)_3$ (R = $SiMe_3$), **1-Gd(III)**, [K(crypt)][$Gd(NR_2)_3$] (crypt = 2.2.2-cryptand), **1-Gd(II)**, $Cp^{tet}{}_3Gd$ (Cp^{tet} = C_5Me_4H), **2-Gd(III)**,

and [K(crypt)][Cp^{tet}_3Gd], **2-Gd(II)**, were compared. The C 1s region in each spectrum of **1-Gd(III)** and **2-Gd(III)**, Figure 9.3, shows expected differences from the C 1s region in each spectrum of **1-Gd(II)** and **2-Gd(II)**, Figure 9.4, specifically that more peaks are present in the Ln(II) spectra due to the presence of the $[K(crypt)]^+$ counter ion. The C 1s region of **1-Gd(III)** shows a single peak at 281.9 eV which has been assigned to the methyl group of the $SiMe_3$ substituent in the $N(SiMe_3)_2$ ligand, Table 9.1. In comparison, the C 1s region of **1-Gd(II)** shows a peak at 281.5 eV ($SiMe_3$) and a peak at 283.2 eV which corresponds to the crypt in the [K(crypt)]+ counter ion. The C 1s region of **2-Gd(III)** shows two peaks at 281.5 eV and 282.6 eV which can be assigned to the ring carbons of the Cp^{tet} ligand, Cp_{ring}, and the methyl groups of the Cp^{tet} ligand, Cp_{Me}, respectively. The Cp_{ring} carbons were assigned to lower binding energies than the Cp_{Me} carbons due to the negative charge that is delocalized in the cyclopentadienide ring. In comparison, the C 1s region of **2-Gd(II)** shows peaks at 283.2 eV (crypt), 281.5 eV (Cp_{Me}), and 280.4 eV (Cp_{ring}). These features are consistent with the data that was previously reported on Cp'_3Gd and [K(crypt)][Cp'_3Gd] complexes ($Cp' = C_5H_4SiMe_3$).[8]

Table 9.1. The binding energies for **1-Gd(III)**, **2-Gd(III)**, **1-Gd(II)**, **and 2-Gd(II)** C 1s region.

	Crypt	**Si*Me*$_3$**	**Cp$_{Me}$**	**Cp$_{ring}$**
1-Gd(III)	-	281.9	-	-
2-Gd(III)	-	-	282.6	281.5
1-Gd(II)	283.2	281.5	-	-
2-Gd(II)	283.2	-	281.5	280.4

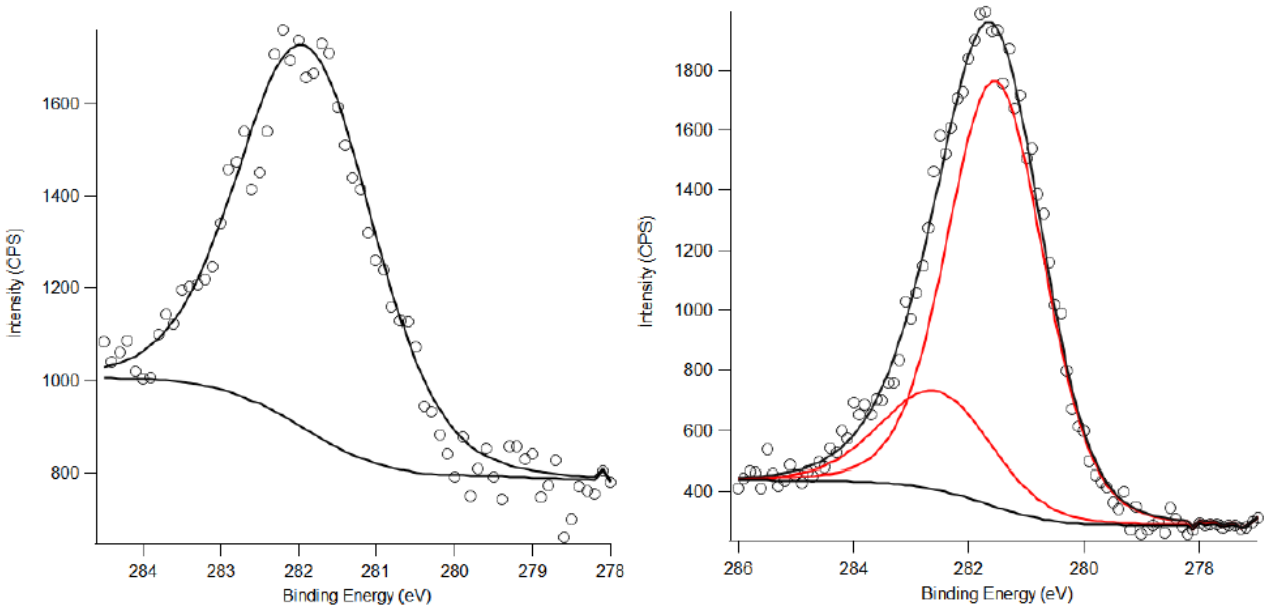

Figure 9.3. C 1s XPS region of **1-Gd(III)**(left) and **2-Gd(III)**(right). The black circles indicate the photoelectron spectrum and the red lines indicate fits.

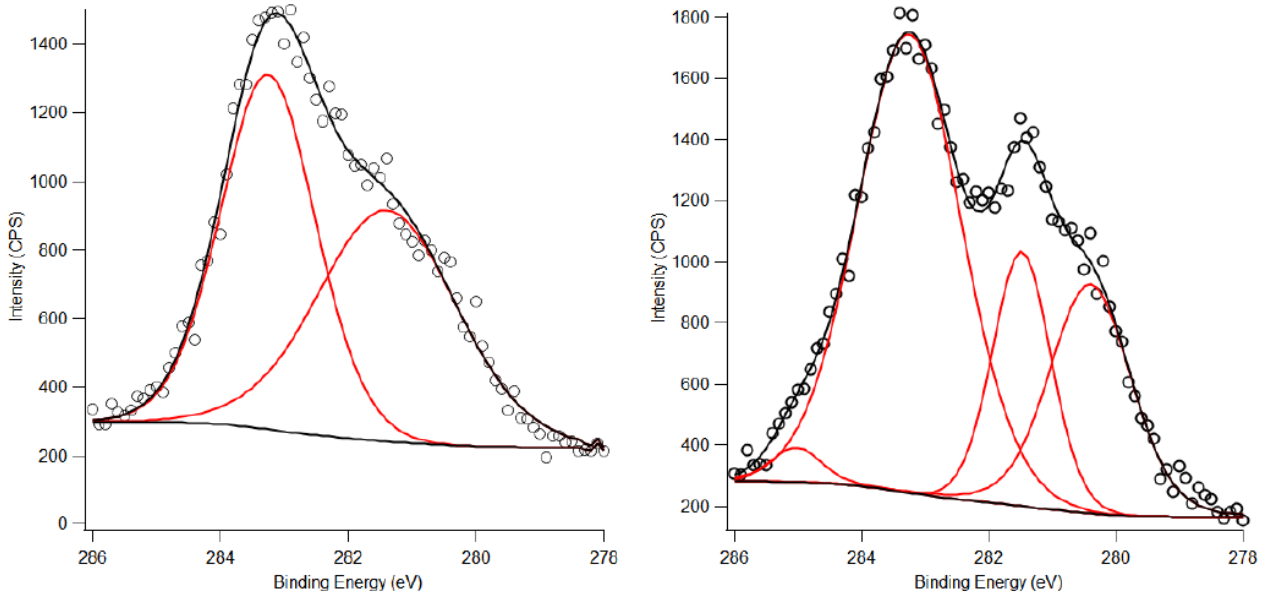

Figure 9.4. C 1s XPS region of **1-Gd(II)**(left) and **2-Gd(II)**(right). The black circles indicate the photoelectron spectrum and the red lines indicate fits.

3d Region. The XPS binding energies (BE) of the 3d region of $Gd(NR_2)_3$, **1-Gd(III)**, [K(crypt)][$Gd(NR_2)_3$], **1-Gd(II)**, Cp^{tet}_3Gd, **2-Gd(III)**, and [K(crypt)][Cp^{tet}_3Gd], **2-Gd(II)**, were compared. Whereas the XPS studies reported in 2021[8] have some overlap in the 4d region from the $4d_{3/2}$ and $4d_{5/2}$ peaks, the 3d region for these Gd complexes has good separation between the $3d_{3/3}$ and $3d_{5/2}$ peaks. For **1-Gd(III)**, BE($3d_{5/2}$) = 1184.3 eV and BE($3d_{3/2}$) = 1216.5 eV. For **1-Gd(II)**, BE($3d_{5/2}$) = 1182.6 eV and BE($3d_{3/2}$) = 1215.1 eV. For **2-Gd(III)**, BE($3d_{5/2}$) = 1184.2 eV and BE($3d_{3/2}$) = 1216.4 eV; for **2-Gd(II)**, BE($3d_{5/2}$) = 1182.8 eV; BE(3d3/2) = 1215.4 eV, Table 3. For both pairs, a shift to lower binding energies of approximately 1 eV is observed from the Gd +3 oxidation state to the Gd +2 oxidation state, Figure 9.5. This is similar to the shift previously observed for Cp'_3Gd and [K(crypt)][Cp'_3Gd].[8]

Table 9.2. The binding energies for **1-Gd(III)**, **2-Gd(III)**, **1-Gd(II)**, **and 2-Gd(II)** 3d region.

	$3d_{5/2}$	**$3d_{3/2}$**
1-Gd(III)	1184.3	1216.5
2-Gd(III)	1184.2	1216.4
1-Gd(II)	1182.6	1215.1
2-Gd(II)	1182.8	1215.4

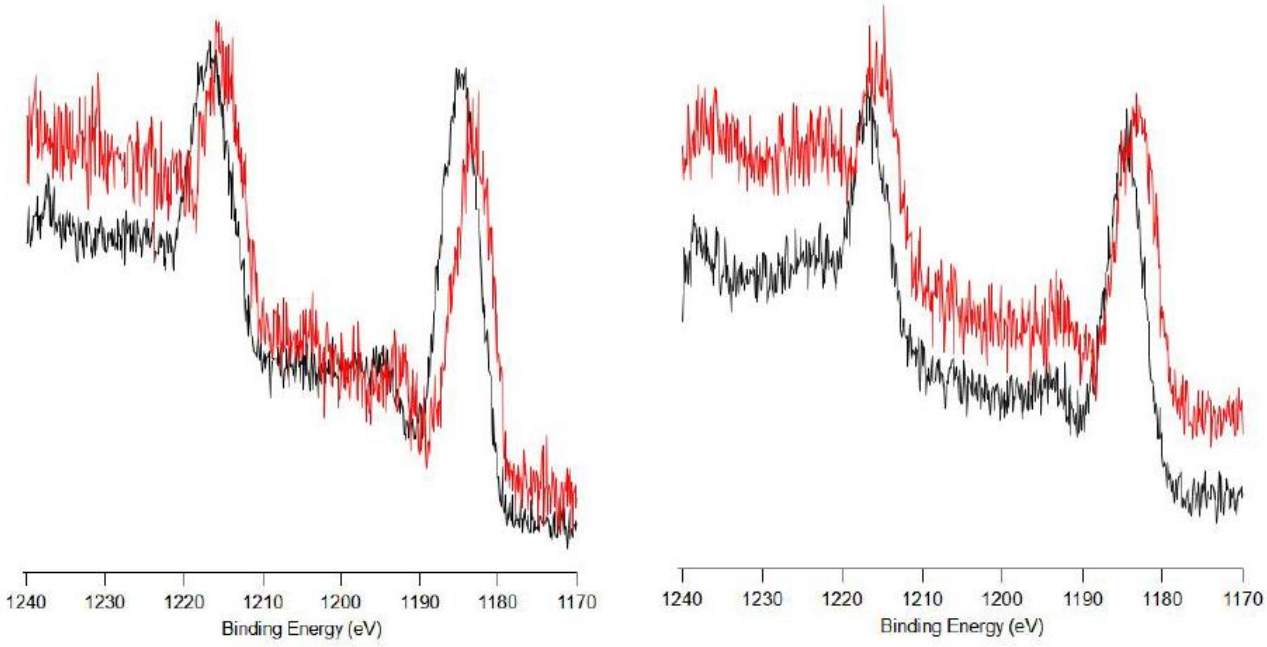

Figure 9.5. Overlay of the 3d region of **1-Gd(III)**(black) and **1-Gd(II)** (red) (left) and overlay of the 3d region of **2-Gd(III)** (black) and **2-Gd(II)** (red)(right).

Valence Region. The valence regions of $[Gd(NR_2)_3]^{1-}$ and $[Cp^{tet}_3Gd]^{1-}$ were examined, but unlike that of $[Cp'_3Gd]^{1-}$, it was difficult to assign a peak to a $5d^1$ electron. Between Cp'_3Gd and $[Cp'_3Gd]^{1-}$, the valence band is clearly changed. However, the only distinguishable difference that appears in the $[Gd(NR_2)_3]^{1-}$ and $[Cp^{tet}_3Gd]^{1-}$ spectra comes from a peak attributed to crypt at ~14 eV, Figure 9.6.

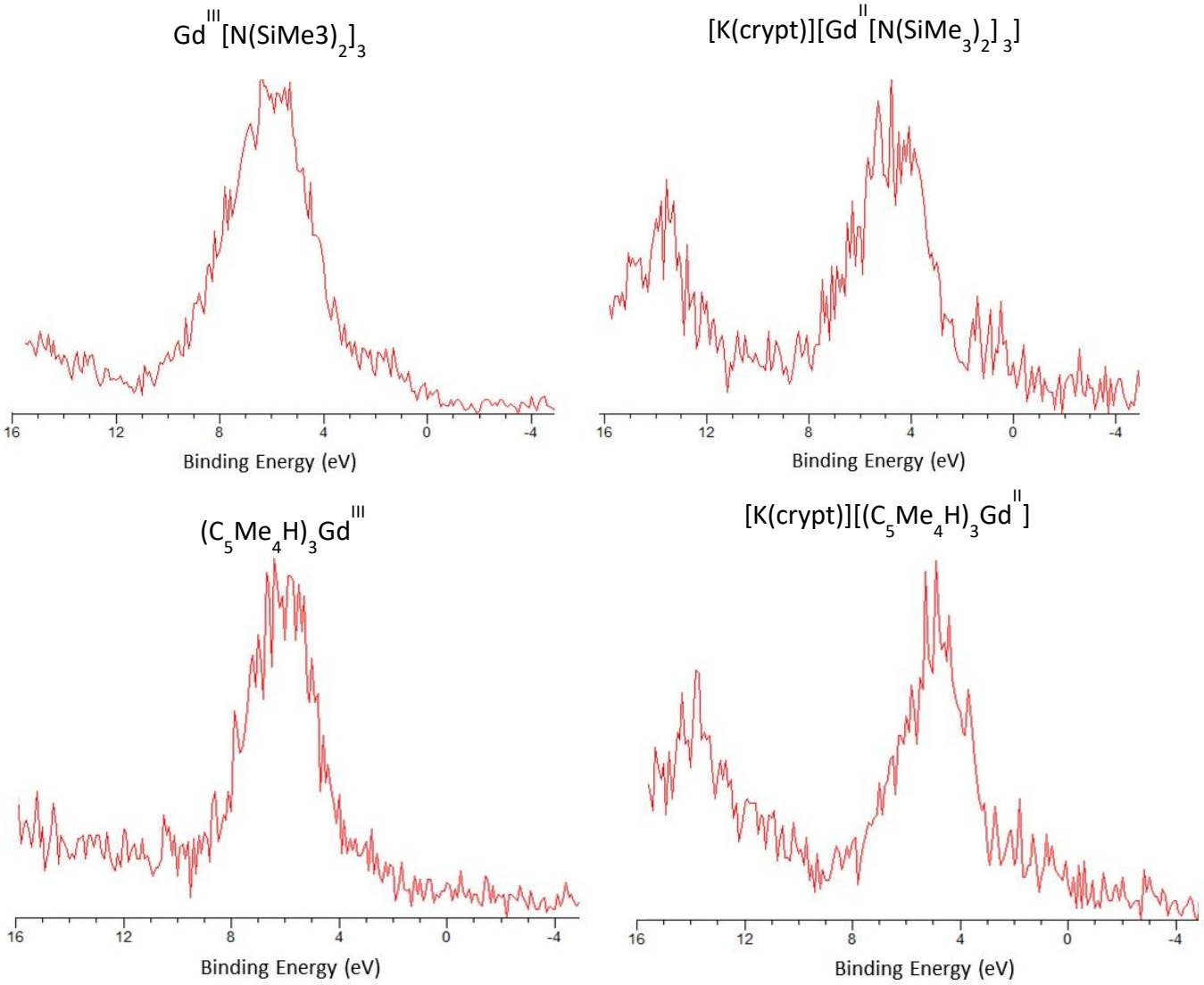

Figure 9.6. Valence bands of **1-Gd(III)** (top left), **1-Gd(II)** (top right), **2-Gd(III)** (bottom left), and **2-Gd(II)** (bottom right).

Conclusion

Gadolinium was investigated in these XPS studies because it was thought that the isolated $^8S_{7/2}$ ground state of Gd(III) would allow for a more simple assignment of the valence region compared to other lanthanide metals, but this was not the case. It may be that, with these complexes, it is difficult to see the $5d^1$ peak appear in the +2 spectra because of the close energy to the 4f orbitals. While it has been shown that it is possible to collect XPS data on these highly

reactive non-traditional molecular complexes, the data are difficult to analyze. In comparison to the XANES result where there is a substantial energy difference between the $4f^{n+1}$ and $4f^n5d^1$ ions, XPS data show an approximately 1 eV shift from the +2 to the +3 oxidation state for both traditional and non-traditional metals.

Experimental

XPS was performed on a Kratos Axis Supra DLD spectrometer (Kratos Analytical Ltd.) with monochromated Al Kα radiation (1486.6 eV) at 10-mA emission current and 15-kV anode voltage with a base pressure of 1 x 10-9 Torr. Experiments were performed with the charge neutralizer with a filament current of 1.8 A and a bias of 3.0V. Spectra were collected with a fixed-analyzer transmission mode, survey scans were collected with a pass energy of 20 eV. All samples were mounted on a stainless steel stub with double-sided copper tape in a nitrogen–filled glovebox attached to the instrument. Samples were synthesized according to the literature.[9, 10] The samples were placed in a Schlenk tube with a Teflon screw cap and then placed on a high-vacuum line (10^{-5} Torr) overnight to remove any residual solvent. The Schlenk tube was then transferred to a N_2 glovebox which is directly attached to the AXIS Supra by a Kratos Analytical XPS instrument. In the glovebox, the lanthanide samples were then mounted on a stainless-steel stub with double-sided copper tape. The stub was then transferred from the glovebox into the XPS instrument for measurement. No changes to the crystal color or size were observed during transfer between gloveboxes, and there was no observable oxidation or hydrolysis of the lanthanide complexes in the photoelectron spectra.Peak fitting was performed with CasaXPS software (Casa Software Ltd.) using a Shirely baseline and 70% Gaussian – 30% Lorentzian function for the peaks.

References

1. Fieser, M. E.; MacDonald, M. R.; Krull, B. T.; Bates, J. E.; Ziller, J. W.; Furche, F.; Evans, W. J., Structural, spectroscopic, and theoretical comparison of traditional vs recently discovered Ln(2+) ions in the [K(2.2.2-cryptand)][$(C_5H_4SiMe_3)_3$Ln] complexes: the variable nature of Dy(2+) and Nd(2+). *J. Am. Chem. Soc.* **2015,** *137* (1), 369-82.

2. Hitchcock, P. B.; Lappert, M. F.; Maron, L.; Protchenko, A. V., Lanthanum does form stable molecular compounds in the +2 oxidation state. *Angew. Chem. Int. Ed.* **2008,** *47* (8), 1488-91.

3. MacDonald, M. R.; Bates, J. E.; Fieser, M. E.; Ziller, J. W.; Furche, F.; Evans, W. J., Expanding rare-earth oxidation state chemistry to molecular complexes of holmium(II) and erbium(II). *J. Am. Chem. Soc.* **2012,** *134* (20), 8420-3.

4. MacDonald, M. R.; Bates, J. E.; Ziller, J. W.; Furche, F.; Evans, W. J., Completing the series of +2 ions for the lanthanide elements: synthesis of molecular complexes of Pr^{2+}, Gd^{2+}, Tb^{2+}, and Lu^{2+}. *J. Am. Chem. Soc.* **2013,** *135* (26), 9857-68.

5. MacDonald, M. R.; Ziller, J. W.; Evans, W. J., Synthesis of a crystalline molecular complex of Y^{2+}, [(18-crown-6)K][$(C_5H_4SiMe_3)_3$Y]. *J. Am. Chem. Soc.* **2011,** *133* (40), 15914-7.

6. Woen, D. H.; Chen, G. P.; Ziller, J. W.; Boyle, T. J.; Furche, F.; Evans, W. J., Solution Synthesis, Structure, and CO_2 Reduction Reactivity of a Scandium(II) Complex, Sc[$N(SiMe_3)_2$]$_3$. *Angew. Chem. Int. Ed.* **2017,** *56* (8), 2050-2053.

7. Fieser, M. E.; Ferrier, M. G.; Su, J.; Batista, E.; Cary, S. K.; Engle, J. W.; Evans, W. J.; Lezama Pacheco, J. S.; Kozimor, S. A.; Olson, A. C.; Ryan, A. J.; Stein, B. W.; Wagner, G. L.; Woen, D. H.; Vitova, T.; Yang, P., Evaluating the electronic structure of formal Ln(II) ions in [Ln(II)$(C_5H_4SiMe_3)_3]^{1-}$ using XANES spectroscopy and DFT calculations. *Chem. Sci.* **2017,** *8* (9), 6076-6091.

8. Huh, D. N.; Bruce, J. P.; Ganesh Balasubramani, S.; Ciccone, S. R.; Furche, F.; Hemminger, J. C.; Evans, W. J., High-Resolution X-ray Photoelectron Spectroscopy of Organometallic $(C_5H_4SiMe_3)_3$Ln(III) and $[(C_5H_4SiMe_3)_3$Ln(II)$]^{1-}$ Complexes (Ln = Sm, Eu, Gd, Tb). *J. Am. Chem. Soc.* **2021,** *143* (40), 16610-16620.

9. Jenkins, T. F.; Woen, D. H.; Mohanam, L. N.; Ziller, J. W.; Furche, F.; Evans, W. J., Tetramethylcyclopentadienyl Ligands Allow Isolation of Ln(II) Ions across the Lanthanide Series in [K(2.2.2-cryptand)][$(C_5Me_4H)_3$Ln] Complexes. *Organometal.* **2018,** *37* (21), 3863-3873.

10. Ryan, A. J.; Darago, L. E.; Balasubramani, S. G.; Chen, G. P.; Ziller, J. W.; Furche, F.; Long, J. R.; Evans, W. J., Synthesis, Structure, and Magnetism of Tris(amide) [Ln$N(SiMe_3)_2)_3]^{1-}$ Complexes of the Non-traditional +2 Lanthanide Ions. *Eur. J. Chem.* **2018,** *24* (30), 7702-7709.

Appendix A

Reaction of *in. situ.* [K(crypt)][$Cp_3^{tet}La$] with NO

Introduction

It was previously reported that the reaction of nitric oxide with the radical $(N_2)^{3-}$bridged complex, $\{K(THF)_6\{[(R_2N)_2Y(THF)]_2[\mu\text{-}\eta^2\text{:}\eta^2\text{-}N_2]\}$ (R = $SiMe_3$),[1] resulted in the exchange of the bridging ligand with nitric oxide and the formation of a radical $(NO)^{2-}$ bridged complex, $\{[(R_2N)_2Y(THF)]_2[\mu\text{-}\eta^2\text{:}\eta^2\text{-}NO]\}$.[2] Upon discovery of this rare species, it became of interest to find other example. This appendix describes the reaction of of *in. situ.* generated [K(crypt)][$Cp_3^{tet}La$] (Cp^{tet} = C_5Me_4H) with NO in attempt to synthesize another $(NO)^{2-}$ complex.

Results and Discussion

$Cp_3^{tet}La$ and KC_8 were loaded into an H-tube on one side while THF was separated on the other. The H-tube was charged with an NO atmosphere. THF was condensed on to the $Cp_3^{tet}La$ and KC_8 and allowed to react under the NO atmosphere. After several minutes, the yellow solution turned to orange. EPR of the solution gave a spectrum with a 14-line pattern centered at g= 2.002, with hyperfine splitting of 90 G, Figure A1. Hyperfine splitting from nitrogen is not observed. This result suggests the presence of a radical species, but it has not yet been determined what that species could be. If this was an $(NO)^{2=}$ ion bridged by two La ions, the spectrum should be much more complicated. Even if nitrogen hyperfine were not present, the spectrum from two La ions should be a 15-line pattern.

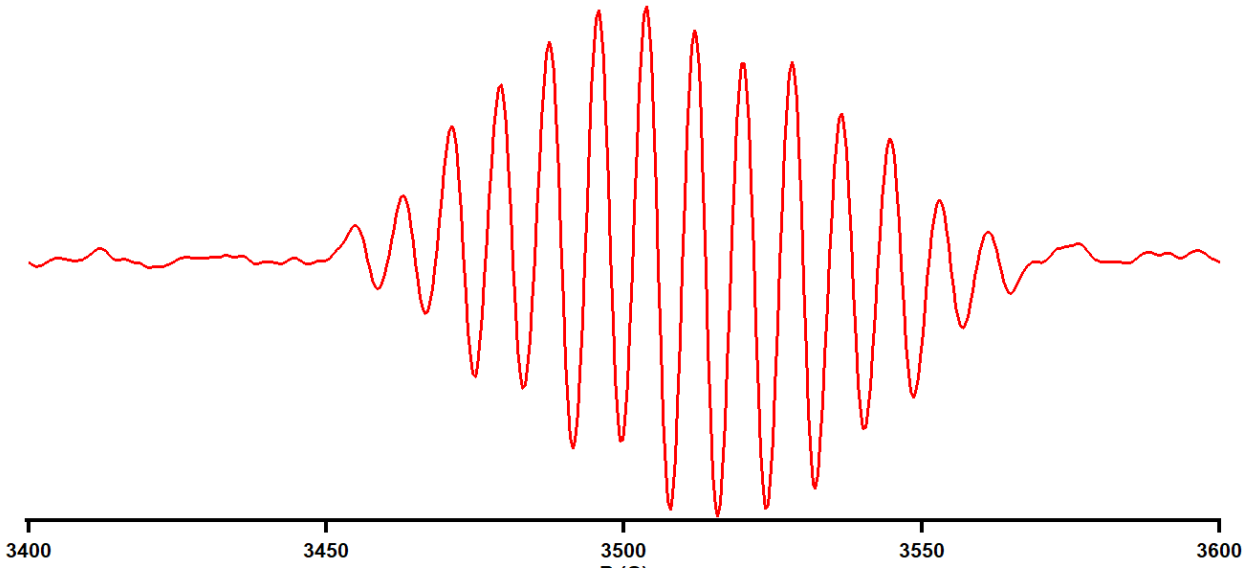

Figure A.1. X-band EPR spectrum of the reaction of NO *in. situ.* generated [K(crypt)][$Cp_3^{tet}La$] collected in THF at 298 K.

References

1. Fang, M., Bates, J. E., Lorenz, S. E., Lee, D. S., Rego, D. B., Ziller, J. W., Furche, F., Evans, W. J. $(N_2)^{3-}$ Radical Chemistry via Trivalent Lanthanide Salt/Alkali Metal Reduction of Dinitrogen: New Syntheses and Examples of $(N_2)^{2-}$ and $(N_2)^{3-}$ Complexes and Density Functional Theory Comparisons of Closed Shell Sc^{3+}, Y^{3+}, and Lu^{3+} versus $4f^9$ Dy^{3+}. Inorg. Chem. **2011**, *50*, 1459–1469.

2. Evans, W. J., Fang, M., Bates, J. E., Furche, F., Ziller, J. W., Kiesz, M. D., Zink, J. I. Isolation of a radical dianion of nitrogen oxide $(NO)^{2-}$. *Nat. Chem.* **2010**, *2*, 644-647